01 May 1994

Behavior of web elements with openings subjected to bending, shear and the combination of bending and shear

Ming-Yang Shan

Roger A. LaBoube
Missouri University of Science and Technology, laboube@mst.edu

Wei-wen Yu
Missouri University of Science and Technology, wwy4@mst.edu

CIVIL ENGINEERING STUDY 94-2
COLD-FORMED STEEL SERIES

Final Report

BEHAVIOR OF WEB ELEMENTS WITH OPENINGS SUBJECTED TO BENDING, SHEAR AND THE COMBINATION OF BENDING AND SHEAR

by

Ming-Yang Shan
Research Assistant

Roger A. LaBoube
Wei-Wen Yu
Project Directors

A Research Project Sponsored by

American Iron and Steel Institute

and Metal Lath/Steel Framing Association Division
National Association of Architectural Metal Manufacturers

May 1994

DEPARTMENT OF CIVIL ENGINEERING
UNIVERSITY OF MISSOURI-ROLLA
ROLLA, MISSOURI

PREFACE

The current design criteria for cold-formed steel members published by the American Iron and Steel Institute (1986,1991) do not provide sufficient information for the design of web elements with openings. The primary objective of this investigation was to study the structural behavior of cold-formed steel C-sections with web openings.

This study deals with the structural behavior of beam webs subjected to bending moment, shear force and combined bending moment and shear force. This report presents a summary of experimental study and findings of analytical results.

The test results indicate that the current AISI Specification does not account for the behavior of C-section members with web openings. Design recommendations are proposed to predict the strength of cold-formed steel beams with web openings.

This report is based on a thesis presented to the Faculty of the Graduate School of the University of Missouri-Rolla in partial fulfillment of the requirements for the degree of Doctor of Philosophy.

This investigation was sponsored by the American Iron and Steel Institute (AISI) and Metal/Lath Steel Framing Association (MLSFA). The technical guidance was provided by the MLSFA-AISI Joint Task Force: J.E. Sullivan (chairman), C. Bissey, R.L. Brockenbrough, C.R. Clauer, E.R.

diGirolamo, S.J. Errera, E.R. Estes, Jr., L. Hernandez, A.L. Johnson, K.H. Klippstein, J.P. Matsen, W.R. Midgley, T.B. Pekoz, N. Peterson, G.S. Ralph, R.M. Schuster, T.W. Trestain, and R.A. LaBoube. Thanks are also extended to R.B. Haws and K.L. Cole, AISI Staff, and A.L. Sisco, MLSFA Staff, for their assistance.

TABLE OF CONTENTS

TABLE OF CONTENTS (CONTINUED)

TABLE OF CONTENTS (CONTINUED)

TABLE OF CONTENTS (CONTINUED)

List of Illustrations

List of Illustrations (Continued)

List of Tables

List of Tables (Continued)

List of Tables (Continued)

List of Tables (Continued)

I. INTRODUCTION

A. GENERAL

During recent years, the use of cold-formed steel members in building construction and other areas has increased vastly, because of their favorable strength-to-weight ratio, ease of fabrication, and ease of erection and installation. Various types of cross sections have been developed for use in buildings and other applications.

In cold-formed steel structural members, the web elements sometimes have different shapes of openings, or punchouts, which give the convenience of easy installation of utility service. The presence of such openings may change the stress distribution within the member's web, alter its buckling characteristics and reduce its ultimate load-carrying capacity depending on the shape, size and arrangement of holes, in the cross section. Although structural elements containing web openings are widely employed, only a small amount information is available for the design and analysis.

The current design criteria for cold-formed steel beams are based on the "Specification for the Design of Cold-Formed Steel Structural Members" (1,2). However AISI Specifications do not have complete design provisions for webs having openings or punchouts. The Specifications only address the situation of local buckling behavior for solid webs and webs with circular holes. Therefore, the load-carrying capacity of members with web holes must be determined experimentally.

To investigate the structural behavior of a cold-formed steel member with a perforated web element and to gain an understanding of the effect of openings in web on load-carrying capacity, a research project "Behavior of Web Elements with Openings" has been conducted at the University of Missouri-Rolla (UMR). This project was conducted under the sponsorship of the American Iron and Steel Institute (AISI) and the Metal Lath/Steel Framing Association. This study has included both an experimental and an analytical investigation. Based on findings of the study, appropriate design recommendations are proposed for cold-formed steel members having a perforated web.

This report summarizes the experimental studies that used C-sections with or without punchouts. Two different web opening geometries were studied. This report also formulates design recommendations for the behavior of beams with web openings, or punchouts, when subjected to bending moment, shear force and a combined shear force and bending moment.

B. PURPOSE OF INVESTIGATION

The main purpose of this experimental investigation has been to study the behavior of cold-formed steel C-sections with and without web openings subjected to a pure bending, pure shear and a combination of bending and shear. The research has developed new design equations or modifications of current design equations in the Specification. Also, the correlation between existing design criteria and the actual

behavior of a beam composed of C-shaped members with and without punchouts in web elements has been examined in this study.

C. SCOPE OF INVESTIGATION

This study consisted of experimental and analytical investigations of the structural behavior of cold-formed steel C-sections with and without web openings subjected to pure bending, pure shear and a combined bending and shear.

In the first phase of the investigation, available literature and research reports relating to beam members with web openings and current cold-formed steel design specification have been studied. A summary of this review and current design criteria is given in Section II.

Section III illustrates the distortional buckling mode which is different from the local buckling mode, which has been the prominent buckling mode considered by the AISI Specifications. The studies on the behavior of distortional mode of buckling are discussed and two approximate models are proposed to evaluate the load carrying capacity.

Section IV contains the experimental test setup and test procedure for each test beam member subjected to pure bending. Also, the test results and evaluation of test data using the current AISI Specification are shown in this Section. Modified design methods are developed to accurately predict the flexural behavior of web elements with openings.

The shear behavior of web elements with openings is discussed in Section V. Experimental results and comparisons of tested and theoretical values computed by using the AISI LRFD Specification are presented in this Section. Finally, the shear reduction factors for C-section members with a web element having an elliptical opening are developed and are compared with Davis and Yu's study for the web element with a circular opening.

Investigation of the behavior of combined bending and shear of webs having a elliptical hole is presented in Section VI. Based on the findings in Sections IV and V, the test results are analyzed using the shear reduction factors to compute the shear strengths. The effective net section approach is used to calculate the moment capacities. The interaction relationships are examined and design recommendations to the current AISI Specification are proposed for C-shaped members with elliptical web openings subjected to combined bending moment and shear force.

II. REVIEW OF LITERATURE

A. GENERAL

A survey of literature was conducted to review the previous works relative to the ultimate strength of cold-formed steel sections with web openings subjected to bending, shear or a combination of bending and shear. Design recommendations, based on research findings to date, are also summarized.

The first design standard for cold-formed steel members was the "Specification for the Design of Light Gage Steel Structural Members" which was published by the American Iron and Steel Institute in 1946. Based on the findings of numerous research studies and industry experience, this specification has been revised several times. The AISI Cold-Formed Steel Design Manual now is the accepted design standard and used widely (3). There are no design provisions available in the AISI Specification for the design of cold-formed steel members with perforated elements subjected to bending, shear and combined bending and shear. A summary of current design criteria will be discussed in this review.

All available literature relative to the bending behavior of cold-formed steel members with web openings are summarized in Part B. The theoretical concepts, experimental works, and analysis of the test results are discussed briefly.

Previous experimental and analytical studies on the shear behavior of perforated webs of cold-formed steel sections are reviewed in Part C.

Previous investigations of the structural behavior of cold-formed steel members with web openings subjected to a combination of bending moment and shear force are discussed in Part D.

A summary of current design specifications and design guidelines governing the design of beam webs subjected to bending, shear, or a combination bending moment and shear force are presented in Sections B, C, and D.

B. ANALYTICAL INVESTIGATION OF BENDING BEHAVIOR

1. Previous Work on Local Buckling. In 1967 and 1968, Redwood and McCutcheon (4,5,6) studied wide-flange beams containing one or two unreinforced openings of various shapes. The beams used in this investigation consisted of 8-in. web depth, 5.25-in. flange width, 0.308-in. flange thickness, 0.230-in. web thickness, 4.5-in. depth of opening, and 36 ksi yield stress. Circular, elliptical, or rectangular holes located at the mid-depth of the beam web were tested. The test results (6) indicate that the moment capacity of the sections with single and double circular openings was approximately 64-72 percent of the plastic moment. For beams with an elliptical hole, the moment capacity was about 41-92 percent of the plastic moment. A single rectangular opening

reduced the moment capacity to 40 percent of the plastic moment.

Hoglund (7), in 1971, presented an experimental and theoretical study of the behavior of thin plate I-girders having both circular and square web openings. Girders with very thin webs were used. Three girders having web slenderness ratios ranging from 200 to 300, and hole depth to web depth ratios varying from 0.25 to 0.67 were tested. Adequate lateral support was provided in Hoglund's test program, and therefore, lateral-torsional buckling was precluded. Based on the test results, Hoglund indicates that the reduction in bending strength of a girder having web openings centered at mid-depth, is small because the flanges carry most of the bending moment. In 1990 (8), in a report to the Metal Lath/Steel Framing Association LaBoube summarized Hoglund's findings and compared the test results to a computed moment capacity using the AISI Specification. From the analysis of the test results and computed capacities, LaBoube concluded that Section C3.1.1 of the AISI Specification which employs an effective section modulus evaluated at the yield stress can accurately predict the moment capacity.

In view of the limited information available on the behavior of beams having slender webs, an experimental study was undertaken by Redwood, Baranda and Daly in 1978 (9), and analysis of the experimental results was performed by Redwood and Uenoya in 1979 (10). The purpose of these studies was to determine if local buckling is a problem for perforated beams

in building structures, and to determine the primary parameters influencing this buckling. The experimental study used thin webbed I-beams with circular and rectangular unreinforced holes having web slenderness ratios in the range 60 to 80, and ratios of the hole depth to web depth ranging from 0.135 to 0.627. The test results (9) showed the buckling of a perforated web is influenced by many different parameters but more tests need to be performed to determine precisely the actual parameters to influence the buckling behavior. Based on these studies, a straightforward way of checking the web stability (11) was developed and a simplified design approach was presented for beams with mid-depth holes undergoing elastic-plastic buckling behavior (10).

Numerous studies (12,13,14,15,16,17) addressed the behavior of beams with reinforced web holes. The type of reinforcement consisted of horizontal bars welded to the web above and below the openings. This reinforcement technique is widely used because of the economy and ease of fabrication. These investigations emphasized the ultimate strength analysis of beams with web openings. These studies focused primarily on rectangular holes, having a particular form of web reinforcement. In 1980 Shrivastava and Redwood (18) presented design recommendations for W-shaped beams with and without reinforced holes. Both rectangular and circular holes with the height of the openings between 30%-70% of the beam depth were studied. The study compares the test results with

equations developed by Redwood and Uenoya (10), Redwood (13), Kussman and Cooper (19), and Shrivastava and Redwood (20).

Another experimental investigation of lateral buckling behavior of narrow rectangular and I-beams containing rectangular web openings was carried out to determine the effect of web openings on the critical load by Shanmugam and Thevendran (21). Twenty three cantilevers and 23 simply supported beams having narrow rectangular sections, and 13 cantilevers and 13 simple supported beams were tested. The test results show that the approximate method based on the energy approach can predict the critical load accurately. Also, the results indicated that the buckling load of the beams of narrow rectangular and I-sections will reduce when the openings exist and the reduction depends on the number, spacing and size of openings in the web.

2. Current Design Criteria. The moment capacity of a cold-formed steel member is fundamentally governed by local buckling. The AISI Specifications employ the concept of an effective width to account for the local buckling and post-buckling strength of the compression elements. The calculated moment, M_{uc}, of a cross section is determined by the product of the effective section modulus, S_e, based on the effective areas of beam flanges and web, and yield strength of the material, F_y. Therefore, the ultimate moment capacity can be calculated as:

$$M_{uc} = S_e F_y \qquad (1)$$

The effective width of web is calculated by using the following equations shown in Section B2 of the AISI Specification. The effective widths, b_1 and b_2, as shown in Fig. 1, are determined from the following formulas:

$$b_1 = b_e/(3-\psi) \quad (2)$$

For $\psi \leq -0.236$

$$b_2 = b_e/2 \quad (3)$$

b_1+b_2 shall not exceed the compression portion of the web calculated on the basis of the effective section.

For $\psi > -0.236$

$$b_2 = b_e-b_1 \quad (4)$$

where b_e = Effective width b determined as follows:

$$b_e = w \text{ when } \lambda \leq 0.673 \quad (5)$$

$$b_e = \rho w \text{ when } \lambda > 0.673 \quad (6)$$

where $w = h$ = Flat width of the web element

$$\rho = (1-0.22/\lambda)/\lambda \quad (7)$$

$$\lambda = (1.052/\sqrt{k})(w/t)\sqrt{(f_1/E)} \quad (8)$$

$$k = 4+2(1-\psi)^3+2(1-\psi) \quad (9)$$

$$\psi = f_2/f_1 \quad (10)$$

f_1, f_2 = Stresses shown in Fig. 1 calculated on the basis of effective section.

Based on the equations shown in Section B4 of the AISI Specification, the effective width of compression flange and edge-stiffener, as shown in Fig. 1, are determined.

More information regarding the use of effective width equations is presented in Part II.

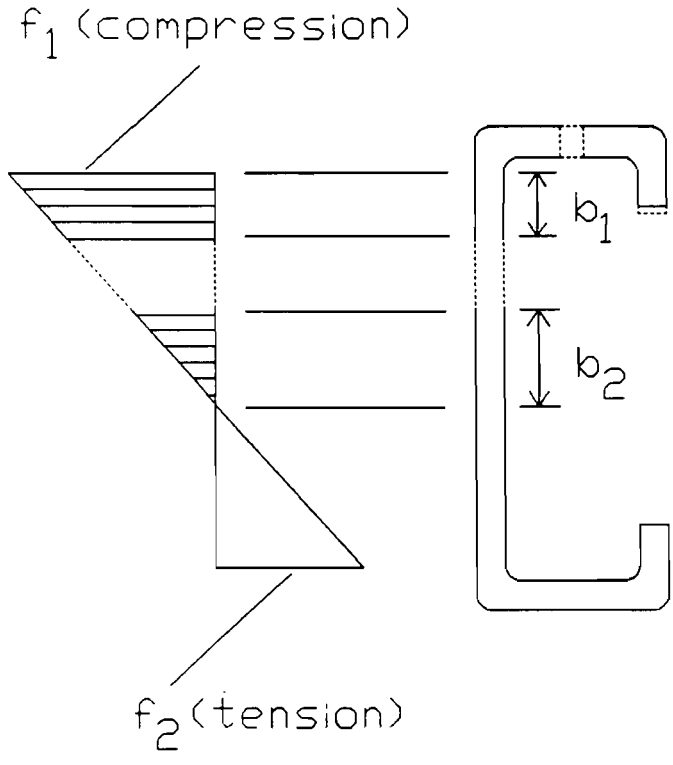

Figure 1. AISI Specification for the Effective Elements

3. Previous Work on Distortional Buckling. Studies on the distortional mode of buckling behavior have been conducted by Lau and Hancock (22) for rack, hat and channel sections; Kwon and Hancock (23) studied channel sections formed from high strength steels; Bernard, Bridge and Hancock (24,25) investigated the behavior of trapezoidal deck sections with V-stiffeners; Bernard, Bridge and Hancock (26) studied the distortional buckling of trapezoidal sections with flat hat stiffeners; and Charnvarnichborikan and Polyzois (27,28) explored the behavior of Z-sections. A detailed discussion on this buckling mode will be presented in Section III.

C. ANALYTICAL INVESTIGATION OF SHEAR BEHAVIOR

1. Previous Work. In the past, several research efforts have focused on the influence of the holes in flat plates subjected to shear. One of the prominent research efforts was performed by Narayanan and Der-Avanessian in 1983 and 1984 (29,30,31,32,33). They studied the ultimate shear capacity of a plate girder with its web containing rectangular openings. Seventy tests were completed with web slenderness ratios ranging from 200 to 360; the ratio of web plate width to depth was 1.0 and 1.5; and the hole sizes did not exceed one-half the depth of web plate or one-half the width of the web plate. Based on a parametric study of the test results (33), an approximate method for computing the ultimate shear capacity was developed and a procedure to design the reinforcement was generated.

An experimental study of the buckling behavior of a square plate with square openings was conducted by Chow and Narayanan in 1984. Shear buckling coefficients that accounted for the square plate having square openings were proposed (34).

Based on the experimental information from numerous research studies, suggested guidelines employing the assumption that the allowable shear stress be taken as 40 percent of the tensile yield stress, and the shear force causes a secondary bending moment above and below the hole within a beam section with a web punchout were made by Fowler, Marino, Palmer, Rewood, Snell and Bower in 1971 (35). The

following two design criteria were proposed, depending on elastic or plastic behavior, for a perforated web subjected to shear:

a. Allowable Stress Design (Elastic Design). The maximum allowable shear stress, F_{vH}, is determined as:

(a). For transverse shear stress:

$$F_{vH} = (1-H/D_b)F_v \tag{11}$$

(b). For the secondary bending moment:

$$F_{vH} = (P_t/P_b)F_v \tag{12}$$

where

F_{vH} = The reduced maximum allowable shear stress at section through a hole

F_v = The present maximum allowable shear stress

t = Web thickness

H = The depth of hole

A_h = The length of hole

D_b = The depth of beam

$P_t = (1-H/D_b)^2(1+8A_f/A_w-H/D_b)$

$P_b = 4(H/D_b)(A_h/H)(1+4A_f/A_w-H/D_b)$

A_f = The area of the web

A_w = The product of D_b and t

The smaller value of F_{vH} calculated by utilizing the above two equations should be used as the maximum shear stress. The above equations indicate that both the length and depth of the hole will influence the maximum allowable stress.

b. Ultimate Load Design (Plastic Design). The ultimate shear load for a beam with an unreinforced web hole is also

controlled by the smaller of the transverse shear and the secondary bending moment. The reduced ultimate shear force, V_{uH}, is determined as:

(a). For $s > p(1-H/D_b)$:

$$V_{uH} = (1-H/D_b)\sqrt{\alpha/(1+\alpha)}V_u \quad (13)$$

(b). For $s < p(1-H/D_b)$:

$$V_{uH} = [4M_T+(n-1)4m]/[A_h+(n-1)p] \leq (s/p)V_u \quad (14)$$

where

V_{uH} = The reduced ultimate shear force

V_u = Maximum shear force

s = Minimum width of web post between adjacent web holes

p = Center-to-center distance between holes

M_T = Plastic moment of tee section

n = Number of adjacent web holes

m = Plastic moment of web between adjacent web holes

$$\alpha = 0.75(H/A_h)^2(D_b/H-1)^2 \quad (15)$$

Both allowable stress and ultimate load design approaches have been experimentally verified to give a good prediction of the shear strength for a beam member with unreinforced web holes.

Yu and Davis studied the structural behavior of cold-formed steel members with perforated elements in 1973 (36,37). Based on twelve tests of back-to-back channel sections having web depth to thickness ratios ranging from 66.2 to 99.5, and the ratio of hole width to web depth varying from 0 to 0.504, the authors concluded that the presence of circular hole will reduce the shear capacity. Yu and Davis defined the reduced

shear capacity, $q_s V_{cr}$, where V_{cr} is the shear buckling force in the elastic and inelastic ranges. The reduction factor, q_s, is applicable for a circular opening located at mid-depth in a web element. This reduction factor, q_s, is expressed as:

$$q_s = 1.0-1.1(d/h) \quad (16)$$

where d = The diameter of a circular hole

h = The clear distance between flanges measured along the plane of the web

Based on a finite element study, a shear reduction factor, q'_s, for both circular and rectangular openings was derived by Redwood and Uenoya (10). This shear reduction factor, q'_s, is represented by:

(a). For rectangular hole:

$$q'_s = 1.24 - 1.16\ (a''/h') - 0.17\ (b'/a'') \quad (17)$$

(b). For circular hole:

$$q'_s = 1.15 - 1.05\ (2r'/h') \quad (18)$$

where

a'' = Height of hole

h' = Clear height of web

b' = Half-length of a rectangular hole

r' = Radius of a circular hole

LaBoube evaluated the findings of Chow and Narayanan's (34) and the results of Yu and Davis's (36) and recommended that Eq. 16 could be used for both circular and rectangular web openings (8).

2. <u>Current Design Criteria.</u> For solid web elements subjected to shear alone, the design strength can be estimated

by applying the equations from Section C3.2 of the 1991 Edition of the AISI LRFD Specification (2). These nominal equations also serve as the basis for the shear strength equations given in the AISI ASD Specification (1). The shear force at any section shall not exceed the allowable shear, V_a, calculated as follows:

(a). For $h/t \leq \sqrt{Ek_v/F_y}$:

$$V_n = 0.577F_yht \tag{19}$$

(b). For $\sqrt{Ek_v/F_y} < h/t \leq 1.415\sqrt{Ek_v/F_y}$:

$$V_n = 0.64t^2k_vF_yE \tag{20}$$

(c). For $h/t > 1.415\sqrt{Ek_v/F_y}$:

$$V_n = 0.905Ek_vt^3/h \tag{21}$$

where

V_n = Nominal shear strength of web

t = Web thickness

h = Depth of the flat portion of the web measured along the plane of the web

k_v = Shear buckling coefficient determined as follows:

1. For unreinforced webs, $k_v = 5.34$
2. For beam webs with transverse stiffeners satisfying the requirements of Section B6

when $a'/h \leq 1.0$

$$k_v = 4.00+5.34/(a'/h)^2 \tag{22}$$

when $a'/h > 1.0$

$$k_v = 5.34+4.00/(a'/h)^2 \tag{23}$$

where a' = The shear panel length for unreinforced web element

= Distance between transverse stiffeners for reinforced web elements

D. ANALYTICAL INVESTIGATION OF A COMBINATION OF BENDING AND SHEAR BEHAVIOR

1. Previous Work. There was no literature reported on the design of web elements with openings under combined loading.

2. Current Design Criteria. The current AISI Specification, in Section C3.3, addresses the ultimate strength of web elements without openings under a load combination of bending and shear. For beams with unreinforced webs, the applied moment, M, and applied shear, V, shall satisfy the following interaction equation:

$$(M/M_a)^2 + (V/V_a)^2 \leq 1.0 \quad (24)$$

For beams with transverse web stiffeners, the applied moment, M, and applied shear, V, shall not exceed M_a and V_a, respectively. When $M/M_a > 0.5$ and $V/V_a > 0.7$, then M and V shall satisfy the following interaction equation:

$$0.6(M/M_a)+(V/V_a) \leq 1.3 \quad (25)$$

where M_a = Allowable moment when bending along exists

V_a = Allowable shear force when shear alone exists

III. DISTORTIONAL BUCKLING BEHAVIOR

A. GENERAL

Channel sections and other sections of monosymmetry may undergo a mode of buckling failure called distortional buckling. A mode in which the edge-stiffener and flange element rotate about the flange-web junction.

Research on the topic of the distortional buckling mode has been conducted widely for various cross-section types. In 1985, a detailed investigation on the buckling modes, including local, distortional and flexural-torsional modes, was performed by Hancock (38). The distortional buckling of steel storage rack columns was discussed, and simple design charts for computing the critical stress for the distortional mode of buckling and the buckling half-wavelengths were presented. For all of the sections investigated, the distortional buckling stress was lower than local buckling stress. The test results showed very little post-buckling strength to be available for this mode of buckling. This theoretical and experimental work only dealt with the distortional buckling mode within the elastic range. An analytical model for computing the elastic distortional buckling stress was provided by Lau and Hancock in 1987 (39). The validity of the analytical model was verified by a finite strip buckling analysis. Further work on both the elastic and the inelastic range of buckling resulted in a set of design curves. The design curves are based on tests using a variety

of cross sections, including lipped channels, hat sections and two types of channels used for industrial steel storage racks (22). In 1992, Charnvarnichborikarn and Polyzois (27,28) predicted the strength of Z-section columns using a simplified formula derived from Lau and Hancock's design curves to calculate the distortional stress. The distortional buckling stress in the flange-lip stiffener elements was taken as the critical stress for the entire section. The researchers used a theoretical distortional buckling model developed on the assumption that local buckling of the web initiated distortional buckling of the flange-lip stiffeners. Good correlation was demonstrated between the theoretical results and experimental results.

B. ANALYTICAL FORMULATIONS

The following discussion is based on two approximate models for considering the distortional buckling. A comparison of the test results and computed moment based on the behavior of these two models is presented in Section IV.

1. Model A: This approximate theoretical model assumed that the combination of flange and lip stiffener is undistorted and rotates about the junction of the flange and web, as shown in Fig. 2b. This model was derived by Lau and Hancock in 1987 (39). The effects of the web on the flanges are represented by a lateral spring and a rotational spring. By considering equilibrium of forces in the plane of x and y directions and the equilibrium of moments about the shear

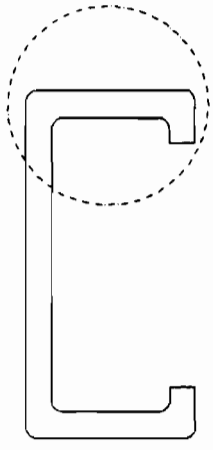

(a) Real section

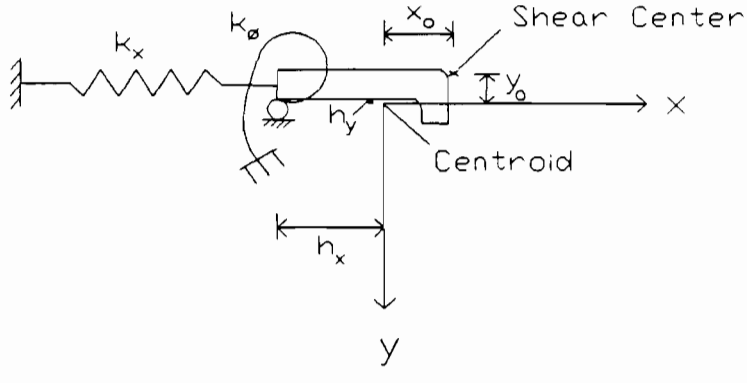

(b) Model A

Figure 2. Analytical Model A for Distortional Buckling

center, three simultaneous differential equations were determined as follows:

$$EI_y\frac{d^4u}{dz^4}+EI_{xy}\frac{d^4v}{dz^4}+P_f\left(\frac{d^2u}{dz^2}-y_o\frac{d^2\phi}{dz^2}\right)+k_x[u+(y_o-h_y)\phi] = 0 \quad (26)$$

$$EI_x\frac{d^4v}{dz^4}+EI_{xy}\frac{d^4u}{dz^4}+P_f\left(\frac{d^2v}{dz^2}-x_o\frac{d^2\phi}{dz^2}\right)+Q_y = 0 \quad (27)$$

$$EI_w\frac{d^4\phi}{dz^4}-\left(GJ-\frac{I_o}{A}P_f\right)\frac{d^2\phi}{dz^2}-P_f\left(x_o\frac{d^2v}{dz^2}-y_o\frac{d^2u}{dz^2}\right)$$
$$+k_x[u+(y_o-h_y)\phi](y_o-h_y)-Q_y(x_o-h_x)+k_\phi\phi = 0 \quad (28)$$

where u,v, and ϕ are the horizontal, vertical, and rotational displacements, k_x and k_ϕ are the horizontal and rotational restraints, I_0 is the polar second moment of area about the shear center and Q_y is the intensity of reaction force distributed continuously along the support and acts in the y-direction. In Eqs. 26 and 27, the first two terms are derived from the bending strength of the section about the y and x axes, respectively. The third terms demonstrate the effect of lateral compressive force P_f on the rotation of cross section. The last terms represent the lateral reaction forces acting along the support with respect to the x and y axes. In Eq. 28, the first three terms are derived from non-uniform torsion of a thin-walled open cross section, whereas the last three terms are the torque caused by the two lateral reactions and the torsional restraint at the elastic support, respectively.

The general solutions were obtained by solving simultaneous differential Eqs. 26 to 28.

By applying several simplifications, the design formula for the distortional buckling load as given by Lau and Hancock, P_{cr}, can be expressed as follows (39):

$$P_{cr} = \frac{E}{2}[(\alpha_1+\alpha_2)+\sqrt{[(\alpha_1+\alpha_2)^2-4\alpha_3]}] \tag{29}$$

$$\text{where } \alpha_1 = \frac{\eta}{\beta_1}(I_x b_f^2+0.039J\lambda^2)+\frac{k_\phi}{\beta_1\eta E} \tag{29a}$$

$$\alpha_2 = \eta(I_y+\frac{2}{\beta_1}\bar{y}b_f I_{xy}) \tag{29b}$$

$$\alpha_3 = \eta(\alpha_1 I_y-\frac{\eta}{\beta_1}I_{xy}^2 b_f^2) \tag{29c}$$

$$\beta_1 = \bar{x}^2+\frac{(I_x+I_y)}{A} \tag{29d}$$

$$\beta_2 = I_w+I_x(x_o-h_x)^2 \tag{29e}$$

$$\beta_3 = I_{xy}(x_o-h_x) \tag{29f}$$

$$\beta_4 = \beta_2+(y_o-h_y)[I_y(y_o-h_y)-2\beta_3] \tag{29g}$$

$$\lambda = 4.80(\frac{I_x b_f^2 b_w}{t^3})^{0.25} \tag{29h}$$

$$\eta = (\frac{\pi}{\lambda})^2 \tag{29i}$$

The elastic distortional buckling stress, σ_d, is obtained as

$$\sigma_d = \frac{P_{cr}}{A} \qquad (30)$$

where A is the gross section area of the flange and edge stiffener as defined and shown in Fig. 2b.

The nominal elastic or inelastic distortional buckling stress, F_d, is given by (22):

$$F_d = F_y\left(1-\frac{F_y}{4\sigma_d}\right) \quad ; \text{ when } \sigma_d \geq \frac{F_y}{2} \qquad (31)$$

$$F_d = F_y\left[0.55\left(\sqrt{\frac{F_y}{\sigma_d}}-3.6\right)^2+0.237\right] \quad ; \text{ when } \sigma_d < \frac{F_y}{2} \qquad (32)$$

where F_d = The nominal elastic or elastic distortional buckling stress

F_y = Yield strength

σ_d = The elastic distortional buckling stress

Equation 31 is based on the Johnston parabola (40) for inelastic buckling. Based on the test results, Eq. 32 was derived by Kwon and Hancock for elastic buckling (22,41). Equations 31 and 32 consider the post-buckling strength of a section which may buckle in the distortional or mixed local-distortional mode in the elastic range.

The rotational restraint, k_ϕ, as derived by Lundquist, Stowell, and Schuette (42), and rederived by Lau and Hancock (43) approaches a constant of $2D/b_w$,

$$k_\phi = \frac{2D}{b_w} = \frac{Et^3}{5.46b_w} \qquad (33)$$

where D = Plate flexural rigidity per unit width

$= Et^3/[12(1-\nu^2)]$

b_w = Depth of web

E = Young's modulus

t = thickness

ν = Poisson's ratio

= 0.3

Equation 34 was developed by Charnvarnichborikarn (27,28) when investigating the distortional buckling mode of Z-sections,

$$k_\phi = \frac{Et^3}{4.00b_w} \tag{34}$$

The Winter formula (44) expressed as the following equation is commonly used to determine the ultimate post buckling load-carrying capacity of plates in compression.

$$\frac{b_e}{b} = \sqrt{\frac{\sigma_{el}}{F_y}}\left[1-0.22\sqrt{\frac{\sigma_{el}}{F_y}}\right] \tag{35}$$

where b_e is the effective part of the plate width and σ_{el} is the elastic local buckling stress.

Based on the test results from axially loaded members (22,41), Kwon and Hancock modified Eq. 35 using the elastic distortional or elastic mixed local-distortional mode buckling stress (σ_d). Therefore, Eq. 35 becomes:

$$\frac{b_e}{b} = 1 \quad ;\lambda \leq 0.673 \tag{36}$$

$$\frac{b_e}{b} = \sqrt{\frac{\sigma_d}{F_y}}\left[1-0.22\sqrt{\frac{\sigma_d}{F_y}}\right] \quad ;\lambda \geq 0.673 \tag{37}$$

$$\text{where } \lambda = \sqrt{\frac{F_y}{\sigma_d}} \tag{38}$$

In subsequent work, Kwon and Hancock increased the exponent of the (σ_d/F_y) term in Eq. 37 from 0.5 to 0.6 and raised the 0.22 coefficient to 0.25 to account for unconservative estimates under certain circumstances. Thus, the effective width formulas for the distortional buckling are given as follows:

$$\frac{b_e}{b} = 1 \quad ;\lambda \leq 0.561 \tag{39}$$

$$\frac{b_e}{b} = \left(\frac{\sigma_d}{F_y}\right)^{0.6}\left[1-0.25\left(\frac{\sigma_d}{F_y}\right)^{0.6}\right] \quad ;\lambda > 0.561 \tag{40}$$

$$\text{where } \lambda = \sqrt{\frac{F_y}{\sigma_d}} \tag{41}$$

Equations 39, 40 and 41 can be used to compute the effective width of flange and lip stiffeners undergoing distortional buckling, and the web having a local-distortional buckling behavior. This concept of effective widths can be performed for all elements of the cross section likely to undergo the pure distortional mode or the distortional buckling mode interacting with local buckling assuming distortional buckling before or at the same time as local buckling.

Based on this model, the elastic distortional buckling stress (σ_d) is obtained from Eqs. 29 and 30 and the nominal

moment, $M_{uc,d}$, given in Eq. 42 can be calculated by using Eqs. 31 and 32 to determine the nominal elastic or inelastic distortional buckling stress (F_d) and Eqs. 39, 40 and 41 to compute the effective section modulus ($S_{ex,d}$).

$$M_{uc,d} = F_d S_{ex,d} \tag{42}$$

2. Model B: Another approach for computing the elastic distortional buckling stress was proposed by Serrette and Pekoz (45). This model treats the web and flange as an elastically restrained beam (Fig. 3). The distortional buckling mode in this model assumes rotation of the web and compression flange is along the axis of the web and tension flange. Using the model shown in Fig. 3, the moment expression for distortional buckling stress with constraints defined by rotational and extensional springs located at the web-tension flange junction was evaluated. In this model, which assumes that distortional buckling occurs before local buckling, no lateral displacement is allowed at the web-tension flange junction because the whole section is assumed to be laterally stable. Two differential equations for flexure about x and y axes respectively, and one equation for the equilibrium of moments about the shear center were developed. The solution for the elastic distortional buckling moment, $M_{cr,d}$, is given as:

$$M_{cr,d} = \frac{\alpha_1+\alpha_2}{\alpha_3} \tag{43}$$

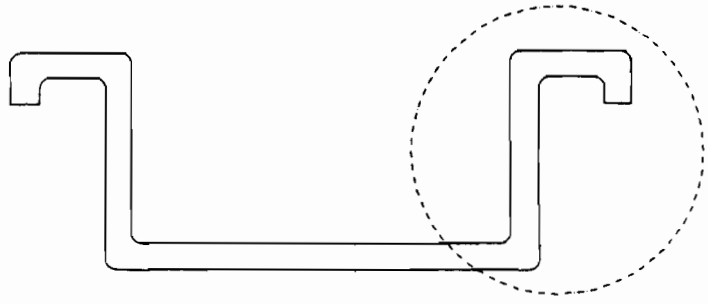

(a) Real section

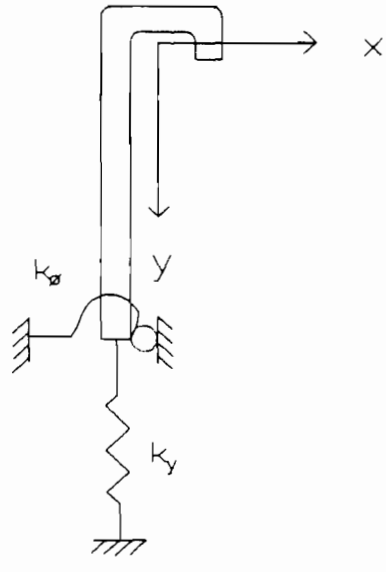

(b) Model B

Figure 3. Analytical Model B for Distortional Buckling

$$\text{where } \alpha_1 = (EI_{xy}\eta\theta^2+k_y\xi)^2 \tag{43a}$$

$$\alpha_2 = -(EI_x\theta^2+k_y)(EC_w\theta^2+EI_y\eta^2\theta^2+GJ\theta+k_y\xi^2+k_\phi) \tag{43b}$$

$$\alpha_3 = -(2\eta+\beta_1)(EI_x\theta^2+k_y)\theta \tag{43c}$$

$$\eta = y_o-h_y' \tag{43d}$$

$$\xi = x_o-h_x' \tag{43e}$$

$$\theta = \frac{\pi^2}{L_e^2} \tag{43f}$$

E = Young's modulus

G = Shear modulus

I_x = Moment of inertia about the x-axis (normal to the web)

I_y = Moment of inertia about the y-axis (parallel to the web)

I_{xy} = Product moment of inertia

C_w = Warping constant

J = Torsion constant

k_y = Elastic extensional spring constant

k_ϕ = Elastic rotational spring constant

β_1 = Geometric parameter

L_e = Effective unsupported length of the leg

x_o = Location of the shear center relative to the centroid, along an axis parallel to the x-axis

y_o = Location of the shear center relative to the centroid, along an axis parallel to the y-axis

h_x' = Distance from the web-tension flange junction to the centroid, along an axis parallel to the x-axis

h_y' = Distance from the web-tension flange junction to the centroid, along an axis parallel to the y-axis

The linear elastic extensional spring constant, k_y, was assumed to be zero for panels typically found in industry, and the linear elastic rotational restraint constant, k_ϕ, was dependent on the distortional buckling mode and local buckling capacity of the web. For the sections with a width-to-thickness ratio of the tension flange less than 400, and having symmetric and non-symmetric buckling modes, the rotational spring constants may be determined, respectively, as:

$$k_{\phi,s} = \frac{Et^3}{(1-\nu^2)(6w_f+4w_w)}\gamma \qquad (44)$$

$$k_{\phi,as} = \frac{Et^3}{(1-\nu^2)(2w_f+4w_w)}\gamma \qquad (45)$$

If the tension flange width-to-thickness exceeds 400, the rotational spring constants for symmetric and non-symmetric modes were estimated by:

$$k_{\phi,s-as} = \frac{Et^3}{(1-\nu^2)(\frac{3}{4}w_f+4w_w)}\gamma \qquad (46)$$

where E = Young's modulus

t = Thickness of the section

ν = Poisson's ratio

w_f = Width of the tension flange

w_w = Depth of the web in the leg under consideration

γ = Ratio of the elastic local buckling stress in the web to the buckling stress required for the web to be fully effective

The elastic buckling stress, $F_{cr,d}$, corresponding to $M_{cr,d}$ is expressed as:

$$F_{cr,d} = \frac{M_{cr,d}}{S_g} \tag{47}$$

where S_g is the gross section modulus for the section shown by Fig. 3a, and the nominal compressive stress, F_n, is determined as follows:

$$F_n = F_{cr,d} \quad ; \quad F_{cr,d} \leq \frac{F_y}{2} \tag{48}$$

$$F_n = F_y\left(1-\frac{F_y}{4F_{cr,d}}\right) \quad ; \quad F_{cr,d} > \frac{F_y}{2} \tag{49}$$

where F_y is the yield strength of the material

Finally the ultimate moment, $M_{uc,d}$, is computed by:

$$M_{uc,d} = F_n S_{en} \tag{50}$$

where S_{en} is the effective section modulus determined by using the AISI Specification (1) effective width provisions and the nominal compressive stress (F_n).

IV. FLEXURAL BEHAVIOR OF WEB ELEMENTS WITH OPENINGS

A. GENERAL

Two test sequences for the investigation of flexural behavior have been completed at UMR. Test sequence No. 1 conducted by Batson (46) investigated sections with web openings fabricated from relatively low yield strength material. Test sequence No. 2 examined sections both with and without web openings. Specimens in test sequence No. 2 had yield strengths higher than those used for sequence No. 1. Specimens having wider flanges and different web opening geometries, type H and type T (Fig. 4), were also considered in test sequence No. 2. Test sequence No. 3 was conducted by Schuster (47) at the University of Waterloo and is also summarized herein. The results of these three test sequences have been analyzed and evaluated to develop an analytical model to account for the flexural behavior of C-section members with or without web punchouts. This section summarizes the UMR test procedure, test results, and the evaluation of the research to date. Design recommendations depending on the local or distortional buckling of the beam members are also proposed herein.

B. EXPERIMENTAL STUDY

The objective of the experimental investigation was to evaluate the buckling behavior and ultimate strength of beam webs with openings, and to develop modified equations, as

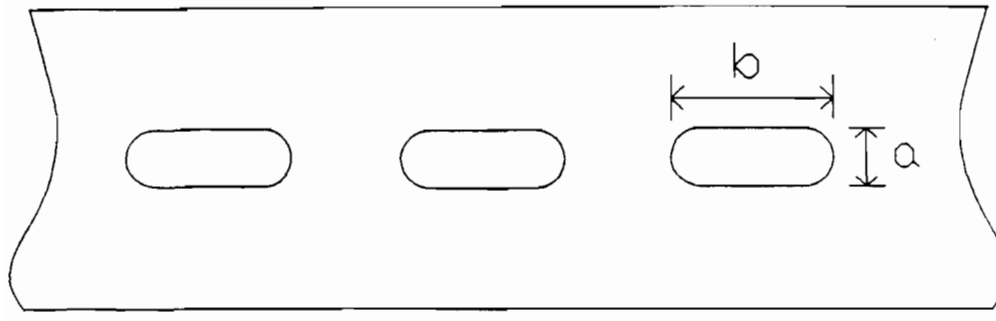

(a) Specimen type H

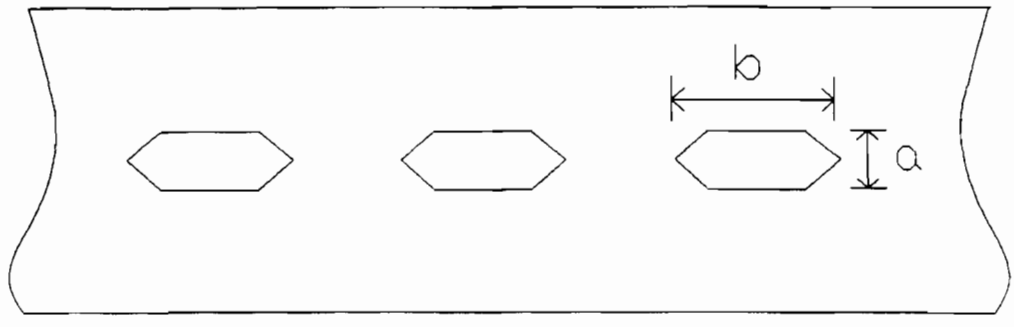

(b) Specimen type T

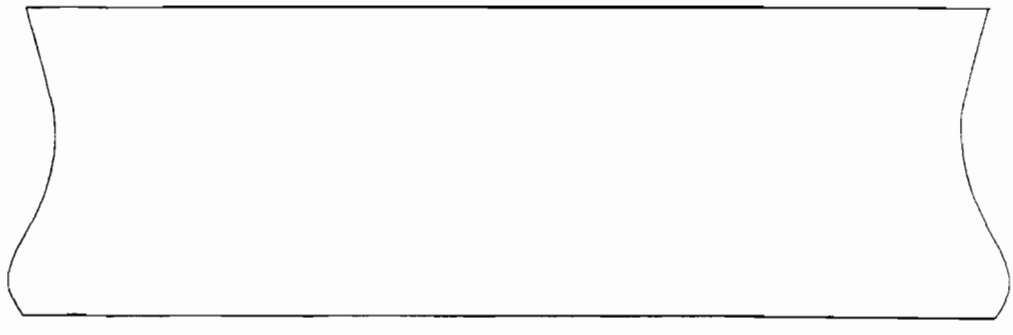

(c) Specimen type N

Figure 4. Specimen Type

necessary, for predicting the bending strength of beam members. Test sequence Nos. 1 and 2 were performed in the Engineering Research Laboratory of the University of Missouri-Rolla, and test sequence No. 3 was completed in the Structures Laboratory of University of Waterloo in Canada. For all test sequences, the web openings for specimens type H and type T (Fig. 4) were located at 24 inches on center as illustrated in Fig. 5. Test sequence No. 1 had two web opening sizes 4 x 1.5 inch and 2 x 0.75 inch where a=1.5 and 0.75 inch and b=2 and 4 inch. Test sequence No. 2 had 4 x 1.5 and 4.5 x 1.5 inch openings, and test sequence No. 3 contained 4.02 x 1.50, 4.53 x 2.48, 4.65 x 1.69 and 4.61 x 2.52 inch web openings. The dimensions for test sequence No. 3 were converted from metric dimensions.

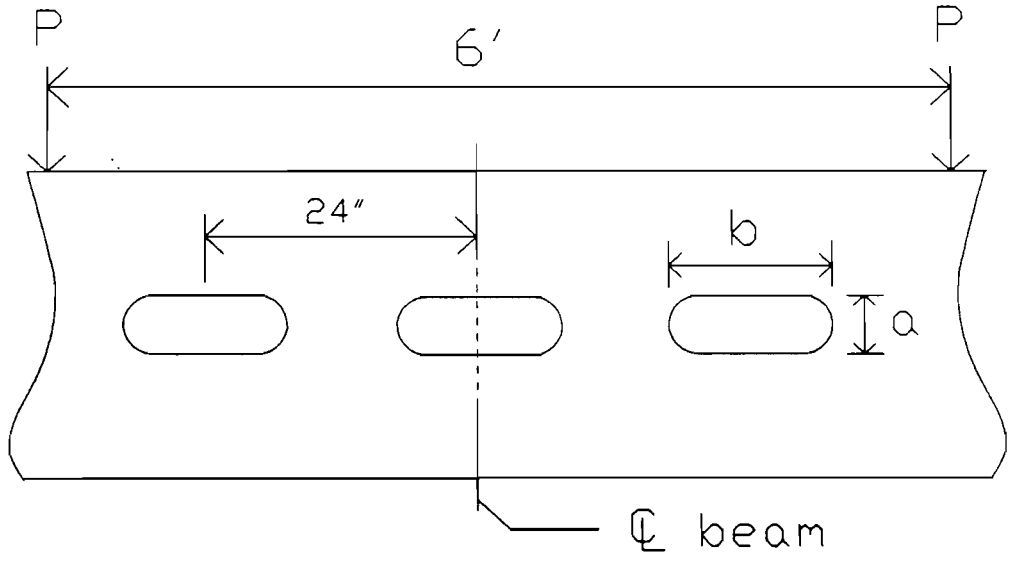

Figure 5. Load and Opening Configurations

TABLE I DIMENSIONS OF BENDING TEST SPECIMENS (UMR TEST SEQUENCE No. 1)

Beam Specimen No.	Cross-Section Dimenisions (inches)											Hole Geom. (in.)	
	Thick.	D1	D2	B1	B2	B3	B4	d1	d2	d3	d4	b	a
2,16,1&2(H)	0.062	2.51	2.51	1.61	1.61	1.63	1.61	0.40	0.45	0.42	0.43	2	0.75
2,20,1&2(H)	0.039	2.50	2.48	1.60	1.60	1.60	1.60	0.42	0.41	0.42	0.41	2	0.75
2,20,3&4(H)	0.039	2.51	2.52	1.59	1.62	1.58	1.60	0.36	0.42	0.47	0.41	2	0.75
3,14,1&2(H)	0.077	3.68	3.68	1.65	1.64	1.63	1.63	0.57	0.55	0.56	0.52	4	1.50
3,14,3&4(H)	0.077	3.69	3.69	1.63	1.62	1.64	1.63	0.53	0.53	0.62	0.55	4	1.50
3,18,1&2(H)	0.044	3.75	3.65	1.56	1.56	1.57	1.58	0.58	0.56	0.58	0.54	4	1.50
3,18,3&4(H)	0.044	3.65	3.64	1.56	1.58	1.56	1.57	0.56	0.57	0.54	0.54	4	1.50
3,20,1&2(H)	0.044	3.65	3.71	1.56	1.64	1.55	1.59	0.52	0.56	0.55	0.56	4	1.50
3,20,3&4(H)	0.044	3.67	3.69	1.56	1.59	1.55	1.61	0.60	0.56	0.52	0.59	4	1.50
12,14,1&2(H)	0.098	12.08	12.07	1.64	1.63	1.69	1.63	0.69	0.60	0.60	0.62	4	1.50
12,14,3&4(H)	0.098	12.05	12.00	1.64	1.60	1.67	1.71	0.65	0.64	0.65	0.64	4	1.50
12,16,1&2(H)	0.055	11.96	11.97	1.57	1.57	1.57	1.56	0.50	0.61	0.52	0.43	4	1.50
12,16,3&4(H)	0.055	12.07	11.96	1.56	1.57	1.57	1.58	0.42	0.53	0.58	0.53	4	1.50

Note: See Fig. 5 for the symbols used for the hole geometry.
See Fig. 6 for the symbols used for dimensions.
Specimen Designation: 12,14,1&2(H)
12-Nominal Depth
14-Gage Number
1&2-Individual Cross Section
(H)-Web Opening Geometry
(N)-No Web Opening

TABLE II DIMENSIONS OF BENDING TEST SPECIMENS (UMR TEST SEQUENCE NO. 2)

Beam Specimen No.	Cross-Section Dimensions(inches)											Hole Geom. (in.)	
	Thick.	D1	D2	B1	B2	B3	B4	d1	d2	d3	d4	b	a
2B,16,1&2(H)	0.059	2.46	2.46	1.62	1.63	1.62	1.61	0.47	0.46	0.51	0.51	4.0	1.5
2B,16,3&4(H)	0.059	2.47	2.46	1.63	1.62	1.62	1.63	0.47	0.52	0.52	0.46	4.0	1.5
2B,16,1&2(N)	0.057	2.48	2.48	1.62	1.63	1.61	1.61	0.45	0.45	0.51	0.51	---	---
2B,16,3&4(N)	0.057	2.48	2.48	1.61	1.63	1.63	1.61	0.51	0.46	0.47	0.51	---	---
2B,20,1&2(H)	0.033	2.42	2.42	1.63	1.64	1.63	1.62	0.42	0.42	0.50	0.50	4.0	1.5
2B,20,3&4(H)	0.033	2.42	2.43	1.63	1.64	1.63	1.62	0.42	0.41	0.50	0.50	4.0	1.5
2B,20,1&2(N)	0.033	2.44	2.44	1.63	1.64	1.63	1.62	0.41	0.40	0.49	0.50	---	---
2B,20,3&4(N)	0.033	2.46	2.45	1.63	1.63	1.61	1.61	0.39	0.40	0.52	0.51	---	---
3B,14,1&2(H)	0.071	3.65	3.62	1.62	1.66	1.63	1.63	0.54	0.55	0.49	0.50	4.0	1.5
3B,14,3&4(H)	0.071	3.64	3.63	1.63	1.62	1.62	1.63	0.54	0.47	0.49	0.54	4.0	1.5
3B,18,1&2(H)	0.044	3.61	3.63	1.61	1.65	1.65	1.62	0.51	0.52	0.50	0.50	4.0	1.5
3B,18,3&4(H)	0.044	3.62	3.63	1.62	1.66	1.65	1.64	0.50	0.50	0.52	0.52	4.0	1.5
3B,18,1&2(N)	0.044	3.66	3.68	1.66	1.61	1.62	1.66	0.52	0.47	0.47	0.52	---	---
3B,18,3&4(N)	0.044	3.64	3.64	1.66	1.64	1.65	1.63	0.49	0.49	0.50	0.48	---	---
3B,20,1&2(H)	0.036	3.61	3.60	1.63	1.62	1.63	1.62	0.46	0.47	0.46	0.47	4.0	1.5
3B,20,3&4(H)	0.036	3.61	3.61	1.64	1.63	1.64	1.63	0.46	0.47	0.47	0.47	4.0	1.5
3B,20,5&6(H)	0.036	3.60	3.60	1.63	1.63	1.62	1.63	0.46	0.46	0.46	0.47	4.0	1.5
3B,20,1&2(T)	0.029	3.56	3.57	1.62	1.65	1.68	1.60	0.59	0.64	0.62	0.61	4.5	1.5
3B,20,3&4(T)	0.029	3.56	3.56	1.62	1.68	1.69	1.61	0.58	0.63	0.62	0.57	4.5	1.5
3B,20,1&2(N)	0.035	3.60	3.60	1.63	1.62	1.63	1.63	0.47	0.47	0.46	0.46	---	---
3B,20,3&4(N)	0.035	3.60	3.60	1.63	1.63	1.63	1.63	0.48	0.46	0.46	0.47	---	---
3B,20,5&6(N)	0.035	3.59	3.60	1.63	1.62	1.62	1.62	0.47	0.47	0.47	0.46	---	---

TABLE II (CONTINUED) DIMENSIONS OF BENDING TEST SPECIMENS (UMR TEST SEQUENCE No. 2)

Beam Specimen No.	Cross-Section Dimensions(inches)											Hole Geom. (in.)	
	Thick.	D1	D2	B1	B2	B3	B4	d1	d2	d3	d4	b	a
6B,18,1&2(H)	0.046	6.06	6.05	1.62	1.62	1.55	1.55	0.47	0.47	0.50	0.50	4.0	1.5
6B,18,3&4(H)	0.046	6.05	6.02	1.62	1.62	1.55	1.55	0.47	0.48	0.50	0.51	4.0	1.5
6C,18,1&2(H)	0.048	5.96	5.96	1.98	1.99	1.98	1.99	0.64	0.59	0.59	0.64	4.0	1.5
6C,18,3&4(H)	0.048	5.95	5.98	1.97	1.98	1.99	1.98	0.60	0.65	0.64	0.63	4.0	1.5
6D,18,1&2(H)	0.046	6.02	6.02	2.42	2.43	2.43	2.43	0.70	0.62	0.62	0.70	4.0	1.5
6D,18,3&4(H)	0.046	6.02	6.02	2.43	2.43	2.43	2.43	0.70	0.70	0.61	0.62	4.0	1.5
6B,20,1&2(H)	0.033	5.92	5.92	1.63	1.62	1.52	1.53	0.44	0.47	0.44	0.42	4.0	1.5
8A,14,1&2(H)	0.074	8.06	8.06	1.38	1.38	1.38	1.38	0.49	0.48	0.41	0.43	4.0	1.5
8A,14,3&4(H)	0.074	8.07	8.07	1.38	1.38	1.38	1.38	0.50	0.41	0.41	0.50	4.0	1.5
8A,14,5&6(H)	0.074	8.07	8.07	1.37	1.38	1.38	1.37	0.41	0.50	0.49	0.41	4.0	1.5
8A,14,7&8(H)	0.065	8.03	8.03	1.39	1.39	1.39	1.40	0.43	0.48	0.48	0.45	4.0	1.5
8A,14,9&10(H)	0.065	8.04	8.04	1.39	1.38	1.38	1.38	0.46	0.44	0.45	0.48	4.0	1.5
8A,14,1&2(N)	0.073	8.08	8.08	1.38	1.38	1.38	1.38	0.47	0.47	0.41	0.42	---	---
8A,14,3&4(N)	0.073	8.08	8.08	1.38	1.38	1.38	1.38	0.48	0.40	0.39	0.49	---	---
8A,14,5&6(N)	0.073	8.07	8.07	1.37	1.38	1.38	1.38	0.47	0.46	0.40	0.42	---	---
8A,14,7&8(N)	0.066	8.03	8.04	1.39	1.40	1.40	1.39	0.50	0.43	0.42	0.51	---	---
8A,14,9&10(N)	0.066	8.03	8.05	1.40	1.39	1.39	1.39	0.44	0.48	0.48	0.44	---	---
8B,14,1&2(T)	0.067	8.05	8.05	1.64	1.63	1.64	1.64	0.63	0.64	0.67	0.66	4.5	1.5
8B,14,3&4(T)	0.067	8.05	8.04	1.64	1.64	1.64	1.64	0.64	0.64	0.66	0.65	4.5	1.5
8B,14,5&6(T)	0.065	8.02	8.02	1.63	1.64	1.64	1.63	0.64	0.63	0.64	0.63	4.5	1.5
8B,14,7&8(T)	0.065	8.03	8.03	1.63	1.63	1.63	1.63	0.66	0.61	0.61	0.66	4.5	1.5

TABLE II (CONTINUED) DIMENSIONS OF BENDING TEST SPECIMENS (UMR TEST SEQUENCE No. 2)

Beam Specimen No.	Cross-Section Dimensions(inches)											Hole Geom. (in.)	
	Thick.	D1	D2	B1	B2	B3	B4	d1	d2	d3	d4	b	a
8B,14,1&2(N)	0.068	8.05	8.05	1.63	1.64	1.63	1.63	0.63	0.66	0.65	0.64	---	---
8B,14,3&4(N)	0.068	8.05	8.05	1.63	1.63	1.63	1.63	0.63	0.65	0.65	0.63	---	---
8B,14,5&6(N)	0.064	8.03	8.03	1.62	1.63	1.63	1.63	0.62	0.65	0.65	0.62	---	---
8B,14,7&8(N)	0.064	8.03	8.03	1.63	1.63	1.62	1.63	0.67	0.59	0.59	0.67	---	---
8D,14,1&2(T)	0.065	7.95	7.96	2.48	2.50	2.47	2.49	0.64	0.48	0.47	0.62	4.5	1.5
8D,14,3&4(T)	0.065	7.95	7.95	2.47	2.49	2.47	2.48	0.66	0.48	0.45	0.61	4.5	1.5
8D,14,1&2(N)	0.064	7.96	7.97	2.50	2.50	2.50	2.50	0.60	0.51	0.49	0.59	---	---
8D,14,3&4(N)	0.064	7.97	7.97	2.49	2.50	2.50	2.50	0.59	0.50	0.50	0.60	---	---
8B,18,1&2(H)	0.045	7.95	7.94	1.59	1.58	1.58	1.58	0.47	0.47	0.48	0.47	4.0	1.5
8D,18,1&2(H)	0.046	8.00	8.00	2.42	2.45	2.44	2.43	0.61	0.69	0.69	0.62	4.0	1.5
8D,18,3&4(H)	0.046	8.00	8.00	2.42	2.45	2.45	2.43	0.60	0.70	0.70	0.60	4.0	1.5
8A,20,1&2(H)	0.031	7.93	7.93	1.38	1.39	1.38	1.38	0.41	0.44	0.45	0.43	4.0	1.5
8A,20,3&4(H)	0.031	7.93	7.92	1.37	1.38	1.39	1.37	0.45	0.43	0.43	0.44	4.0	1.5
8A,20,1&2(N)	0.031	7.93	7.93	1.38	1.38	1.37	1.38	0.40	0.45	0.46	0.41	---	---
8A,20,3&4(N)	0.031	7.94	7.93	1.37	1.38	1.38	1.36	0.46	0.42	0.39	0.44	---	---
8B,20,1&2(T)	0.031	7.97	7.97	1.63	1.64	1.63	1.62	0.61	0.61	0.60	0.62	4.5	1.5
8B,20,3&4(T)	0.031	7.96	7.96	1.63	1.63	1.62	1.63	0.62	0.58	0.58	0.62	4.5	1.5
8B,20,5&6(T)	0.031	7.95	7.95	1.63	1.63	1.63	1.63	0.61	0.60	0.60	0.61	4.5	1.5
8B,20,7&8(T)	0.031	7.95	7.95	1.63	1.63	1.64	1.63	0.61	0.62	0.61	0.62	4.5	1.5
8B,20,1&2(N)	0.031	7.95	7.98	1.63	1.65	1.64	1.64	0.62	0.62	0.62	0.61	---	---
8B,20,3&4(N)	0.031	7.95	7.96	1.63	1.64	1.63	1.63	0.62	0.62	0.62	0.62	---	---
8B,20,5&6(N)	0.031	7.95	7.95	1.63	1.63	1.63	1.63	0.61	0.61	0.61	0.61	---	---

TABLE II (CONTINUED) DIMENSIONS OF BENDING TEST SPECIMENS (UMR TEST SEQUENCE No. 2)

Beam Specimen No.	Cross-Section Dimensions(inches)											Hole Geom. (in.)	
	Thick.	D1	D2	B1	B2	B3	B4	d1	d2	d3	d4	b	a
8D,20,1&2(T)	0.043	7.94	7.94	2.49	2.45	2.45	2.49	0.64	0.59	0.59	0.64	4.5	1.5
8D,20,3&4(T)	0.043	7.94	7.94	2.46	2.46	2.44	2.48	0.64	0.59	0.59	0.65	4.5	1.5
8D,20,5&6(T)	0.043	7.95	7.95	2.49	2.46	2.45	2.48	0.62	0.62	0.62	0.63	4.5	1.5
8D,20,1&2(N)	0.043	7.94	7.95	2.49	2.45	2.45	2.50	0.64	0.60	0.58	0.65	---	---
8D,20,3&4(N)	0.043	7.95	7.95	2.49	2.45	2.46	2.49	0.65	0.58	0.58	0.65	---	---
12B,16,1&2(H)	0.060	11.95	11.95	1.63	1.63	1.63	1.63	0.53	0.54	0.52	0.53	4.0	1.5
12B,16,3&4(H)	0.060	11.98	12.02	1.63	1.63	1.62	1.63	0.47	0.50	0.55	0.53	4.0	1.5
12B,16,5&6(H)	0.060	11.96	11.97	1.63	1.63	1.63	1.63	0.51	0.50	0.51	0.52	4.0	1.5
12B,16,7&8(H)	0.060	11.97	11.96	1.63	1.63	1.62	1.63	0.48	0.55	0.56	0.49	4.0	1.5
12B,16,1&2(N)	0.062	11.95	11.94	1.63	1.63	1.63	1.63	0.51	0.55	0.54	0.48	---	---
12B,16,3&4(N)	0.062	11.96	11.98	1.64	1.63	1.63	1.63	0.46	0.55	0.56	0.49	---	---

Note: Specimen Designation: 8A,14,1&2(H)
8-Nominal Depth
A-Flange Width Designation
14-Gage Number
1&2-Individual Cross Section
(H)-Web Opening Geometry
(T)-Web Opening Geometry
(N)-No Web Opening

TABLE III DIMENSIONS OF BENDING TEST SPECIMENS (SCHUSTER TEST SEQUENCE No. 3)

Beam Specimen No.	Cross-Section Dimenisions (inches)											Hole Geom. (in.)	
	Thick.	D1	D2	B1	B2	B3	B4	d1	d2	d3	d4	b	a
BS1(N)	0.048	7.99	7.99	1.61	1.61	1.61	1.61	0.47	0.47	0.47	0.47	----	----
BS2(N)	0.048	7.99	7.99	1.61	1.61	1.61	1.61	0.47	0.47	0.47	0.47	----	----
BP4-40(H)	0.047	7.99	7.99	1.61	1.61	1.61	1.61	0.47	0.47	0.47	0.47	4.02	1.50
BP5-40(H)	0.047	7.99	7.99	1.61	1.61	1.61	1.61	0.47	0.47	0.47	0.47	4.02	1.50
BP6-40(H)	0.047	7.99	7.99	1.61	1.61	1.61	1.61	0.47	0.47	0.47	0.47	4.02	1.50
BP7-65(H)	0.047	7.99	7.99	1.58	1.58	1.58	1.58	0.47	0.47	0.47	0.47	4.53	2.48
BP8-65(H)	0.047	7.99	7.99	1.61	1.58	1.61	1.58	0.47	0.47	0.47	0.47	4.53	2.48
BP9-65(H)	0.047	7.99	7.99	1.61	1.58	1.58	1.58	0.47	0.47	0.47	0.47	4.53	2.48
CS1(N)	0.048	7.99	7.99	1.58	1.58	1.58	1.58	0.51	0.51	0.51	0.51	----	----
CS2(N)	0.048	8.03	7.99	1.58	1.58	1.58	1.58	0.51	0.51	0.51	0.51	----	----
CS3(N)	0.048	8.03	7.99	1.61	1.58	1.58	1.58	0.51	0.51	0.51	0.51	----	----
CP4-40(T)	0.048	7.99	7.99	1.58	1.58	1.58	1.58	0.51	0.51	0.51	0.51	4.65	1.69
CP5-40(T)	0.048	7.99	7.99	1.58	1.61	1.58	1.58	0.51	0.51	0.51	0.51	4.65	1.69
CP6-40(T)	0.048	8.03	8.03	1.61	1.61	1.58	1.58	0.51	0.51	0.51	0.51	4.65	1.69
CP7-65(T)	0.048	7.99	7.99	1.61	1.61	1.61	1.61	0.51	0.51	0.51	0.51	4.61	2.52
CP8-65(T)	0.048	8.03	7.99	1.58	1.61	1.58	1.61	0.51	0.51	0.51	0.51	4.61	2.52
CP9-65(T)	0.048	7.99	7.99	1.61	1.61	1.61	1.61	0.51	0.51	0.51	0.51	4.61	2.52

Note: Specimen Designation: BP4-40
B-Section Type
P-Perforated Web
4-Test No.
40-Depth of Perforation in mm

1. Preparation of Beam Specimens. Five different depth industry standard C-sections were tested at UMR. The sections had nominal web depths of 2.5, 3.625, 6, 8 and 12 inches. Various thickness and yield strengths were also tested. Test sequence No. 3 only considered a nominal web depth of 8 inches. The cross-sectional dimensions, thickness and size of web openings for each test specimen are recorded in Tables I, II and III.

The desired span length of each beam specimen was cut from a 20 foot long C-section. The specimen was fabricated such that a web hole be located at the center of the test specimen span. Each beam test specimen consisted of two C-shaped beams connected together using 3/4 x 3/4 x 1/8 inch aluminum angles and self-drilling screws. See Fig. 6. The aluminum angles were located every 6 inches along the top and bottom of the individual C-section to prevent lateral buckling for test sequence No. 2. Test sequence Nos. 1 and 3 used angles spaced at 12 inches.

In order to determine the strain distribution in the web element during testing, electrical resistance strain gages were mounted to one C-section of each test specimen. The strain gages were located at mid-span (Fig. 7). In addition, strain gages were also mounted on the compression and tension flanges to determine the bending stresses in both flanges.

Side channels were attached to the beam webs with self-drilling screws at the location of loading (Fig. 8). The side channels were used to support the bearing plates. The load

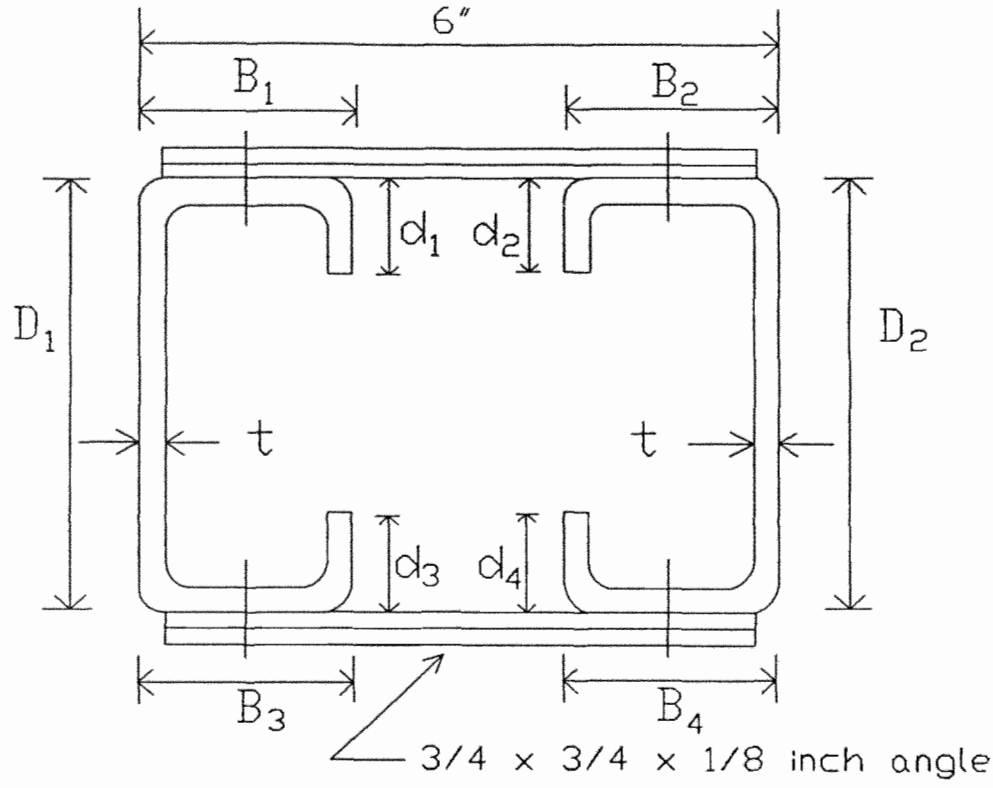

Figure 6. Typical Cross Section of Test Specimens

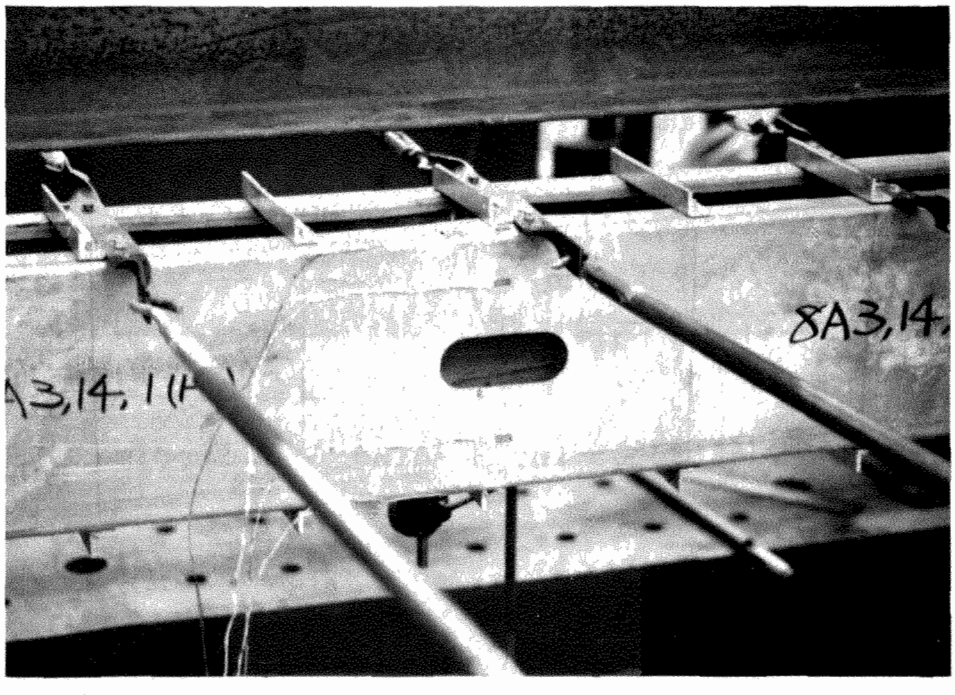

Figure 7. Location of Strain Gages for Beam Specimens

applied to the I-beam was transferred to the bearing plates which in turn introduced the load through the side channels into the webs of the test beam. This loading arrangement avoided the direct stress from the load and cross I-beam on the web element which may have caused web crippling. In order to prevent the beam webs at the location of side channels from rotating, the 3/4 x 3/4 x 1/8 inch aluminum angles were used to connect side channels together on the top.

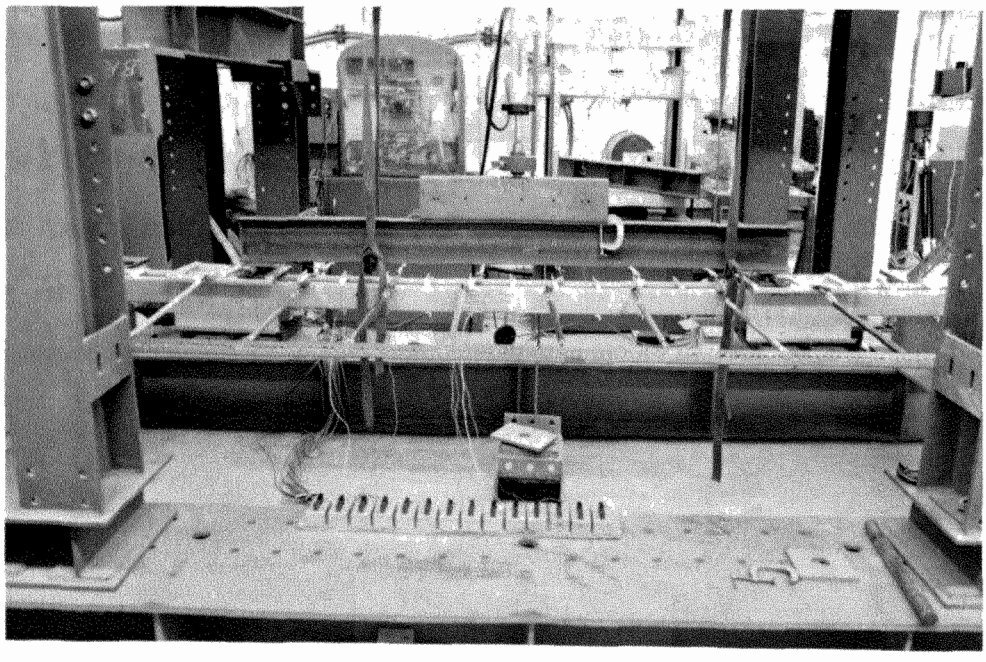

Figure 8. Test Setup for Bending Test Specimens

2. Testing of Specimens

a. Tensile Coupon Tests. The mechanical properties of the steels, for each test specimen, were established by

standard tensile coupon tests. Three coupons were cut from the web element of each specimen type, and prepared in accordance with ASTM A370. The coupons were tested in a 150,000 pound Tinus-Olsen universal testing machine which was linked to the computer software package Labtech Notebook. The average property values obtained for each material from the coupon tests were used. Tables IV, V and VI list the tensile test data for thickness, yield strength (F_y), ultimate tensile strength (F_u) and percent elongation in 2 inches gage length.

TABLE IV MATERIAL PROPERTIES OF BENDING TEST SPECIMENS (UMR TEST SEQUENCE No. 1)

Specimen No.	Thickness (in.)	F_y (ksi)	F_u (ksi)	Elongation (%)
2,16(H)	0.062	37.23	48.86	38
2,20(H)	0.039	33.70	48.02	44
3,14(H)	0.077	63.72	78.42	23
3,18(H)	0.044	46.92	60.32	31
3,20(H)	0.044	46.82	60.31	31
12,14(H)	0.098	35.93	47.43	35
[illegible]16(H)	0.055	49.11	57.50	32

TABLE V MATERIAL PROPERTIES OF BENDING TEST SPECIMENS (UMR TEST SEQUENCE No. 2)

Specimen No.	Thickness (in.)	F_y (ksi)	F_u (ksi)	Elongation (%)
2B,16(H)	0.059	53.59	74.74	39.1
2B,16(N)	0.057	58.00	77.81	36.5
2B,20(H)	0.033	67.15	71.50	35.4
2B,20(N)	0.033	64.67	75.15	32.8
3B,14(H)	0.071	81.36	104.28	21.9
3B,14(N)	0.076	77.60	109.81	20.3
3B,18(H)	0.044	53.13	70.16	24.0
3B,18(N)	0.044	62.74	80.67	13.5
3B,20(H)	0.036	63.71	78.95	29.2
3B,20(T)	0.029	25.51	68.99	51.6
3B,20(N)	0.035	60.70	81.56	33.3
6B,18(H)	0.046	47.17	67.06	41.4
6C,18(H)	0.048	75.08	83.80	15.6
6D,18(H)	0.046	30.77	55.11	54.7
6B,20(H)	0.033	93.26	97.31	4.6
8A,14(H)	0.074	31.04	54.81	50.0
8A,14(H)	0.065	56.29	81.91	31.3
8A,14(N)	0.073	29.76	56.70	46.9
8A,14(N)	0.066	55.76	81.24	32.8
8B,14(T)	0.067	32.58	54.78	56.3
8B,14(T)	0.065	53.14	80.98	34.4
8B,14(N)	0.068	36.54	54.78	50.8
8B,14(N)	0.064	53.33	81.12	34.4
8D,14(T)	0.065	54.71	81.06	32.0
8D,14(N)	0.064	50.37	76.69	34.4
8B,18(H)	0.045	72.32	74.49	29.7
8D,18(H)	0.046	22.00	59.06	54.7
8A,20(H)	0.031	37.96	67.61	38.5
8A,20(N)	0.031	39.74	71.99	40.6
8B,20(T)	0.031	44.89	80.69	37.5
8B,20(N)	0.031	42.97	79.09	38.3
8D,20(T)	0.043	38.59	64.26	46.9
8D,20(N)	0.043	38.60	64.76	45.3
12B,16(H)	0.060	60.64	74.70	37.5
12B,16(N)	0.062	61.61	74.24	39.1

TABLE VI MATERIAL PROPERTIES OF BENDING TEST SPECIMENS (SCHUSTER TEST SEQUENCE No. 3)

Specimen No.	Thickness (in.)	F_y (ksi)	F_u (ksi)	Elongation (%)
BS(N)	0.047	39.30	52.21	31.3
BP(H)	0.047	38.87	50.76	31.1
CS(N)	0.048	48.01	52.07	35.8
CP(T)	0.047	49.02	52.21	36.3

b. Testing of Beam Specimens

(i). Test Setup. A similar test setup was used for all three test sequences, the following details pertain specifically to the UMR test setup. Each specimen was tested as a simply supported beam. Two concentrated loads were applied a distance of six feet apart positioning a hole at mid-span as shown in Fig. 5 for all tests in test sequence Nos. 1 and 2. This loading configuration provided a constant moment region between the applied loads.

The load was applied using a hydraulic jack and transmitted to a cross beam, which distributed the load as two concentrated loads to the test specimen. An electronic load cell placed between the jack and the cross beam measured the applied load. Figure 8 shows the test setup. For each test specimen, the span length and the distance from the end support to the applied load, x, are given in Tables VII, VIII and IX.

TABLE VII TEST RESULTS FOR BENDING TEST SPECIMENS (UMR TEST SEQUENCE No. 1)

Beam Specimen No.	Span Length (ft)	x (in.)	P (kips)
2,16,1&2(H)	12.5	39	1.04
2,20,1&2(H)	12.5	39	0.46
2,20,3&4(H)	12.5	39	0.46
3,14,1&2(H)	12.5	39	3.70
3,14,3&4(H)	12.5	39	3.54
3,18,1&2(H)	12.5	39	1.35
3,18,3&4(H)	12.5	39	1.37
3,20,1&2(H)	12.5	39	1.35
3,20,3&4(H)	12.5	39	1.43
12,14,1&2(H)	16.0	60	7.16
12,14,3&4(H)	16.0	60	7.50
12,14,5&6(H)	16.0	60	7.95
12,14,7&8(H)	16.0	60	7.98
12,16,1&2(H)	16.0	60	4.38
12,16,3&4(H)	16.0	60	4.79

TABLE VIII TEST RESULTS FOR BENDING TEST SPECIMENS (UMR TEST SEQUENCE No. 2)

Beam Specimen No.	Span Length (ft)	x (in.)	P (kips)
2B,16,1&2(H)	12.5	39	1.345
2B,16,3&4(H)	12.5	39	1.360
2B,16,1&2(N)	12.5	39	1.585
2B,16,3&4(N)	12.5	39	1.620
2B,20,1&2(H)	12.5	39	0.600
2B,20,3&4(H)	12.5	39	0.635
2B,20,1&2(N)	12.5	39	0.770
2B,20,3&4(N)	12.5	39	0.760

TABLE VIII (CONTINUED) TEST RESULTS FOR BENDING TEST SPECIMENS (UMR TEST SEQUENCE No. 2)

Beam Specimen No.	Span Length (ft)	x (in.)	P (kips)
3B,14,1&2(H)	12.5	39	4.310
3B,14,3&4(H)	12.5	39	4.255
3B,18,1&2(H)	12.5	39	1.600
3B,18,3&4(H)	12.5	39	1.510
3B,18,1&2(N)	12.5	39	2.440
3B,18,3&4(N)	12.5	39	2.150
3B,20,1&2(H)	12.5	39	1.200
3B,20,3&4(H)	12.5	39	1.100
3B,20,5&6(H)	12.5	39	1.335
3B,20,1&2(T)	12.5	39	0.425
3B,20,3&4(T)	12.5	39	0.455
3B,20,1&2(N)	12.5	39	1.170
3B,20,3&4(N)	12.5	39	1.255
3B,20,5&6(N)	12.5	39	1.405
6B,18,1&2(H)	16.0	60	1.640
6B,18,3&4(H)	16.0	60	1.700
6C,18,1&2(H)	16.0	60	3.425
6C,18,3&4(H)	16.0	60	3.445
6D,18,1&2(H)	16.0	60	1.670
6D,18,3&4(H)	16.0	60	1.700
6B,20,1&2(H)	16.0	60	1.150
8A,14,1&2(H)	16.0	60	3.675
8A,14,3&4(H)	16.0	60	3.700
8A,14,5&6(H)	16.0	60	3.640
8A,14,7&8(H)	16.0	60	4.370
8A,14,9&10(H)	16.0	60	4.310
8A,14,1&2(N)	16.0	60	3.825
8A,14,3&4(N)	16.0	60	3.900
8A,14,5&6(N)	16.0	60	3.880
8A,14,7&8(N)	16.0	60	4.380
8A,14,9&10(N)	16.0	60	4.480
8B,14,1&2(T)	16.0	60	3.225
8B,14,3&4(T)	16.0	60	3.890
8B,14,5&6(T)	16.0	60	3.735
8B,14,7&8(T)	16.0	60	5.375
8B,14,9&10(T)	16.0	60	5.260

TABLE VIII (CONTINUED) TEST RESULTS FOR BENDING TEST SPECIMENS (UMR TEST SEQUENCE No. 2)

Beam Specimen No.	Span Length (ft)	x (in.)	P (kips)
8B,14,1&2(N)	16.0	60	4.250
8B,14,3&4(N)	16.0	60	4.200
8B,14,5&6(N)	16.0	60	5.200
8B,14,7&8(N)	16.0	60	5.190
8D,14,1&2(T)	16.0	60	5.895
8D,14,3&4(T)	16.0	60	5.925
8D,14,1&2(N)	16.0	60	5.780
8D,14,3&4(N)	16.0	60	5.975
8B,18,1&2(H)	16.0	60	2.760
8D,18,1&2(H)	16.0	60	2.100
8D,18,3&4(H)	16.0	60	1.840
8A,20,1&2(H)	16.0	60	1.005
8A,20,3&4(H)	16.0	60	0.985
8A,20,1&2(N)	16.0	60	1.055
8A,20,3&4(N)	16.0	60	1.070
8B,20,1&2(T)	16.0	60	1.370
8B,20,3&4(T)	16.0	60	1.370
8B,20,5&6(T)	16.0	60	1.425
8B,20,7&8(T)	16.0	60	1.380
8B,20,1&2(N)	16.0	60	1.440
8B,20,3&4(N)	16.0	60	1.440
8B,20,5&6(N)	16.0	60	1.425
8D,20,1&2(T)	16.0	60	2.540
8D,20,3&4(T)	16.0	60	2.650
8D,20,5&6(T)	16.0	60	2.600
8D,20,1&2(N)	16.0	60	2.660
8D,20,3&4(N)	16.0	60	2.600
12B,16,1&2(H)	16.0	60	6.485
12B,16,3&4(H)	16.0	60	6.440
12B,16,5&6(H)	16.0	60	6.385
12B,16,7&8(H)	16.0	60	6.665
12B,16,1&2(N)	16.0	60	6.500
12B,16,3&4(N)	16.0	60	6.755

TABLE IX TEST RESULTS FOR BENDING TEST SPECIMENS (SCHUSTER TEST SEQUENCE No. 3)

Beam Specimen No.	Span Length (ft)	x (in.)	P (kips)
BS1(N)	14	72	3.12
BS2(N)	14	72	3.18
BP4-40(H)	14	72	3.16
BP5-40(H)	14	72	3.07
BP6-40(H)	14	72	3.18
BP7-65(H)	14	72	3.14
BP8-65(H)	14	72	3.18
BP9-65(H)	14	72	3.18
CS1(N)	14	72	3.34
CS2(N)	14	72	3.34
CS3(N)	14	72	3.43
CP4-40(T)	14	72	3.45
CP5-40(T)	14	72	3.28
CP6-40(T)	14	72	3.47
CP7-65(T)	14	72	3.44
CP8-65(T)	14	72	3.41
CP9-65(T)	14	72	3.40

The ends of the beam test specimen were laterally supported by vertical rollers to prevent lateral movement of the ends (Fig. 9). To prevent premature failure of the beam due to lateral-torsional buckling, lateral braces were also attached to the central portion of the beam. The details of the typical bracing scheme are shown in Fig. 10. A dial gage was placed under the beam to measure the vertical deflection of the test specimen at midspan.

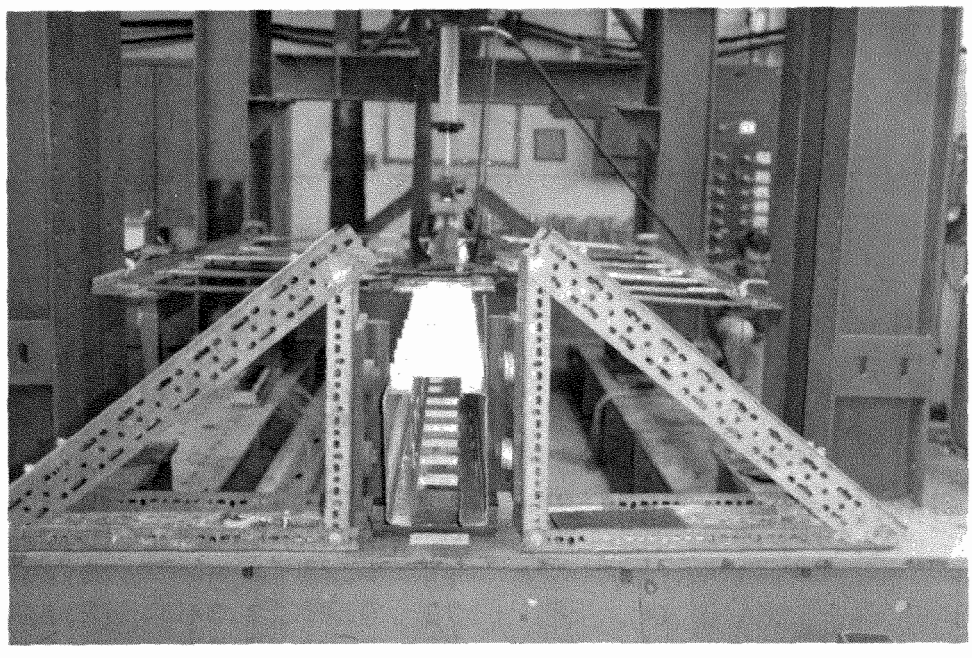

Figure 9. Support at Ends of Beams

(ii). Test Procedure. For the UMR test program, each test specimen was loaded to failure. Prior to testing, the possible failure load was estimated based on the yield moment, $M_y = S_e F_y$. During each test, the load was applied to the test specimen in predetermined increments using a hydraulic jack. Small increments were used when the load approached the failure load. For each increment of loading, the load and strain gage readings were recorded to a data file using a data acquisition system and personal computer. In addition, for each load increment the vertical displacement at mid-span of the beam was measured by using a dial gage. The load was

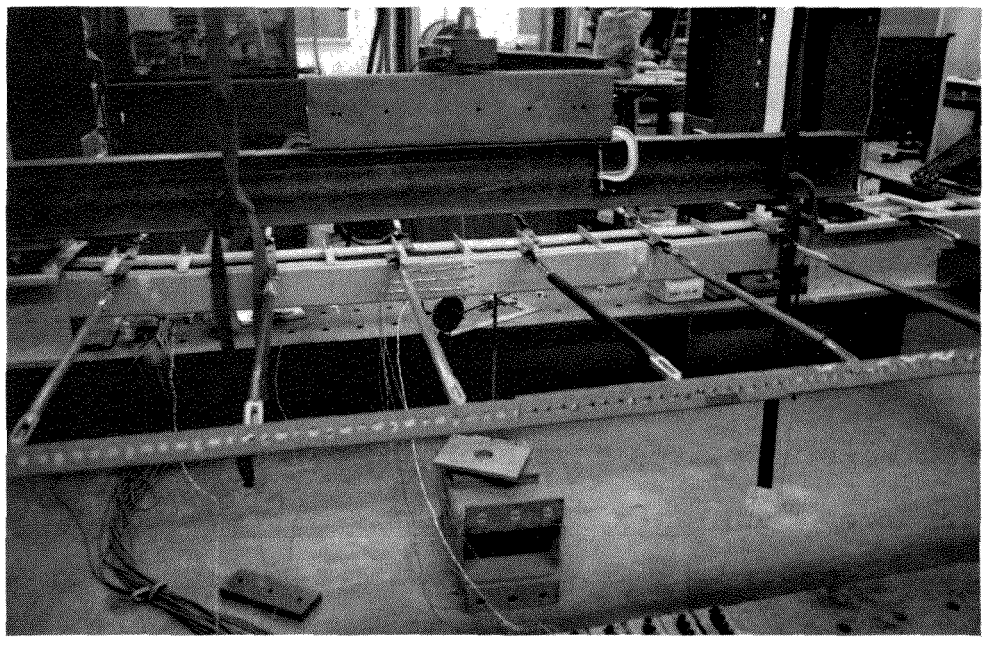

(a) Side view

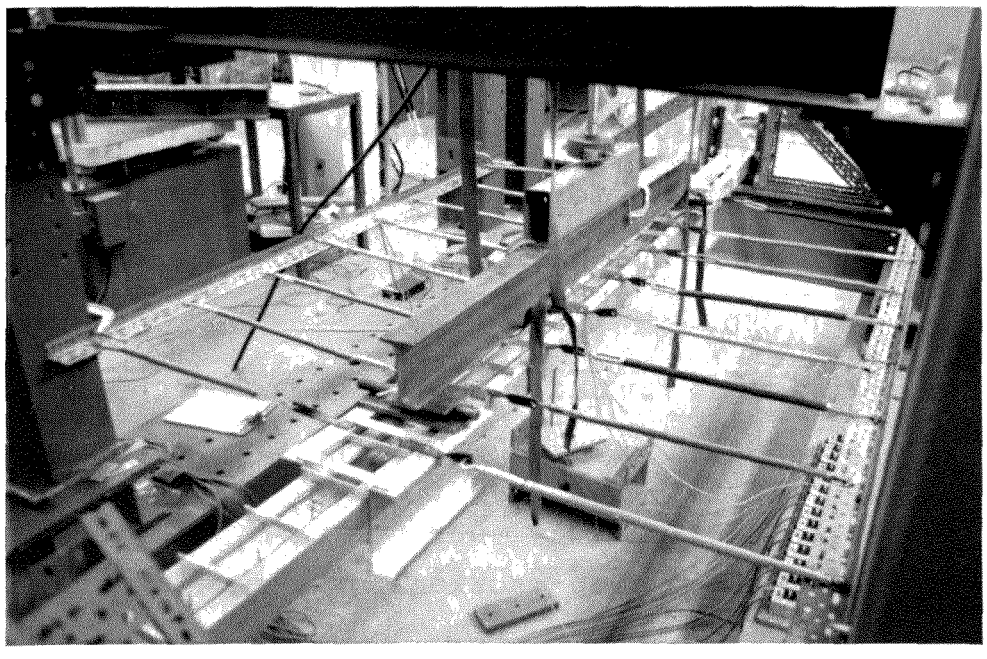

(b) Top view

Figure 10. Typical Bracing System

increased in increments until the beam reached failure and could no longer sustain additional load.

3. Test Results. The applied failure load, P, for each test specimen is recorded in Tables VII, VIII and IX. The value of P is the total load applied by the hydraulic jack at mid-span of the test specimen. The dead load due to the cross beam and bearing plates have been accounted for in the moment calculations. Tables X, XI and XII list the tested moment capacity, M_{ut}, for each test specimen, as well as the predicted moment capacity, M_{uc}, calculated according to Eqs. 1-10.

a. Test Sequence No. 1: A total of 15 tests were conducted in this test sequence. The cross-sectional dimensions, material properties and test results are summarized in Tables I, IV and VII, respectively. Table X compares the tested and calculated moment capacities.

The ratio of M_{ut}/M_{uc} for the 2.5 inch deep sections varied from 0.947 to 1.046 and has a mean of 0.995 and a standard deviation of 0.050.

The mean moment ratio for the 3.625 inch deep sections is 0.888 with a range of 0.864 to 0.920 and a standard deviation of 0.024.

For the 12 inch deep sections, the mean moment ratio, M_{ut}/M_{uc}, is 0.743. The moment ratio ranges from 0.679 to 0.814 with a standard deviation of 0.047.

b. Test Sequence No. 2: A total of 76 beam tests were completed in this test sequence. Twenty-nine beam tests were

TABLE X COMPARISON OF TEST RESULTS BASED ON 1986 AISI SPECIFICATION FOR BENDING TEST SPECIMENS (UMR TEST SEQUENCE No. 1)

Beam Specimen No.	h/t	a/h	w/h	M_{ut} (k-in.)	M_{uc} (k-in.)	$(M_{ut})/(M_{uc})$
2,16,1&2(H)	33.43	0.362	0.572	23.37	22.35	1.046
2,20,1&2(H)	53.92	0.357	0.575	11.85	12.51	0.947
2,20,3&4(H)	54.46	0.353	0.564	11.95	12.04	0.993
Mean						0.995
Standard Deviation						0.050
3,14,1&2(H)	41.77	0.466	0.364	75.17	82.30	0.913
3,14,3&4(H)	41.80	0.466	0.362	72.01	81.02	0.889
3,18,1&2(H)	74.99	0.455	0.354	29.32	33.93	0.864
3,18,3&4(H)	73.68	0.463	0.358	29.70	33.93	0.875
3,20,1&2(H)	74.42	0.458	0.353	29.31	33.84	0.866
3,20,3&4(H)	74.48	0.458	0.354	30.78	33.46	0.920
Mean						0.888
Standard Deviation						0.024
12,14,1&2(H)	118.01	0.130	0.100	219.52	323.42	0.679
12,14,3&4(H)	117.52	0.130	0.099	229.87	326.30	0.704
12,14,5&6(H)	117.77	0.130	0.097	243.37	323.64	0.752
12,14,7&8(H)	117.77	0.130	0.097	244.27	320.54	0.762
12,16,1&2(H)	209.87	0.130	0.099	135.97	181.89	0.748
12,16,3&4(H)	210.77	0.129	0.098	148.27	182.18	0.814
Mean						0.743
Standard Deviation						0.047

TABLE XI COMPARISON OF TEST RESULTS BASED ON 1986 AISI SPECIFICATION FOR BENDING TEST SPECIMENS (UMR TEST SEQUENCE No. 2)

Beam Specimen No.	h/t	a/h	w/h	M_{ut} (k-in.)	M_{uc} (k-in.)	$(M_{ut})/(M_{uc})$ (H), (T)[1]	$(M_{ut})/(M_{uc})$ (N)[2]
2B,16,1&2(H)	34.37	0.740	0.587	29.17	29.90	0.976	---
2B,16,3&4(H)	34.48	0.737	0.586	29.47	30.23	0.975	---
2B,16,1&2(N)	36.04	---	0.579	33.85	31.09	---	1.089
2B,16,3&4(N)	35.98	---	0.580	34.54	31.32	---	1.103
2B,20,1&2(H)	61.96	0.734	0.611	14.65	17.19	0.852	---
2B,20,3&4(H)	62.03	0.733	0.611	15.33	17.19	0.892	---
2B,20,1&2(N)	62.47	---	0.607	17.96	16.56	---	1.085
2B,20,3&4(N)	62.94	---	0.597	17.77	16.69	---	1.065
Mean						0.924	1.086
Standard Deviation						0.062	0.016
3B,14,1&2(H)	44.78	0.472	0.367	86.99	89.50	0.972	---
3B,14,3&4(H)	44.75	0.472	0.368	85.68	88.68	0.966	---
3B,18,1&2(H)	73.17	0.466	0.383	34.15	34.85	0.980	---
3B,18,3&4(H)	73.25	0.465	0.383	32.39	35.07	0.924	---
3B,18,1&2(N)	74.30	---	0.378	50.53	39.28	---	1.286
3B,18,3&4(N)	73.53	---	0.387	44.87	39.28	---	1.142
3B,20,1&2(H)	89.50	0.466	0.386	26.35	31.86	0.827	---
3B,20,3&4(H)	89.50	0.466	0.389	24.40	31.73	(0.769)	---
3B,20,5&6(H)	89.26	0.467	0.386	28.88	31.60	0.914	---
3B,20,1&2(T)	110.14	0.470	0.395	11.13	12.24	0.909	---
3B,20,3&4(T)	109.97	0.470	0.401	11.72	12.24	0.957	---
3B,20,1&2(N)	91.99	---	0.386	25.76	29.50	---	(0.873)
3B,20,3&4(N)	91.90	---	0.388	27.42	29.62	---	0.926
3B,20,5&6(N)	91.79	---	0.387	30.34	29.50	---	1.028
Mean						0.931	1.096
Mean						(0.913)*	(1.051)*
Standard Deviation						0.050	0.155
Standard Deviation						(0.072)*	(0.167)*

TABLE XI (CONTINUED) COMPARISON OF TEST RESULTS BASED ON 1986 AISI SPECIFICATION FOR BENDING TEST SPECIMENS (UMR TEST SEQUENCE No. 2)

Beam Specimen No.	h/t	a/h	w/h	M_{ut} (k-in.)	M_{uc} (k-in.)	$(M_{ut})/(M_{uc})$ (H), (T)[1]	(N)[2]
6B,18,1&2(H)	122.85	0.265	0.215	53.58	67.59	0.793	---
6B,18,3&4(H)	122.42	0.266	0.216	55.38	67.68	0.818	---
6C,18,1&2(H)	115.68	0.270	0.284	107.13	106.92	1.002	---
6C,18,3&4(H)	115.78	0.270	0.282	107.73	107.67	1.001	---
6D,18,1&2(H)	122.07	0.267	0.360	54.48	56.12	0.971	---
6D,18,3&4(H)	122.03	0.267	0.360	55.38	55.81	0.992	---
6B,20,1&2(H)	167.79	0.271	0.225	38.88	60.08	(0.647)	---
Mean						0.930	
Mean						(0.889)*	
Standard Deviation						0.097	
Standard Deviation						(0.139)*	
8A,14,1&2(H)	102.69	0.197	0.121	114.63	102.49	1.118	---
8A,14,3&4(H)	102.78	0.197	0.121	115.38	102.61	1.124	---
8A,14,5&6(H)	102.82	0.197	0.120	113.58	102.36	1.110	---
8A,14,7&8(H)	116.75	0.198	0.125	135.48	164.42	0.824	---
8A,14,9&10(H)	116.88	0.197	0.124	133.68	164.42	0.815	---
8A,14,1&2(N)	104.40	---	0.121	119.13	98.22	---	1.213
8A,14,3&4(N)	104.37	---	0.121	121.38	97.68	---	1.243
8A,14,5&6(N)	104.28	---	0.120	120.78	97.68	---	1.236
8A,14,7&8(N)	114.98	---	0.125	135.78	166.99	---	0.813
8A,14,9&10(N)	115.08	---	0.125	138.78	167.33	---	0.829
8B,14,1&2(T)	113.49	0.197	0.156	121.08	113.85	1.064	---
8B,14,3&4(T)	113.41	0.197	0.157	116.43	113.92	1.022	---
8B,14,5&6(T)	116.58	0.198	0.157	165.63	176.28	0.940	---
8B,14,7&8(T)	116.72	0.198	0.156	162.18	175.64	0.923	---
8B,14,1&2(N)	111.79	---	0.155	131.88	128.91	---	1.023
8B,14,3&4(N)	111.75	---	0.156	130.38	128.98	---	1.011
8B,14,5&6(N)	118.55	---	0.156	160.38	173.31	---	0.925
8B,14,7&8(N)	118.55	---	0.156	160.08	172.25	---	0.929
8D,14,1&2(T)	115.62	0.200	0.272	181.23	187.33	0.967	---
8D,14,3&4(T)	115.48	0.200	0.272	182.13	185.68	0.981	---
8D,14,1&2(N)	117.57	---	0.274	177.78	171.50	---	1.037
8D,14,3&4(N)	117.58	---	0.273	183.63	171.90	---	1.068
8B,18,1&2(H)	167.56	0.199	0.157	87.18	112.61	(0.774)	---
8[illegible],18,1&2(H)	165.17	0.197	0.267	67.38	63.01	1.069	---
8D,18,3&4(H)	165.12	0.197	0.268	59.58	62.52	0.953	---

TABLE XI (CONTINUED) COMPARISON OF TEST RESULTS BASED ON 1986 AISI SPECIFICATION FOR BENDING TEST SPECIMENS (UMR TEST SEQUENCE No. 2)

Beam Specimen No.	h/t	a/h	w/h	M_{ut} (k-in.)	M_{uc} (k-in.)	$(M_{ut})/(M_{uc})$ (H),(T)[1]	(N)[2]
8A,20,1&2(H)	243.71	0.199	0.133	34.53	40.28	0.857	---
8A,20,3&4(H)	243.50	0.199	0.133	33.93	40.89	0.830	---
8A,20,1&2(N)	243.65	---	0.133	36.03	40.64	---	0.887
8A,20,3&4(N)	243.89	---	0.132	36.48	40.56	---	0.899
8B,20,1&2(T)	244.97	0.198	0.166	45.48	53.46	0.851	---
8B,20,3&4(T)	244.58	0.198	0.165	45.48	53.37	0.852	---
8B,20,5&6(T)	244.24	0.198	0.165	47.13	53.28	0.885	---
8B,20,7&8(T)	244.27	0.198	0.166	45.78	53.28	0.859	---
8B,20,1&2(N)	244.85	---	0.167	47.58	51.77	---	0.919
8B,20,3&4(N)	244.50	---	0.166	47.58	51.69	---	0.920
8B,20,5&6(N)	244.42	---	0.165	47.13	51.69	---	0.912
8D,20,1&2(T)	175.38	0.199	0.275	80.58	83.93	0.960	---
8D,20,3&4(T)	175.40	0.199	0.273	82.38	83.62	0.985	---
8D,20,5&6(T)	175.51	0.199	0.275	82.38	85.57	0.963	---
8D,20,1&2(N)	175.48	---	0.275	84.18	83.46	---	1.009
8D,20,3&4(N)	175.51	---	0.274	82.38	83.15	---	0.991
Mean						0.952	0.992
Mean						(0.945)*	
Standard Deviation						0.100	0.129
Standard Deviation						(0.104)*	
12B,16,1&2(H)	192.02	0.130	0.104	198.93	255.17	0.780	---
12B,16,3&4(H)	192.81	0.130	0.103	197.52	248.50	0.795	---
12B,16,5&6(H)	192.20	0.130	0.103	195.93	251.17	0.780	---
12B,16,7&8(H)	192.26	0.130	0.103	204.33	249.23	0.820	---
12B,16,1&2(N)	185.61	---	0.103	199.38	264.18	---	0.755
12B,16,3&4(N)	186.05	---	0.103	207.03	262.83	---	0.788
Mean						0.794	0.772
Standard Deviation						0.019	0.023

[1] Web punchouts

[2] No web punchouts

* Statistics including test specimens with lower test to computed ratio given in ( )

TABLE XII COMPARISON OF TEST RESULTS BASED ON 1986 AISI SPECIFICATION FOR BENDING TEST SPECIMENS (SCHUSTER TEST SEQUENCE No. 3)

Beam Specimen No.	h/t	a/h	w/h	M_{ut} (k-in.)	M_{uc} (k-in.)	$(M_{ut})/(M_{uc})$ (H), (T)[1]	$(M_{ut})/(M_{uc})$ (N)[2]
BS1(N)	161.90	---	0.172	74.88	90.86	---	0.824
BS2(N)	161.90	---	0.172	76.21	90.86	---	0.839
BP4-40(H)	163.32	0.194	0.173	75.85	89.16	0.851	---
BP5-40(H)	163.32	0.194	0.173	73.64	89.16	0.826	---
BP6-40(H)	163.32	0.194	0.173	76.21	89.16	0.855	---
BP7-65(H)	163.32	0.322	0.168	75.23	89.08	0.845	---
BP8-65(H)	163.32	0.322	0.170	76.38	89.08	0.857	---
BP9-65(H)	163.32	0.322	0.173	76.21	89.16	0.855	---
CS1(N)	160.50	---	0.167	80.10	105.98	---	0.756
CS2(N)	160.91	---	0.167	80.10	105.98	---	0.756
CS3(N)	160.91	---	0.170	82.22	105.98	---	0.776
CP4-40(T)	161.90	0.220	0.167	82.84	104.86	0.790	---
CP5-40(T)	161.90	0.220	0.170	78.68	104.86	0.750	---
CP6-40(T)	162.72	0.219	0.172	83.37	104.17	0.800	---
CP7-65(T)	161.90	0.327	0.172	81.69	103.68	0.788	---
CP8-65(T)	162.31	0.326	0.169	81.78	104.86	0.780	---
CP9-65(T)	161.90	0.327	0.172	81.87	103.68	0.790	---
Mean						0.816	0.790
Standard Deviation						0.037	0.039

See Table XI for Notes

conducted for test specimens without web openings and 47 beam tests (32 for specimen type H and 15 for specimen type T) were performed for test specimens with web punchouts. The cross-sectional dimensions, material properties and test results are summarized in Tables II, V and VIII, respectively. Table XI

shows the comparison of the tested and calculated moment capacities.

The ratio of M_{ut}/M_{uc} for the 2.5 inch deep sections having web openings varied from 0.852 to 0.976, and has a mean of 0.924 and a standard deviation of 0.062. For those 2.5 inch specimens without web openings, the mean value of M_{ut}/M_{uc} is 1.086 with a standard deviation of 0.016.

For the 3.625 inch deep sections, the value of M_{ut}/M_{uc} ranges from 0.827 to 0.980 with a mean of 0.931 and a standard deviation of 0.050 for test specimens with web openings. For test specimens without web openings, the mean moment ratio is 1.096 with a standard deviation of 0.155.

The value of M_{ut}/M_{uc} varied from 0.647 to 1.002 and 0.774 to 1.069 for the 6 inch and 8 inch deep sections, respectively. The 6 inch deep web members has a mean moment ratio of 0.930 and a standard deviation of 0.097. For the 8 inch deep sections, the test specimens with web openings have a mean moment ratio of 0.952 and a standard deviation of 0.100. The test specimens without web openings have a mean moment ratio of 0.992 and a standard deviation of 0.129. The moment ratio showed no clear difference for the type H and type T specimens.

For the 12 inch deep sections, the ratio of M_{ut}/M_{uc} ranged from 0.755 to 0.788 with a mean of 0.772 and a standard deviation of 0.023 for unpunched webs, and ranged from 0.780 to 0.820 with a mean of 0.794 and a standard deviation of 0.019 for punched webs.

c. Test Sequence No. 3: A total of 17 beam tests were completed in test sequence No. 3 (47). There were 12 beam tests, 6 of each specimen type H and type T, for punched webs and 5 beam tests for unpunched webs. Tables III, VI and IX present the cross-sectional dimensions, material properties and test results, and Table XII presents the comparison of the tested and calculated moment capacities.

For the 8 inch deep sections (Table XII), the ratio of M_{ut}/M_{uc} ranged from 0.756 to 0.839 with a mean of 0.790 and a standard deviation of 0.039 for solid web specimens and ranged from 0.750 to 0.857 with a mean of 0.816 and a standard deviation of 0.037 for perforated web elements. The average moment ratio of specimen type T is lower than that of specimen type H.

4. Evaluation of Test Data. The moment ratio M_{ut}/M_{uc} is a measure of how well the AISI Specification for solid webs estimates the bending strength of C-shaped members with web openings. Tables X, XI and XII list the values of M_{ut}/M_{uc} for each test sequence. A discussion of the test results for three test sequences follows.

The results in test sequence Nos. 1 and 2 show that for the 2.5 inch sections, with an a/h ratio of 0.357, the presence of a web opening has little effect on the flexural strength of the member. However, for the 2.5 inch sections with an a/h ratio of 0.736 the flexural strength of the member is reduced about eight percent, and for the 3.625 inch sections with an a/h ratio of 0.465 the moment capacity is

reduced approximately nine percent. There is 2 percent deduction on moment capacity for 6 inch deep sections with an a/h ratio of 0.267. For 2.5 and 3.625 inch deep sections having a solid web, Table XI presents a mean value of M_{ut}/M_{uc} greater than 1.0. This indicates that the AISI Specification (1) adequately accounted for the local buckling behavior.

For the 6 inch web, the narrow flange (nominally 1.625 inch) test specimens, 6B, have low moment capacities; whereas for 6C and 6D having wider flanges (nominally 2.0 inch and 2.5 inch), the tested and computed moments show a good moment ratio between 0.971 and 1.002. The test results indicate that the narrow flange did not provide adequate edge restraint to the web. Therefore the flange-web interaction appears to have contributed to the low moment ratios.

From Table XI, the 8 inch deep webs did not have the same behavior as 6 inch webs. Some but not all of the 8A test specimens (nominally 1.5 inch) have high moment capacities, whereas for some but not all of the 8B test specimens (nominally 1.625 inch) have low moment capacities. Further analysis of this data will be discussed in a subsequent section of this report.

As indicated by Tables X and XI, for the 12 inch deep sections, there was no significant difference in the tested moment capacity between C-sections with and without web openings. The size of the web opening was small when compare to the depth of the beam web, the opening depth to flat beam depth ratio, a/h, was 0.13, and the failure did not

necessarily occur at the location of a web opening, whereas, the specimens with shallower webs failed by local buckling near a punchout. Figure 11 shows typical buckling failures. Therefore, the low mean moment ratios are not being attributed to the presence of punchouts for the 12 inch deep web.

The test results in Tables X, XI and XII show the AISI Specification overestimated the moment capacity for some of the sections having 6,8 and 12 inch deep webs. A premature web failure resulted from the compression flange undergoing distortional buckling. Therefore, the distortional mode of buckling rather than local buckling behavior controls the design for these test specimens. Because the slender web is unreinforced and lip stiffeners and flanges are small, the distortional buckling mode existed even though there were angles connecting the test specimens. The difference between local and distortional buckling mode is shown in Fig. 12.

5. Development of Modified Design Methods. The test specimens appear to have failed by either local or distortional buckling. The test data (Tables X, XI and XII) indicates that for certain geometries, the moment capacity predicted by the AISI Specification can not be achieved. Therefore, design modifications have been developed. Based on the test results and the analytical study for members having depths of 2.5 and 3.625 inches, failure by local buckling resulted. Three possible modified design methods are discussed in Section 5a for those test specimens governed by local buckling. This section deals with the design of beam

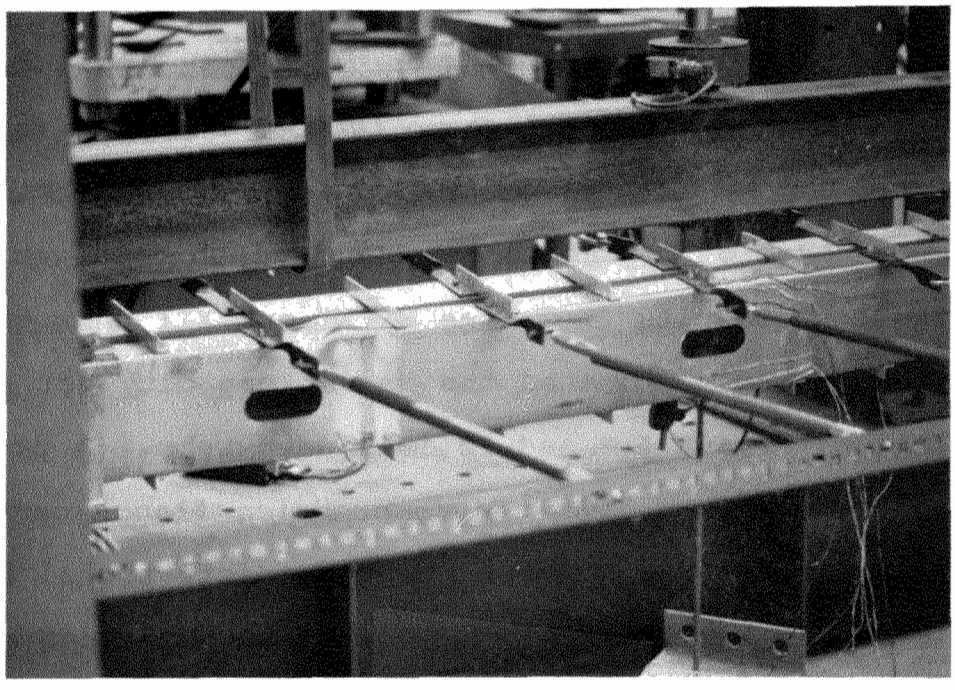

(a) Typical local buckling failure mode

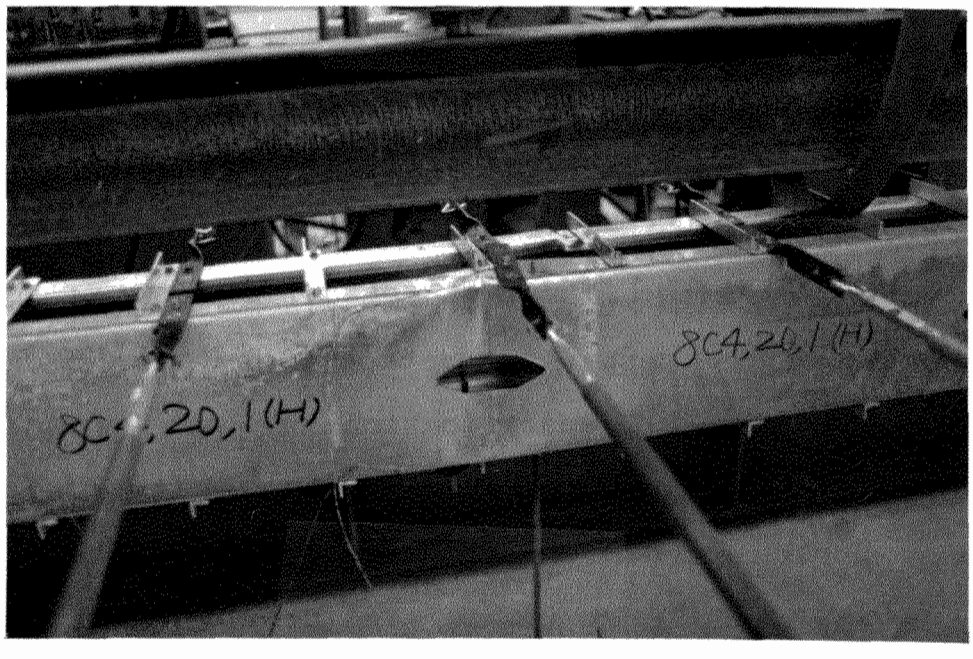

(b) Typical distortional buckling failure mode

Figure 11. Typical Bending Failure Pattern

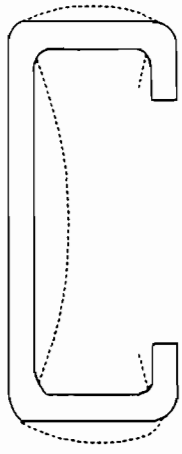

(a) Local buckling mode

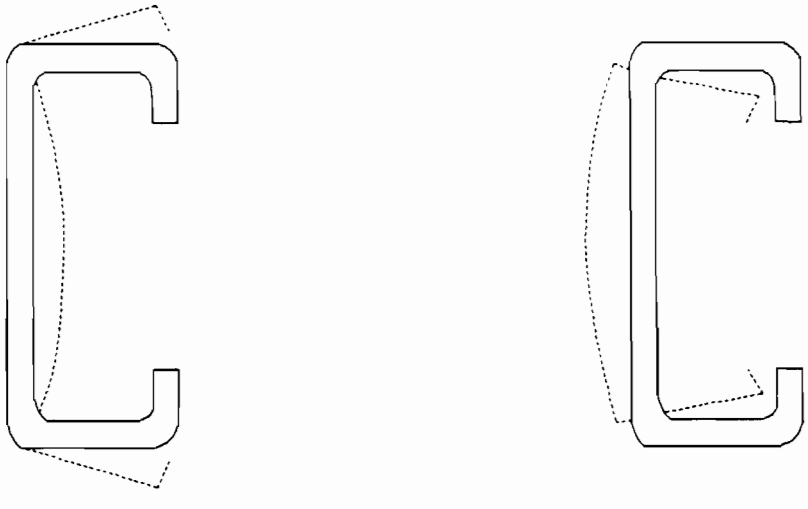

(b) Distortional buckling modes

Figure 12. Local and Distortional Buckling Modes for Compression members

webs using a modified effective web area method, a net section method and an effective net section method. For the 6, 8 and 12 inch deep sections distortional buckling appeared to be the governing limit state. Design approaches are proposed for consideration in Part 5b. These design approaches include an Australian model, a modified buckling load approach, a modified buckling coefficient approach and the Cornell method. The computed bending moments, according to each design approach, are compared with the available test moments.

a. Local Buckling. For test specimens that failed by local buckling and subsequent yielding, the test data (Tables X and XI) indicates that for certain geometries, the moment capacity predicted by the AISI Specification, Eqs. 1-10, can not be achieved. The presence of openings in the web element influenced the failure load, and resulted in low moment ratios. Therefore, three alternate techniques for computing the moment capacity have been examined.

(i). Method I - AISI formuli using modified effective web area: This method consists of reducing the effective section modulus based on the solid web by making a simple modification on the AISI effective width equations (Eqs. 1-10). In this method, the value of width b_2 (Fig. 1), is set to zero to account for the web opening. By only using width b_1 for the effective width of the compression portion of the web to determine the effective section modulus, S_{ufm}, the moment capacity, M_{ufm}, can be computed by the following equation:

$$M_{ufm} = S_{ufm} F_y \quad (52)$$

in which S_{ufm} is the effective section modulus evaluated at a yield stress, F_y, with b_2=0. Tables XIII and XIV show the results of this analysis.

TABLE XIII COMPARISON OF TEST RESULTS BASED ON 1986 AISI SPECIFICATION, b_2=0.0 FOR BEAM SPECIMENS HAVING LOCAL BUCKLING BEHAVIOR (UMR TEST SEQUENCE No. 1)

Beam Specimen No.	h/t	a/h	w/h	M_{ut} (k-in)	M_{ufm} (k-in)	$(M_{ut})/(M_{ufm})$
2,16,1&2(H)	33.43	0.362	0.572	23.37	17.02	1.373
2,20,1&2(H)	53.92	0.357	0.575	11.85	11.90	0.996
2,20,3&4(H)	54.46	0.353	0.564	11.95	11.90	1.004
Mean						1.124
Standard Deviation						0.215
3,14,1&2(H)	41.77	0.466	0.364	75.17	80.13	0.938
3,14,3&4(H)	41.80	0.466	0.362	72.01	75.90	0.949
3,18,1&2(H)	74.99	0.455	0.354	29.32	32.99	0.889
3,18,3&4(H)	73.68	0.463	0.358	29.70	32.90	0.903
3,20,1&2(H)	74.42	0.458	0.353	29.31	33.18	0.883
3,20,3&4(H)	74.48	0.458	0.354	30.78	31.58	0.975
Mean						0.923
Standard Deviation						0.037

Notes: M_{ut} = Tested moment capacities
M_{ufm} = Moment capacity based on 1986 AISI Specification, b_2=0.0

TABLE XIV COMPARISON OF TEST RESULTS BASED ON 1986 AISI SPECIFICATION, b_2=0.0 FOR BEAM SPECIMENS HAVING LOCAL BUCKLING BEHAVIOR (UMR TEST SEQUENCE No. 2)

Beam Specimen No.	h/t	a/h	w/h	M_{ut} (k-in)	M_{ufm} (k-in)	$(M_{ut})/(M_{ufm})$
2B,16,1&2(H)	34.37	0.740	0.587	29.17	28.35	1.029
2B,16,3&4(H)	34.48	0.737	0.586	29.47	28.61	1.030
2B,20,1&2(H)	61.96	0.734	0.611	14.65	16.34	0.897
2B,20,3&4(H)	62.03	0.733	0.611	15.33	16.33	0.939
Mean						0.974
Standard Deviation						0.067
3B,14,1&2(H)	44.78	0.472	0.367	86.99	87.00	1.000
3B,14,3&4(H)	44.75	0.472	0.368	85.68	83.27	1.029
3B,18,1&2(H)	73.17	0.466	0.383	34.15	33.36	1.024
3B,18,3&4(H)	73.25	0.465	0.383	32.39	33.07	0.979
3B,20,1&2(H)	89.50	0.466	0.386	26.35	29.14	0.904
3B,20,3&4(H)	89.50	0.466	0.389	24.40	29.04	(0.840)
3B,20,5&6(H)	89.26	0.467	0.386	28.88	28.98	0.997
3B,20,1&2(T)	110.14	0.470	0.395	11.13	12.00	0.923
3B,20,3&4(T)	109.97	0.470	0.401	11.72	12.00	0.976
Mean						0.979
Mean						(0.964)*
Standard Deviation						0.045
Standard Deviation						(0.062)*

See Table XIII for Notes

* Includes Beam Specimen No. 3B,20,3&4(H)

(ii). Method II - net section approach: Another approach to improve the computed strength for the test specimens having higher a/h ratios was developed based on the net section of the cross section. This method employs the net

section to compute the ultimate bending moment, M_{ufn}, determined by the following formula:

$$M_{ufn} = S_{ufn} F_y \quad (53)$$

The section modulus, S_{ufn}, was based on the net section considering the depth of the web opening. A typical net section is shown in Fig. 13. The results of computed ultimate bending moment, M_{ufn}, and an analysis of the ratios of M_{ut}/M_{ufn} are summarized in Tables XV and XVI.

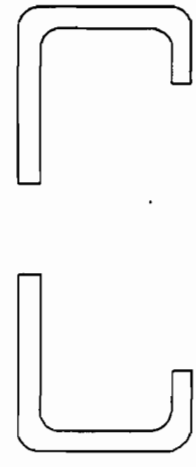

Figure 13. Net Section for Net Web Area

(iii). Method III - effective net section approach: The net section moment capacity (Method II), M_{ufn}, does not recognize the potential for a reduction in moment capacity that may occur due to local buckling of the web and flange. To account for local buckling and postbuckling strength, the effective width concept was used. The local buckling in the

TABLE XV COMPARISON OF TEST RESULTS BASED ON NET SECTION APPROACH FOR BEAM SPECIMENS HAVING LOCAL BUCKLING BEHAVIOR (UMR TEST SEQUENCE No. 1)

Beam Specimen No.	h/t	a/h	w/h	M_{ut} (k-in)	M_{ufn} (k-in)	$(M_{ut})/(M_{ufn})$
2,16,1&2(H)	33.43	0.362	0.572	23.37	22.05	1.060
2,20,1&2(H)	53.92	0.357	0.575	11.85	12.14	0.976
2,20,3&4(H)	54.46	0.353	0.564	11.95	11.65	1.026
Mean						1.021
Standard Deviation						0.042
3,14,1&2(H)	41.77	0.466	0.364	75.17	81.98	0.917
3,14,3&4(H)	41.80	0.466	0.362	72.01	73.42	0.981
3,18,1&2(H)	74.99	0.455	0.354	29.32	33.81	0.867
3,18,3&4(H)	73.68	0.463	0.358	29.70	33.77	0.879
3,20,1&2(H)	74.42	0.458	0.353	29.31	32.34	0.906
3,20,3&4(H)	74.48	0.458	0.354	30.78	34.08	0.903
Mean						0.909
Standard Deviation						0.040

Notes: M_{ut} = Tested moment capacities
M_{ufn} = Moment capacity based on the net section

TABLE XVI COMPARISON OF TEST RESULTS BASED ON NET SECTION APPROACH FOR BEAM SPECIMENS HAVING LOCAL BUCKLING BEHAVIOR (UMR TEST SEQUENCE No. 2)

Beam Specimen No.	h/t	a/h	w/h	M_{ut} (k-in)	M_{ufn} (k-in)	$(M_{ut})/(M_{ufn})$
2B,16,1&2(H)	34.37	0.740	0.587	29.17	27.09	1.077
2B,16,3&4(H)	34.48	0.737	0.586	29.47	27.45	1.074
2B,20,1&2(H)	61.96	0.734	0.611	14.65	13.52	1.084
2B,20,3&4(H)	62.03	0.733	0.611	15.33	13.50	1.136
Mean						1.093
Standard Deviation						0.029

TABLE XVI (CONTINUED) COMPARISON OF TEST RESULTS BASED ON NET SECTION APPROACH FOR BEAM SPECIMENS HAVING LOCAL BUCKLING BEHAVIOR (UMR TEST SEQUENCE No. 2)

Beam Specimen No.	h/t	a/h	w/h	M_{ut} (k-in)	M_{ufn} (k-in)	$(M_{ut})/(M_{ufn})$
3B,14,1&2(H)	44.78	0.472	0.367	86.99	88.82	0.979
3B,14,3&4(H)	44.75	0.472	0.368	85.68	84.77	1.011
3B,18,1&2(H)	73.17	0.466	0.383	34.15	33.79	1.011
3B,18,3&4(H)	73.25	0.465	0.383	32.39	33.48	0.967
3B,20,1&2(H)	89.50	0.466	0.386	26.35	30.06	0.877
3B,20,3&4(H)	89.50	0.466	0.389	24.40	30.11	(0.810)
3B,20,5&6(H)	89.26	0.467	0.386	28.88	29.94	0.965
3B,20,1&2(T)	110.14	0.470	0.395	11.13	10.05	1.107
3B,20,3&4(T)	109.97	0.470	0.401	11.72	10.05	1.166
Mean						1.010
Mean						(0.988)*
Standard Deviation						0.090
Standard Deviation						(0.107)*

See Table XV for Notes

* Includes Beam Specimen No. 3B,20,3&4(H)

flange was accounted for by using the current AISI effective width equations for edge stiffened compression elements. To reflect the influence of web local buckling, the portion of the web above the punchout was treated as an unstiffened compression element with the buckling coefficient taken as 0.43 (Fig. 14). In this approach, the computed moment capacity is determined by the following equation:

$$M_{uen} = S_{uen} F_y \qquad (54)$$

The effective net section modulus, S_{uen}, was based on the net section at the yield stress, F_y. For each test specimen, the

computed moment capacity, M_{uen}, and the ratio of test to computed moment, M_{ut}/M_{uen}, are given in Tables XVII and XVIII.

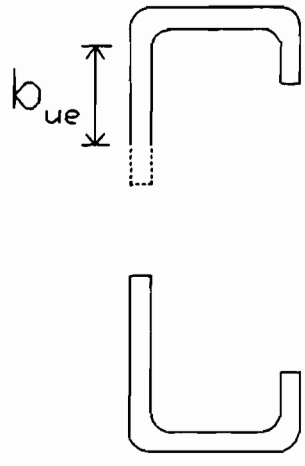

Figure 14. Net Section Using Unstiffened Compression Web Element

(iv). Comparison of tested and computed moment capacities based on Method I, Method II and Method III:

Based on an analysis of the three different methods, Table XIX summarizes the results of the comparison of the tested and computed moment capacities. The comparison of each method for the 22 test specimens that failed by local buckling are discussed in the following Section.

1. AISI Formuli Using Modified Effective Web Area Method: For test specimens having a/h ratios of approximately 0.267 and 0.357, the mean moment ratios for test sequence No. 1 and test sequence No. 2 are 1.011 and 1.124 (Table XIX), respectively.

TABLE XVII COMPARISON OF TEST RESULTS BASED ON EFFECTIVE NET SECTION APPROACH FOR BEAM SPECIMENS HAVING LOCAL BUCKLING BEHAVIOR (UMR TEST SEQUENCE No. 1)

Beam Specimen No.	h/t	a/h	w/h	M_{ut} (k-in)	M_{uen} (k-in)	$(M_{ut})/(M_{uen})$
2,16,1&2(H)	33.43	0.362	0.572	23.37	22.05	1.060
2,20,1&2(H)	53.92	0.357	0.575	11.85	11.97	0.990
2,20,3&4(H)	54.46	0.353	0.564	11.95	11.45	1.044
Mean						1.031
Standard Deviation						0.037
3,14,1&2(H)	41.77	0.466	0.364	75.17	81.02	0.928
3,14,3&4(H)	41.80	0.466	0.362	72.01	72.02	1.000
3,18,1&2(H)	74.99	0.455	0.354	29.32	32.29	0.908
3,18,3&4(H)	73.68	0.463	0.358	29.70	32.26	0.921
3,20,1&2(H)	74.42	0.458	0.353	29.31	30.79	0.952
3,20,3&4(H)	74.48	0.458	0.354	30.78	32.44	0.949
Mean						0.943
Standard Deviation						0.033

Notes: M_{ut} = Tested moment capacities
M_{uen} = Moment capacity based on effective net section

TABLE XVIII COMPARISON OF TEST RESULTS BASED ON EFFECTIVE NET SECTION APPROACH FOR BEAM SPECIMENS HAVING LOCAL BUCKLING BEHAVIOR (UMR TEST SEQUENCE No. 2)

Beam Specimen No.	h/t	a/h	w/h	M_{ut} (k-in)	M_{uen} (k-in)	$(M_{ut})/(M_{uen})$
2B,16,1&2(H)	34.37	0.740	0.587	29.17	26.87	1.086
2B,16,3&4(H)	34.48	0.737	0.586	29.47	27.30	1.079
2B,20,1&2(H)	61.96	0.734	0.611	14.65	13.52	1.084
2B,20,3&4(H)	62.03	0.733	0.611	15.33	13.50	1.136
Mean						1.096
Standard Deviation						0.027

TABLE XVIII (CONTINUED) COMPARISON OF TEST RESULTS BASED ON EFFECTIVE NET SECTION APPROACH FOR BEAM SPECIMENS HAVING LOCAL BUCKLING BEHAVIOR (UMR TEST SEQUENCE No. 2)

Beam Specimen No.	h/t	a/h	w/h	M_{ut} (k-in)	M_{uen} (k-in)	$(M_{ut})/(M_{uen})$
3B,14,1&2(H)	44.78	0.472	0.367	86.99	86.42	1.007
3B,14,3&4(H)	44.75	0.472	0.368	85.68	82.41	1.040
3B,18,1&2(H)	73.17	0.466	0.383	34.15	31.88	1.071
3B,18,3&4(H)	73.25	0.465	0.383	32.39	31.33	1.034
3B,20,1&2(H)	89.50	0.466	0.386	26.35	27.64	0.953
3B,20,3&4(H)	89.50	0.466	0.389	24.40	27.68	(0.882)
3B,20,5&6(H)	89.26	0.467	0.386	28.88	27.52	1.049
3B,20,1&2(T)	110.14	0.470	0.395	11.13	9.69	1.148
3B,20,3&4(T)	109.97	0.470	0.401	11.72	9.69	1.203
Mean						1.063
Mean						(1.043)*
Standard Deviation						0.079
Standard Deviation						(0.095)*

See Table XVII for Notes

* Includes Beam Specimen No. 3B,20,3&4(H)

For test specimens having an a/h ratio of about 0.465, the mean moment ratio without the b_2 =0 modification is 0.913 and with the modification is 0.955 (Table XIX).

For test specimens with an a/h ratio of approximately 0.736, the mean moment ratio is 0.924 without the b_2=0 modification, and 0.974 with a standard deviation of 0.067 when b_2 equals zero (Tables XI, XIV and XIX). This modification provides a slightly improved moment prediction.

Table XIX COMPARISON OF TESTED TO COMPUTED MOMENT CAPACITIES FOR BEAM SPECIMENS HAVING LOCAL BUCKLING BEHAVIOR (UMR TEST SEQUENCES Nos. 1 & 2)

	M(tested)/M(computed)					
	a/h=0.357		a/h=0.465		a/h=0.736	
	MEAN	STD	MEAN	STD	MEAN	STD
1986 AISI	0.995	0.050	0.913	0.046	0.924	0.062
Method I	1.124	0.215	0.955	0.049	0.974	0.067
Method II	1.021	0.042	0.967	0.088	1.093	0.029
Method III	1.031	0.037	1.012	0.087	1.096	0.027

Notes:

Method I: Based on Modified Effective Area (b_2=0)

Method II: Based on Net Section Approach

Method III: Based on Effective Net Section Approach

2. Net Section Approach: By using the net section approach, for test specimens having an a/h ratio of approximately 0.357 (Tables XV and XIX), the mean moment ratio was 1.021 with a standard deviation of 0.042.

For both test sequences, when the a/h ratio was about 0.465, the mean moment ratio is 0.967 (Table XIX). This method shows a 3.3 percent reduction in the accuracy of predicted moment capacity.

For test specimens having an a/h ratio of around 0.736, the mean moment ratio is 1.093 with a standard deviation of 0.029 (Tables XVI and XIX) using the net section, and 0.924 with a standard deviation of 0.062 (Tables XI and XIX) using the AISI Specification without any modification. For specimens with high a/h ratios, this moment modification provides a conservative moment prediction and a low standard deviation.

3. Effective Net Section Approach: By applying this method, for test specimens having a/h of approximately 0.357, the mean moment ratio, M_{ut}/M_{uen} is 1.031 with a standard deviation of 0.037 (Tables XVII and XIX) as compared to a mean of 0.995 with a standard deviation of 0.050 (Tables X and XIX) for the present AISI approach.

For both test sequences with a/h ratio of around 0.465, the mean value for the ratio of M_{ut}/M_{uen} is 1.012 with a standard deviation of 0.087 (Table XIX). With this moment modification, the mean moment increased from 0.913 to 1.012 (Table XIX).

For test specimens having an a/h ratio of around 0.736, the mean moment ratio is 1.096 with a standard deviation of 0.027 (Tables XVIII and XIX) using the effective net section approach, and 0.924 with a standard deviation of 0.062 (Tables XI and XIX) without any modification.

From the above discussion, it can be concluded that the current AISI Specification did not accurately estimate the bending strength for all of C-sections having a web punchout and by using the effective net section approach, good results were obtained for the ratio of the tested to computed ultimate bending capacities for test specimens that failed by local buckling.

b. Distortional Buckling. As previously discussed, the results in Tables X, XI and XII, based on the local buckling failure of the web, did not account for the distortional buckling effects. Distortional buckling will usually occur in the flange of channel sections if the flange and lip stiffener are inadequate to prevent movement normal to the plane of the flange. The distortional mode of buckling appears to have controlled the design for some test specimens, especially the sections with a 6, 8 and 12 inches deep web, and a small lip stiffener and flange. Four possible approaches incorporating the use of distortional mode of buckling to evaluate the computed moment have been investigated.

(i). Method I - Australian Model (39): The approach for computing $M_{uc,d}$ in this model is to use the effective width of web, flange and lip stiffener (Fig. 15) which account for

the distortional buckling behavior when calculating the ultimate moment. The effective section modulus, $S_{ex,d}$, is determined by using the effective width formula for the distortional buckling as given in Eqs. 39, 40 and 41, and the nominal elastic or inelastic distortional buckling stress, F_d, as given by Eqs. 31 and 32. The computed moment capacity was obtained from:

$$M_{uc,d} = S_{ex,d} F_d \qquad (55)$$

By using Eq. 33 for rotational stiffness and Eq. 55 for ultimate moment capacity, the moment capacity and the ratio of tested to computed moment capacity for each beam test specimen were calculated and tabulated in Tables XX, XXI and XXII. The analytical results in Tables XXIV, XXV and XXVI employ Eq. 34 (26,27) to account for the rotational restraint.

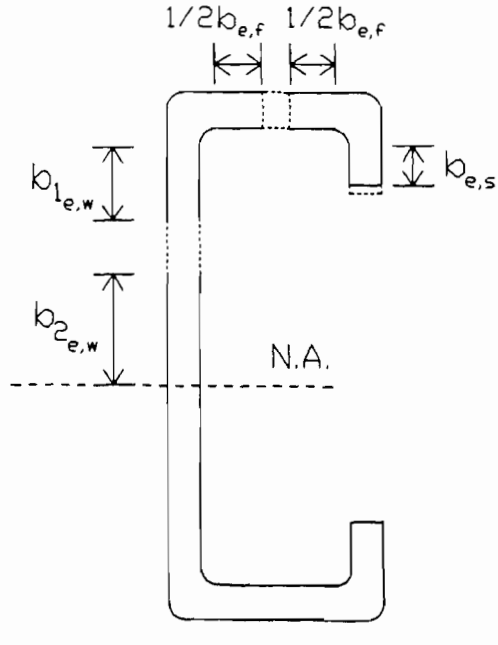

Figure 15. Australian Model for the Effective Elements

A summary of Tables XX, XXI and XXII is shown in Table XXIII. The summary indicates that the mean moment ratio $M_{ut}/M_{uc,d}$ is 0.824 for test sequence No. 1, 1.114 for test sequence No. 2, 1.109 for test sequence No. 3, and 1.078 when the three sequences are combined. Table XXVII summarizes the results of Tables XXIV, XXV and XXVI and presents that the test sequence No. 1 has a mean moment ratio of 0.796, test sequence No. 2 has a mean moment ratio of 1.026, test sequence No. 3 has a mean moment ratio of 1.034 and the combined three sequences has a mean moment ratio of 1.002. An examination of Tables XXIII and XXVII indicates that applying the values of rotational restraint, k_ϕ, in Eq. 33 is a slightly better method to predict the moment capacity.

For the test specimens having 12 inch web depth in test sequence No. 1, this model provides an unconservative prediction of the beam strength. There is a 26 percent reduction in the moment capacity when using the AISI Specification design provision (Tables XXIII and XXVII). When applying this model with different equations for rotational restraint, the moment ratio was 0.824 (Table XX) and 0.796 (Table XXIV). However, a 5 percent reduction (Table XXI) in moment capacity are shown for the 12 inch deep web specimen in test sequence No. 2 when Eq. 33 was applied for rotational stiffness. Note, the yield strengths were 60.64 and 61.61 ksi in test sequence No. 2, whereas F_y was 35.93 and 49.11 ksi in test sequence No. 1.

(ii). Method II - UMR modified distortional buckling load: A study was also undertaken to investigate the relationship between distortional buckling load (P_{cr}) and stiffness of rotational restraint (k_ϕ). According to the analysis summarized in Tables XXII and XXVII, the rotational restraint, k_ϕ, defined by Eqs. 33 and 34 are good expressions to define the distortional buckling behavior. Therefore, a possible design modification employing Eqs. 33 and 34 to compute the distortional buckling load has been developed.

TABLE XX COMPUTATION OF THE ULTIMATE MOMENT CAPACITY AND COMPARISON WITH TEST RESULTS FOR BEAM SPECIMENS HAVING DISTORTIONAL BUCKLING BEHAVIOR (UMR TEST SEQUENCE No. 1)

Beam Specimen No.	h/t	a/h	w/h	$(M_{ut})/(M_{uc,d})$ (1)	(2)*	(3)*	(4)
12,14,1&2(H)	118.01	0.130	0.100	0.679	0.750	0.755	0.899
12,14,3&4(H)	117.52	0.130	0.099	0.704	0.790	0.791	0.948
12,14,5&6(H)	117.77	0.130	0.097	0.752	0.833	0.837	1.000
12,14,7&8(H)	117.77	0.130	0.097	0.762	0.837	0.839	1.004
12,16,1&2(H)	209.87	0.130	0.099	0.748	0.818	0.934	0.836
12,16,3&4(H)	210.77	0.129	0.098	0.814	0.914	1.025	1.005
Mean				0.743	0.824	0.864	0.949
Standard Deviation				0.047	0.055	0.099	0.069

Notes:

(1): Based on 1986 AISI Specification

(2): Based on Method I - Australian Model

(3): Based on Method II - UMR Modified Distortional Buckling Load

(4): Based on Method III - Modified Buckling Coefficient

* Using Eq. 33 for rotational stiffness

TABLE XXI COMPUTATION OF THE ULTIMATE MOMENT CAPACITY AND COMPARISON WITH TEST RESULTS FOR BEAM SPECIMENS HAVING DISTORTIONAL BUCKLING BEHAVIOR (UMR TEST SEQUENCE No. 2)

Beam Specimen No.	h/t	a/h	w/h	$(M_{ut})/(M_{uc,d})$ (1)	(2)*	(3)*	(4)
6B,18,1&2(H)	122.85	0.265	0.215	0.793	1.117	0.975	0.917
6B,18,3&4(H)	122.42	0.266	0.216	0.818	1.151	1.007	0.945
8A,14,7&8(H)	116.75	0.198	0.125	0.824	1.071	0.996	1.030
8A,14,9&10(H)	116.88	0.197	0.124	0.815	1.058	0.981	1.019
8A,14,7&8(N)	114.98	---	0.125	0.813	1.055	0.986	1.004
8A,14,9&10(N)	115.08	---	0.125	0.829	1.079	1.004	1.031
8B,14,5&6(T)	116.58	0.198	0.157	0.940	1.251	1.180	1.114
8B,14,7&8(T)	116.72	0.198	0.156	0.923	1.225	1.156	1.101
8B,14,5&6(N)	118.55	---	0.156	0.925	1.235	1.164	1.103
8B,14,7&8(N)	118.55	---	0.156	0.929	1.233	1.169	1.086
8B,18,1&2(H)	167.56	0.199	0.157	0.774	1.156	1.037	0.802
8A,20,1&2(H)	243.71	0.199	0.133	0.857	1.051	1.008	1.017
8A,20,3&4(H)	243.50	0.199	0.133	0.830	1.025	0.979	0.985
8A,20,1&2(N)	243.65	---	0.133	0.887	1.080	1.052	1.053
8A,20,3&4(N)	243.89	---	0.132	0.899	1.079	1.070	0.980
8B,20,1&2(T)	244.97	0.198	0.166	0.851	1.195	1.191	0.958
8B,20,3&4(T)	244.58	0.198	0.165	0.852	1.202	1.193	0.961
8B,20,5&6(T)	244.24	0.198	0.165	0.885	1.242	1.235	0.997
8B,20,7&8(T)	244.27	0.198	0.166	0.859	1.201	1.200	0.967
8B,20,1&2(N)	244.85	---	0.167	0.919	1.260	1.265	1.039
8B,20,3&4(N)	244.50	---	0.166	0.920	1.263	1.263	1.041
8B,20,5&6(N)	244.42	---	0.165	0.912	1.253	1.249	1.031
12B,16,1&2(H)	192.02	0.130	0.104	0.780	0.957	1.044	0.946
12B,16,3&4(H)	192.81	0.130	0.103	0.795	0.966	1.042	0.961
12B,16,5&6(H)	192.20	0.130	0.103	0.780	0.951	1.030	0.943
12B,16,7&8(H)	192.26	0.130	0.103	0.820	0.985	1.082	0.991
12B,16,1&2(N)	185.61	---	0.103	0.755	0.902	0.982	0.879
12B,16,3&4(N)	186.05	---	0.103	0.788	0.945	1.021	0.956
Mean				0.849	1.114	1.091	0.995
Standard Deviation				0.056	0.114	0.100	0.069

See Table XX for Notes

TABLE XXII COMPUTATION OF THE ULTIMATE MOMENT CAPACITY AND COMPARISON WITH TEST RESULTS FOR BEAM SPECIMENS HAVING DISTORTIONAL BUCKLING BEHAVIOR (SCHUSTER TEST SEQUENCE No. 3)

Beam Specimen No.	h/t	a/h	w/h	$(M_{ut})/(M_{uc,d})$ (1)	(2)*	(3)*	(4)
BS1(N)	161.90	---	0.172	0.824	1.135	1.021	1.051
BS2(N)	161.90	---	0.172	0.839	1.155	1.039	1.070
BP4-40(H)	163.32	0.194	0.173	0.851	1.171	1.054	1.086
BP5-40(H)	163.32	0.194	0.173	0.826	1.137	1.023	1.054
BP6-40(H)	163.32	0.194	0.173	0.855	1.177	1.059	1.091
BP7-65(H)	163.32	0.322	0.168	0.845	1.160	1.053	1.084
BP8-65(H)	163.32	0.322	0.170	0.857	1.177	1.069	1.100
BP9-65(H)	163.32	0.322	0.173	0.855	1.177	1.059	1.091
CS1(N)	160.50	---	0.167	0.756	1.045	0.946	0.927
CS2(N)	160.91	---	0.167	0.756	1.045	0.946	0.927
CS3(N)	160.91	---	0.170	0.776	1.073	0.971	0.947
CP4-40(T)	161.90	0.220	0.167	0.790	1.083	0.977	0.962
CP5-40(T)	161.90	0.220	0.170	0.750	1.029	0.928	0.914
CP6-40(T)	162.72	0.219	0.172	0.800	1.080	0.975	0.962
CP7-65(T)	161.90	0.327	0.172	0.788	1.072	0.958	0.954
CP8-65(T)	162.31	0.326	0.169	0.780	1.069	0.964	0.950
CP9-65(T)	161.90	0.327	0.172	0.790	1.074	0.961	0.956
Mean				0.811	1.109	1.000	1.007
Standard Deviation				0.038	0.053	0.048	0.071

See Table XX for Notes

TABLE XXIII COMPARISON OF TESTED TO COMPUTED MOMENT CAPACITIES (BASED ON TABLES XX, XXI AND XXII)

	M(tested)/M(computed)							
	1986 AISI		Method I		Method II		Method III	
	MEAN	STD	MEAN	STD	MEAN	STD	MEAN	STD
UMR Test Sequence No. 1	0.743	0.047	0.824	0.055	0.864	0.099	0.949	0.069
UMR Test Sequence No. 2	0.849	0.056	1.114	0.114	1.091	0.100	0.995	0.069
SCHUSTER Test Sequence No. 3	0.811	0.038	1.109	0.053	1.000	0.048	1.007	0.071
Combined All Three Sequences	0.823	0.060	1.078	0.131	1.034	0.114	0.994	0.071

See Table XX for Notes

TABLE XXIV COMPUTATION OF THE ULTIMATE MOMENT CAPACITY AND COMPARISON WITH TEST RESULTS FOR BEAM SPECIMENS HAVING DISTORTIONAL BUCKLING BEHAVIOR (UMR TEST SEQUENCE No. 1)

Beam Specimen No.	h/t	a/h	w/h	$(M_{ut})/(M_{uc,d})$ (1)	(2)*	(3)*	(4)
12,14,1&2(H)	118.01	0.130	0.100	0.679	0.737	0.735	0.899
12,14,3&4(H)	117.52	0.130	0.099	0.704	0.776	0.770	0.948
12,14,5&6(H)	117.77	0.130	0.097	0.752	0.819	0.814	1.000
12,14,7&8(H)	117.77	0.130	0.097	0.762	0.823	0.817	1.004
12,16,1&2(H)	209.87	0.130	0.099	0.748	0.767	0.870	0.836
12,16,3&4(H)	210.77	0.129	0.098	0.814	0.855	0.964	1.005
Mean				0.743	0.796	0.828	0.949
Standard Deviation				0.047	0.043	0.081	0.069

Notes:

(1): Based on 1986 AISI Specification

(2): Based on Method I - Australian Model

(3): Based on Method II - UMR Modified Distortional Buckling Load

(4): Based on Method III - Modified Buckling Coefficient

* Using Eq. 34 for rotational stiffness

TABLE XXV COMPUTATION OF THE ULTIMATE MOMENT CAPACITY AND COMPARISON WITH TEST RESULTS FOR BEAM SPECIMENS HAVING DISTORTIONAL BUCKLING BEHAVIOR (UMR TEST SEQUENCE No. 2)

Beam Specimen No.	h/t	a/h	w/h	$(M_{ut})/(M_{uc,d})$ (1)	(2)*	(3)*	(4)
6B,18,1&2(H)	122.85	0.265	0.215	0.793	1.037	0.922	0.917
6B,18,3&4(H)	122.42	0.266	0.216	0.818	1.069	0.953	0.945
8A,14,7&8(H)	116.75	0.198	0.125	0.824	1.022	0.946	1.030
8A,14,9&10(H)	116.88	0.197	0.124	0.815	1.009	0.932	1.019
8A,14,7&8(N)	114.98	---	0.125	0.813	1.008	0.938	1.004
8A,14,9&10(N)	115.08	---	0.125	0.829	1.031	0.955	1.031
8B,14,5&6(T)	116.58	0.198	0.157	0.940	1.186	1.110	1.114
8B,14,7&8(T)	116.72	0.198	0.156	0.923	1.162	1.088	1.101
8B,14,5&6(N)	118.55	---	0.156	0.925	1.170	1.093	1.103
8B,14,7&8(N)	118.55	---	0.156	0.929	1.169	1.098	1.086
8B,18,1&2(H)	167.56	0.199	0.157	0.774	1.012	0.969	0.802
8A,20,1&2(H)	243.71	0.199	0.133	0.857	0.963	0.978	1.017
8A,20,3&4(H)	243.50	0.199	0.133	0.830	0.941	0.941	0.985
8A,20,1&2(N)	243.65	---	0.133	0.887	0.985	1.014	1.053
8A,20,3&4(N)	243.89	---	0.132	0.899	0.987	1.032	0.980
8B,20,1&2(T)	244.97	0.198	0.166	0.851	1.063	1.119	0.958
8B,20,3&4(T)	244.58	0.198	0.165	0.852	1.069	1.122	0.961
8B,20,5&6(T)	244.24	0.198	0.165	0.885	1.106	1.161	0.997
8B,20,7&8(T)	244.27	0.198	0.166	0.859	1.070	1.128	0.967
8B,20,1&2(N)	244.85	---	0.167	0.919	1.128	1.193	1.039
8B,20,3&4(N)	244.50	---	0.166	0.920	1.131	1.193	1.041
8B,20,5&6(N)	244.42	---	0.165	0.912	1.123	1.182	1.031
12B,16,1&2(H)	192.02	0.130	0.104	0.780	0.886	0.959	0.946
12B,16,3&4(H)	192.81	0.130	0.103	0.795	0.893	0.970	0.961
12B,16,5&6(H)	192.20	0.130	0.103	0.780	0.880	0.946	0.943
12B,16,7&8(H)	192.26	0.130	0.103	0.820	0.912	0.995	0.991
12B,16,1&2(N)	185.61	---	0.103	0.755	0.838	0.909	0.879
12B,16,3&4(N)	186.05	---	0.103	0.788	0.877	0.957	0.956
Mean				0.849	1.026	1.023	0.995
Standard Deviation				0.056	0.101	0.090	0.069

See Table XXIV for Notes

TABLE XXVI COMPUTATION OF THE ULTIMATE MOMENT CAPACITY AND COMPARISON WITH TEST RESULTS FOR BEAM SPECIMENS HAVING DISTORTIONAL BUCKLING BEHAVIOR (SCHUSTER TEST SEQUENCE No. 3)

Beam Specimen No.	h/t	a/h	w/h	$(M_{ut})/(M_{uc,d})$ (1)	(2)*	(3)*	(4)
BS1(N)	161.90	---	0.172	0.824	1.064	0.962	1.051
BS2(N)	161.90	---	0.172	0.839	1.083	0.979	1.070
BP4-40(H)	163.32	0.194	0.173	0.851	1.098	0.993	1.086
BP5-40(H)	163.32	0.194	0.173	0.826	1.066	0.964	1.054
BP6-40(H)	163.32	0.194	0.173	0.855	1.103	0.997	1.091
BP7-65(H)	163.32	0.322	0.168	0.845	1.089	0.993	1.084
BP8-65(H)	163.32	0.322	0.170	0.857	1.106	1.009	1.100
BP9-65(H)	163.32	0.322	0.173	0.855	1.103	0.997	1.091
CS1(N)	160.50	---	0.167	0.756	0.971	0.876	0.927
CS2(N)	160.91	---	0.167	0.756	0.971	0.876	0.927
CS3(N)	160.91	---	0.170	0.776	0.997	0.899	0.947
CP4-40(T)	161.90	0.220	0.167	0.790	1.004	0.902	0.962
CP5-40(T)	161.90	0.220	0.170	0.750	0.954	0.857	0.914
CP6-40(T)	162.72	0.219	0.172	0.800	1.001	0.906	0.962
CP7-65(T)	161.90	0.327	0.172	0.788	0.991	0.883	0.954
CP8-65(T)	162.31	0.326	0.169	0.780	0.991	0.891	0.950
CP9-65(T)	161.90	0.327	0.172	0.790	0.993	0.885	0.956
Mean				0.811	1.034	0.933	1.007
Standard Deviation				0.038	0.055	0.054	0.071

See Table XXIV for Notes

TABLE XXVII COMPARISON OF TESTED TO COMPUTED MOMENT CAPACITIES
(BASED ON TABLES XXIV, XXV AND XXVI)

	M(tested)/M(computed)							
	1986 AISI		Method I		Method II		Method III	
	MEAN	STD	MEAN	STD	MEAN	STD	MEAN	STD
UMR Test Sequence No. 1	0.743	0.047	0.796	0.043	0.828	0.081	0.949	0.069
UMR Test Sequence No. 2	0.849	0.056	1.026	0.101	1.023	0.090	0.995	0.069
SCHUSTER Test Sequence No. 3	0.811	0.038	1.034	0.055	0.933	0.054	1.007	0.071
Combined All Three Sequences	0.823	0.060	1.002	0.111	0.973	0.105	0.994	0.071

See Table XXIV for Notes

Based on the regression analysis, the following simplified relationships were derived:

when $k_\phi = Et^3/(5.46b_w)$:

$$P_{cr} = 45.945k_\phi + 1.057 \quad (56)$$

when $k_\phi = Et^3/(4.00b_w)$:

$$P_{cr} = 38.527k_\phi + 1.341 \quad (57)$$

where P_{cr} = The distortional buckling load for the gross section area of the flange and edge stiffener as defined by model A

k_ϕ = The stiffness of rotational restraint

E = Modulus of elasticity of steel

The ultimate moment capacity, $M_{uc,d}$, was computed by using the effective width equations of the AISI Specification with the yield stress replaced by modified distortional buckling stress expressed as followings:

$$M_{uc,d} = F_{d,p}\, S_{ex,p} \quad (58)$$

where $\sigma_d = P_{cr}/A$

P_{cr} = Eqs. 56 or 57

A = The gross section area of the flange and edge stiffener

$F_{d,p}$ = Eqs. 31 or 32

$S_{ex,p}$ = Effective section modulus using AISI effective width equations evaluated at $F_{d,p}$

The computed moment capacities based on Eqs. 33, 34 and 58 are shown in the column No. 3 of Tables XX, XXI, XXII, XXIV, XXV and XXVI, respectively.

Tables XXIII and XXVII show the comparison of the test moment and computed moment based on the Eqs. 33, 34 and 58. A review of Tables XX, XXI, XXII, XXIV, XXV and XXVI indicates a range of $M_{ut}/M_{uc,d}$ ratios from 0.755 to 1.265 with an average of 1.034 and a standard deviation of 0.114, and 0.735 to 1.193 with an average of 0.973 and a standard deviation of 0.105, for the different conditions of rotational stiffness.

Even though Eqs. 33, 34 and 58 provide an acceptable mean estimate of the moment capacity, some of the test specimens in test sequence No. 1 still have low moment ratios.

(iii). Method III - modified buckling coefficient: Because of the complicated calculation for distortional buckling behavior (Eqs. 29 and 29a to 29i), an investigation was undertaken to modify the effective width equations of the AISI Specification. The intent was to derive an appropriate web buckling coefficient that will reflect the distortional buckling behavior or mixed local-distortional buckling behavior. From Section B2 of the AISI Specification, the web buckling coefficient, k, is calculated as follow:

$$k = 4+2(1-\psi)^3+2(1-\psi) \tag{59}$$

$$\psi = \frac{f_2}{f_1} \tag{60}$$

where f_2 and f_1 are calculated on the basis of the effective section (Fig. 1). Equations 59 and 60 were developed to illustrate the local buckling behavior of the C-sections, and do not reflect the distortional buckling behavior. Based on

an analysis of the test data, the web buckling coefficient for distortional buckling varied from 0.26 to 11.80. This compares to a web local buckling coefficient of 20 to 24. Based on a regression analysis, the web distortional buckling coefficient, k, may be represented by the following equations:

$$k = 0.008(h/t)+17000(w/h)(F_y/E) \quad (61)$$

where w = The flat width of flange

h = The flat width of web

t = Thickness

F_y = Yield stress

E = Modulus of elasticity of steel

Equation 61 shows the correlation between buckling coefficient, k, and the ratios of flat width of web to thickness, and flat widths of flange and web. A close examination of Eq. 24 indicates that the primary parameters effecting distortional buckling behavior are the ratios of h/t and w/h, and the yielding stress of material. It seems reasonable that there is some correlation between the web slenderness, and the flat widths of flange and web when the test specimens undergo a mode of distortional buckling.

For each test specimen, the computed moment capacity was evaluated by using the following equation:

$$M_{uc,d} = F_y S_{ex,Fk} \quad (62)$$

where $S_{ex,Fk}$ is the effective section modulus evaluated at F_y using proposed web buckling coefficient (Eq. 61).

Based on Eq. 62, the three test sequences have good correlation between tested and computed ultimate bending

moment. A study of Tables XX, XXI and XXII reveals that satisfactory results were obtained for the tested and computed moment capacities having a mean value of 0.949 for test sequence No. 1, 0.995 for test sequence No. 2, 1.007 for test sequence No. 3 and 0.994 for the three test sequences. The standard deviations are 0.069, 0.069, 0.071 and 0.071 with respect to test sequence No. 1, 2, 3 and the combination of the three sequences. This modified web buckling coefficient not only has improved the moment ratios in test sequence No. 1 which was not achieved by using Method I and Method II, but also provided a good moment ratios range from 0.899 to 1.114 in the three sequences.

(iv). Method IV - Cornell Method: When applying Eq. 47 to compute the elastic distortional buckling ($F_{cr,d}$) and Eq. 50 to determine the ultimate moment ($M_{uc,d}$), all three sequences have a very conservative ratio of $M_{ut}/M_{uc,d}$ as shown in Tables XXVIII, XXIX and XXX. The Cornell model which described the distortional buckling as overall buckling and local-overall buckling interaction is good for the behavior of panel members with a stable tension flange to prevent lateral movement. But for the tests in these three sequences, the model proposed by Hancock, which characterizes the distortional buckling as an interaction between local and lateral buckling can provide a better prediction of the strength of beam members.

TABLE XXVIII COMPUTATION OF THE ULTIMATE MOMENT CAPACITY USING MODIFIED EQUATIONS IN MODEL B AND COMPARISON WITH TEST RESULTS FOR BEAM SPECIMENS HAVING DISTORTIONAL BUCKLING BEHAVIOR (UMR TEST SEQUENCE No. 1)

Beam Specimen No.	M_{ut}	$M_{uc,d}$	$M_{ut}/M_{uc,d}$
12,14,1&2(H)	219.52	215.74	1.018
12,14,3&4(H)	229.87	217.18	1.058
12,14,5&6(H)	243.37	243.54	0.999
12,14,7&8(H)	244.27	243.54	1.003
12,16,1&2(H)	135.97	21.19	6.417
12,16,3&4(H)	148.27	19.56	7.580
Mean			3.013
Standard Deviation			3.109

Note: $M_{uc,d}$ = Moment capacity based on Method IV -- Cornell Method

c. Predicted Moments. An investigation was also undertaken to develop a technique for distinguishing between local buckling and distortional buckling behavior. Based on the moment ratios from Tables X, XI and XII, the following criteria was developed:

(i) If the specimen has the ratio of web opening depth to web depth (a/h) located between 0.35 and 0.74, the value of M_{Rp} can be obtained from the following Eq. 63. If M_{Rp} in Eq. 63 is less than 1.0, local buckling controls and the effective net section approach can be employed to account for the local buckling due to the present of web openings.

TABLE XXIX COMPUTATION OF THE ULTIMATE MOMENT CAPACITY USING MODIFIED EQUATIONS IN MODEL B AND COMPARISON WITH TEST RESULTS FOR BEAM SPECIMENS HAVING DISTORTIONAL BUCKLING BEHAVIOR (UMR TEST SEQUENCE No. 2)

Beam Specimen No.	M_{ut}	$M_{uc,d}$	$M_{ut}/M_{uc,d}$
6B,18,1&2(H)	53.58	42.04	1.275
6B,18,3&4(H)	55.38	42.27	1.310
6B,20,1&2(H)	38.88	6.18	6.291
8A,14,7&8(H)	135.48	92.91	1.458
8A,14,9&10(H)	133.68	92.64	1.443
8A,14,7&8(N)	135.78	98.18	1.383
8A,14,9&10(N)	138.78	103.38	1.342
8B,14,5&6(T)	165.63	102.11	1.622
8B,14,7&8(T)	162.18	101.57	1.597
8B,14,5&6(N)	160.38	96.12	1.668
8B,14,7&8(N)	160.08	95.34	1.679
8B,18,1&2(H)	87.18	14.11	6.177
8A,20,1&2(H)	34.53	5.59	6.181
8A,20,3&4(H)	33.93	5.75	5.905
8A,20,1&2(N)	36.03	5.28	6.826
8A,20,3&4(N)	36.48	5.37	6.796
8B,20,1&2(T)	45.48	7.61	5.974
8B,20,3&4(T)	45.48	7.61	5.980
8B,20,5&6(T)	47.13	7.56	6.237
8B,20,7&8(T)	45.78	7.60	6.020
8B,20,1&2(N)	47.58	7.89	6.033
8B,20,3&4(N)	47.58	7.83	6.074
8B,20,5&6(N)	47.13	7.75	6.080
12B,16,1&2(H)	198.93	25.26	7.875
12B,16,3&4(H)	197.52	24.17	8.174
12B,16,5&6(H)	195.93	24.46	8.009
12B,16,7&8(H)	204.33	24.34	8.395
12B,16,1&2(N)	199.38	26.70	7.468
12B,16,3&4(N)	207.03	26.50	7.813
Mean			4.899
Standard Deviation			2.705

See Table XXVIII for Notes

TABLE XXX COMPUTATION OF THE ULTIMATE MOMENT CAPACITY USING MODIFIED EQUATIONS IN MODEL B AND COMPARISON WITH TEST RESULTS FOR BEAM SPECIMENS HAVING DISTORTIONAL BUCKLING BEHAVIOR (SCHUSTER TEST SEQUENCE No. 3)

Beam Specimen No.	M_{ut}	$M_{uc,d}$	$M_{ut}/M_{uc,d}$
BS1(N)	74.88	31.02	2.414
BS2(N)	76.21	31.02	2.457
BP4-40(H)	75.85	30.25	2.507
BP4-50(H)	73.64	30.25	2.434
BP4-60(H)	76.21	30.25	2.519
BP7-65(H)	75.23	30.07	2.502
BP8-65(H)	76.38	29.97	2.549
BP9-65(H)	76.21	30.25	2.519
CS1(N)	80.10	26.90	2.977
CS2(N)	80.10	26.90	2.977
CS3(N)	82.22	26.91	3.055
CP4-40(T)	82.84	25.39	3.262
CP5-40(T)	78.68	25.39	3.098
CP6-40(T)	83.37	25.10	3.322
CP7-65(T)	81.69	25.33	3.225
CP8-65(T)	81.78	25.46	3.212
CP9-65(T)	81.87	25.33	3.232
Mean			2.839
Standard Deviation			0.354

See Table XXVIII for Notes

when $0.35 \leq a/h < 0.74$:

$$M_{Rp} = [2.373(a/h)-1.100]^3-[(0.919(a/h)-1.331] \quad (63)$$

(ii) If the specimen has an a/h ratio which is not in the range from 0.35 to 0.74, or a w/h ratio which is less than 0.35 for a solid web, Eqs. 64 or 65 can be used to compute the M_{Rp}.

when $w/h < 0.25$:

$$M_{Rp} = -54.487(w/h-0.142)^2+1.109 \quad (64)$$

when $0.25 \leq w/h < 0.35$:

$$M_{Rp} = -11.652(w/h-0.300)^2+1.0967 \quad (65)$$

Equations 64 and 65 indicate that if M_{Rp} is greater than 1.0, then local buckling controls the design and the present AISI Specification can provide an adequate prediction. If M_{Rp} is less than 1.0, the distortional buckling or the interaction of local and distortional buckling governs the design and the previously discussed methods relating to the distortional mode of buckling can be used to predict the bending strength.

(iii) If a solid web cross section having a w/h ratio which is greater than 0.35, the local buckling controls the design and the current AISI Specification equations can predict the moment capacity accurately.

The predicted moment ratios, M_{Rp}, which serve as the basis for Eqs. 63, 64 and 65 are presented in Tables XXXI, XXXII and XXXIII.

TABLE XXXI COMPARISON OF TESTED TO COMPUTED ULTIMATE BENDING MOMENTS AND PERDICTED VALUES OF MOMENT RATIOS (UMR TEST SEQUENCE No. 1)

Beam Specimen No.	h/t	a/h	w/h	M_{Rr}	M_{Rp}
2,16,1&2(H)	33.43	0.362	0.572	1.046	0.985
2,20,1&2(H)	53.92	0.357	0.575	0.947	0.987
2,20,3&4(H)	54.46	0.353	0.564	0.993	0.989
3,14,1&2(H)	41.77	0.466	0.364	0.913	0.903
3,14,3&4(H)	41.80	0.466	0.362	0.889	0.903
3,18,1&2(H)	74.99	0.455	0.354	0.864	0.914
3,18,3&4(H)	73.68	0.463	0.358	0.875	0.906
3,20,1&2(H)	74.42	0.458	0.353	0.866	0.911
3,20,3&4(H)	74.48	0.458	0.354	0.920	0.911
12,14,1&2(H)	118.01	0.130	0.100	0.679	0.899
12,14,3&4(H)	117.52	0.130	0.099	0.704	0.893
12,14,5&6(H)	117.77	0.130	0.097	0.752	0.865
12,14,7&8(H)	117.77	0.130	0.097	0.762	0.865
12,16,1&2(H)	209.87	0.130	0.099	0.748	0.760
12,16,3&4(H)	210.77	0.129	0.098	0.814	0.755

Notes:

$M_{Rr} = (M_{ut}/M_{uc})$

M_{Rp} = Predicted values of the tested to computed moment capacities, based on the Eqs. 63, 64 and 65

TABLE XXXII COMPARISON OF TESTED TO COMPUTED ULTIMATE BENDING MOMENTS AND PREDICTED VALUES OF MOMENT RATIOS (UMR TEST SEQUENCE No. 2)

Beam Specimen No.	h/t	a/h	w/h	M_{Rr}	M_{Rp}
2B,16,1&2(H)	34.37	0.740	0.587	0.976	0.932
2B,16,3&4(H)	34.48	0.737	0.586	0.975	0.928
2B,20,1&2(H)	61.96	0.734	0.611	0.852	0.920
2B,20,3&4(H)	62.03	0.733	0.611	0.892	0.919
3B,14,1&2(H)	44.78	0.472	0.367	0.972	0.898
3B,14,3&4(H)	44.75	0.472	0.368	0.966	0.898
3B,18,1&2(H)	73.17	0.466	0.383	0.980	0.903
3B,18,3&4(H)	73.25	0.465	0.383	0.924	0.904
3B,20,1&2(H)	89.50	0.466	0.386	0.827	0.903
3B,20,3&4(H)	89.50	0.466	0.389	0.769	0.903
3B,20,5&6(H)	89.26	0.467	0.386	0.914	0.903
3B,20,1&2(T)	110.14	0.470	0.395	0.909	0.900
3B,20,3&4(T)	109.97	0.470	0.401	0.957	0.899
6B,18,1&2(H)	122.85	0.265	0.215	0.793	0.678
6B,18,3&4(H)	122.42	0.266	0.216	0.818	0.675
6C,18,1&2(H)	115.68	0.270	0.284	1.002	1.007
6C,18,3&4(H)	115.78	0.270	0.282	1.001	1.006
6D,18,1&2(H)	122.07	0.267	0.360	0.971	0.985
6D,18,3&4(H)	122.03	0.267	0.360	0.992	0.985
6B,20,1&2(H)	167.79	0.271	0.225	(0.647)	(0.734)
8A,14,1&2(H)	102.69	0.197	0.121	1.118	1.007
8A,14,3&4(H)	102.78	0.197	0.121	1.124	1.008
8A,14,5&6(H)	102.82	0.197	0.120	1.110	1.006
8A,14,7&8(H)	116.75	0.198	0.125	0.824	0.934
8A,14,9&10(H)	116.88	0.197	0.124	0.815	0.932
8A,14,1&2(N)	104.40	---	0.121	1.213	1.010
8A,14,3&4(N)	104.37	---	0.121	1.243	1.009
8A,14,5&6(N)	104.28	---	0.120	1.236	1.008
8A,14,7&8(N)	114.98	---	0.125	0.813	0.938
8A,14,9&10(N)	115.08	---	0.125	0.829	0.937
8B,14,1&2(T)	113.49	0.197	0.156	1.064	1.008
8B,14,3&4(T)	113.41	0.197	0.157	1.022	1.007
8B,14,5&6(T)	116.58	0.198	0.157	0.940	0.947
8B,14,7&8(T)	116.72	0.198	0.156	0.923	0.948

TABLE XXXII (CONTINUED) COMPARISON OF TESTED TO COMPUTED ULTIMATE BENDING MOMENTS AND PREDICTED VALUES OF MOMENT RATIOS (UMR TEST SEQUENCE No. 2)

Beam Specimen No.	h/t	a/h	w/h	M_{Rr}	M_{Rp}
8B,14,1&2(N)	111.79	---	0.155	1.023	1.000
8B,14,3&4(N)	111.75	---	0.156	1.011	1.000
8B,14,5&6(N)	118.55	---	0.156	0.925	0.945
8B,14,7&8(N)	118.55	---	0.156	0.929	0.945
8D,14,1&2(T)	115.62	0.200	0.272	0.967	1.016
8D,14,3&4(T)	115.48	0.200	0.272	0.981	1.016
8D,14,1&2(N)	117.57	---	0.274	1.037	1.020
8D,14,3&4(N)	117.58	---	0.273	1.068	1.019
8B,18,1&2(H)	167.56	0.199	0.157	(0.774)	(0.804)
8D,18,1&2(H)	165.17	0.197	0.267	1.069	1.030
8D,18,3&4(H)	165.12	0.197	0.268	0.953	1.031
8A,20,1&2(H)	243.71	0.199	0.133	0.857	0.880
8A,20,3&4(H)	243.50	0.199	0.133	0.830	0.880
8A,20,1&2(N)	243.65	---	0.133	0.887	0.870
8A,20,3&4(N)	243.89	---	0.132	0.899	0.869
8B,20,1&2(T)	244.97	0.198	0.166	0.851	0.812
8B,20,3&4(T)	244.58	0.198	0.165	0.852	0.814
8B,20,5&6(T)	244.24	0.198	0.165	0.885	0.814
8B,20,7&8(T)	244.27	0.198	0.166	0.859	0.813
8B,20,1&2(N)	244.85	---	0.167	0.919	0.820
8B,20,3&4(N)	244.50	---	0.166	0.920	0.822
8B,20,5&6(N)	244.42	---	0.165	0.912	0.825
8D,20,1&2(T)	175.38	0.199	0.275	0.960	1.015
8D,20,3&4(T)	175.40	0.199	0.273	0.985	1.014
8D,20,5&6(T)	175.51	0.199	0.275	0.963	1.015
8D,20,1&2(N)	175.48	---	0.275	1.009	1.015
8D,20,3&4(N)	175.51	---	0.274	0.991	1.014
12B,16,1&2(H)	192.02	0.130	0.104	0.780	0.747
12B,16,3&4(H)	192.81	0.130	0.103	0.795	0.744
12B,16,5&6(H)	192.20	0.130	0.103	0.780	0.745
12B,16,7&8(H)	192.26	0.130	0.103	0.820	0.745
12B,16,1&2(N)	185.61	---	0.103	0.755	0.750
12B,16,3&4(N)	186.05	---	0.103	0.788	0.749

See Table XXXI for Notes

TABLE XXXIII COMPARISON OF TESTED TO COMPUTED ULTIMATE BENDING MOMENTS AND PREDICTED VALVES OF MOMENT RATIOS (SCHUSTER TEST SEQUENCE No. 3)

Beam Specimen No.	h/t	a/h	w/h	M_{Rr}	M_{Rp}
BS1(N)	161.90	---	0.172	0.824	0.905
BS2(N)	161.90	---	0.172	0.839	0.905
BP4-40(H)	163.32	0.194	0.173	0.851	0.905
BP5-40(H)	163.32	0.194	0.173	0.826	0.905
BP6-40(H)	163.32	0.194	0.173	0.855	0.905
BP7-65(H)	163.32	0.322	0.168	0.845	0.920
BP8-65(H)	163.32	0.322	0.170	0.857	0.913
BP9-65(H)	163.32	0.322	0.173	0.855	0.905
CS1(N)	160.50	---	0.167	0.756	0.888
CS2(N)	160.91	---	0.167	0.756	0.889
CS3(N)	160.91	---	0.170	0.776	0.882
CP4-40(T)	161.90	0.220	0.167	0.790	0.882
CP5-40(T)	161.90	0.220	0.170	0.750	0.875
CP6-40(T)	162.72	0.219	0.172	0.800	0.869
CP7-65(T)	161.90	0.327	0.172	0.788	0.867
CP8-65(T)	162.31	0.326	0.169	0.780	0.876
CP9-65(T)	161.90	0.327	0.172	0.790	0.867

See Table XXXI for Notes

C. SUMMARY AND DESIGN RECOMMENDATIONS ON FLEXURAL BEHAVIOR

1. Summary. To obtain the objective of this investigation, which was to study the flexural behavior of C-shaped members with or without web openings subjected to a pure bending moment, a total 108 beam specimen tests have been performed and evaluated. Ninety-one beam specimens were

tested at UMR and 17 beam tests were conducted at the University of Waterloo. There were 34 beam specimens that failed by the distortional mode of buckling or mixed local and distortional mode of buckling at UMR and all 17 tests conducted at the University of Waterloo had a distortional mode of buckling or interaction of local and distortional mode of buckling. Based on the study reported herein, the following conclusions can be drawn:

a. This study indicates that there are two buckling modes, and the current AISI Specification does not adequately represent these buckling modes. This research has developed satisfactory techniques for evaluating both buckling modes.

b. For specimens whose failure was attributed to local buckling, an effective net section approach, satisfactorily predicts the bending strength for all test specimens.

c. Four simplified approaches for evaluating the ultimate bending moment for beam members having a deep web, narrow flanges and small edge stiffeners which undergo the distortional or mixed local and distortional buckling behavior has been developed.

d. For test specimens undergoing a distortional mode of buckling, an effective width approach that employs a modified web buckling coefficient, provides a satisfactory prediction for the ultimate moment capacity for all of the beam specimens having failed by distortional buckling behavior.

e. Criteria were developed to evaluate the controlling mode of buckling, i.e. local or distortional buckling.

2. Design Recommendations. Based on the findings of this project relating to the moment capacity of a beam member with or without web openings, the following design recommendations are proposed for consideration.

a. The buckling modes of local and distortional buckling are distinguished by the ratios of a/h and w/h, and Eqs. 63, 64 and 65.

b. For those beam members with web openings having $0.350 \leq a/h \leq 0.740$ and $M_{Rp} < 1.0$, the local buckling behavior controls the design and the effective net section approach can be used to predict the moment capacity. The ultimate moment capacity shall be determined by the following:

$$M_{uen} = S_{uen} F_y \qquad (66)$$

where S_{uen} = Effective net section modulus based on the net section and yield stress, F_y

F_y = Yield stress

The effective width of the portion of the web above the punchout, b_{ue} is treated as an unstiffened compression element and calculated by using the following equations:

b_{ue} = Effective width determined as follows:

$b_{ue} = w_u$ when $\lambda \leq 0.673$

$b_{ue} = \rho w_u$ when $\lambda > 0.673$

where

w_u = Flat width of the portion of the web element above the punchout

$\rho = (1-0.22/\lambda)/\lambda$

$\lambda = (1.052/\sqrt{k})(w_u/t)\sqrt{(F_y/E)}$

$k = 0.43$

where

w = Flat width of the portion of the web element above the punchout

t = Thickness

F_y = Yield stress

E = Modulus of elasticity of steel

The portion of the web below the punchout is assumed to be fully effective and the effective width of the flange and edge stiffener are calculated using the current AISI Specification equations.

c. For beam members with or without web openings having $0.25 \leq w/h \leq 0.35$ and $M_{Rp} < 1.0$, and undergoing a distortional mode of buckling, the modified buckling coefficient approach can be employed to predict the moment capacity. The ultimate moment capacity shall be determined by the following:

$$M_{uc,d} = S_{ex,FK} F_y \qquad (67)$$

where $S_{ex,FK}$ = The effective section modulus evaluated at F_y using the modified web buckling coefficient

F_y = Yield stress

The effective width of web, b_1 and b_2, are calculated by using the following equations:

$b_1 = b_e/(3+\psi)$

For $\psi \leq -0.236$

$b_2 = b_e/2$

b_1+b_2 shall not exceed the compression portion of the web calculated on the basis of the effective section.

For $\psi > -0.236$

$b_2 = b_e-b_1$

where

b_e = Effective width b determined as follows:

$b_e = w$ when $\lambda \leq 0.673$

$b_e = \rho w$ when $\lambda > 0.673$

where

$w = h$ = Flat width of the web element

$\rho = (1-0.22/\lambda)/\lambda$

$\lambda = (1.052/\sqrt{k})(w/t)\sqrt{(f_1/E)}$

$k = 0.008(h/t)+17000(w'/h)(F_y/E)$

$\psi = f_2/f_1$

where

$w = h$ = Flat width of the web element

w' = Flat width of the flange element

t = Thickness

F_y = Yield stress

E = Modulus of elasticity of steel

f_1, f_2 = Stresses shown in Fig. 1 calculated on the basis of effective section.

The effective width of the flange and edge stiffener are calculated using the current AISI Specification equations.

V. SHEAR BEHAVIOR OF WEB ELEMENTS WITH OPENINGS

A. GENERAL

The purpose of this phase of the research has been to investigate the shear behavior of a single web with openings when subjected to a constant shear force. A survey of the limited amount of literature has been conducted to determine the ultimate shear capacity of web elements with openings. UMR tests concentrate on the effect of the presence of elliptical web openings in C-shaped members. In view of the void of design criteria in the current AISI Specification, the results have been analyzed and evaluated to develop a load reduction factor for the shear behavior of C-section members with web elements having an elliptical opening.

This section is concerned with the test procedure, test results, and the analysis of the results for this study. The results of this investigation are summarized. Based on the findings of this study, appropriate design equations have been developed and presented herein. The design equations will also be considered in the following study of the behavior of combined bending and shear. The comparison relative to the results of Davis and Yu's for the web element with a circular opening are also discussed.

B. EXPERIMENTAL STUDY

The objective of the experimental investigation was to determine the strength of a beam with unreinforced and

reinforced webs having holes subjected to a pure shear force. The shear strength of a cold-formed steel member with a perforated web was studied with consideration of the slenderness ratio of the web, h/t and the ratio of web opening depth to web depth, a/h. It was found in the previous research (29,30,31,32,33,34) that these two parameters seem to effect the shear capacity. Thus, the objective for this investigation was to experimentally determine the shear strength, and compare the tested shear strength with the computed shear strength of beam webs determined by the theoretical equations as given by the AISI Specification (1) for solid webs, and to develop appropriate shear reduction equations for design. The experimental results are also compared to a shear reduction equation derived by Davis and Yu (36) for circular holes.

A total of 26 beam specimens were completed in this study. These beam specimens having either a 4 x 1.5 inch or 2 x 0.75 inch web opening located at the mid-height of the web were tested. The dimensions of the web openings are listed in Table XXXIV. For those deeper sections (6, 8 and 12 inches), the test specimens were treated as reinforced webs, whereas the test specimens with web depths of 2.5 and 3.625 inches were tested with unreinforced webs.

The range of parameters considered in the beam test specimens of this test program are given as follows:

$h/t = 34.43$ to 210.32

$a/h = 0.130$ to 0.739

TABLE XXXIV DIMENSIONS OF TEST SPECIMENS SUBJECTED TO SHEAR

Beam Specimen No.	Cross-Section Dimenisions (inches)											Hole Geom. (in.)	
	Thick.	D1	D2	B1	B2	B3	B4	d1	d2	d3	d4	b	a
SU-4	0.071	3.65	3.63	1.63	1.64	1.63	1.63	0.54	0.51	0.49	0.52	4	1.50
SU-5	0.059	2.47	2.46	1.63	1.63	1.62	1.62	0.47	0.49	0.52	0.49	4	1.50
SU-6	0.033	2.42	2.43	1.63	1.64	1.63	1.62	0.42	0.42	0.50	0.50	4	1.50
SU-8	0.039	2.51	2.50	1.60	1.61	1.59	1.60	0.39	0.42	0.45	0.41	2	0.75
SU-9	0.044	3.70	3.65	1.56	1.57	1.57	1.58	0.57	0.57	0.56	0.50	4	1.50
SU-10	0.077	3.69	3.69	1.64	1.63	1.64	1.63	0.55	0.54	0.59	0.54	4	1.50
SR-12	0.055	12.02	11.97	1.57	1.57	1.57	1.57	0.46	0.57	0.55	0.48	4	1.50
SR-13	0.045	7.95	7.94	1.59	1.58	1.58	1.58	0.47	0.47	0.48	0.47	4	1.50
SR-14	0.046	6.06	6.04	1.62	1.62	1.55	1.55	0.47	0.48	0.50	0.51	4	1.50
SR-15	0.046	8.00	8.00	2.42	2.45	2.45	2.43	0.61	0.70	0.70	0.61	4	1.50

Notes: 1. See Fig. 5 for the symbols used for the hole geometry.
2. See Fig. 6 for the symbols used for dimensions.
3. SU: Single Unreinforced (Web)
4. SR: Single Reinforced (Web)

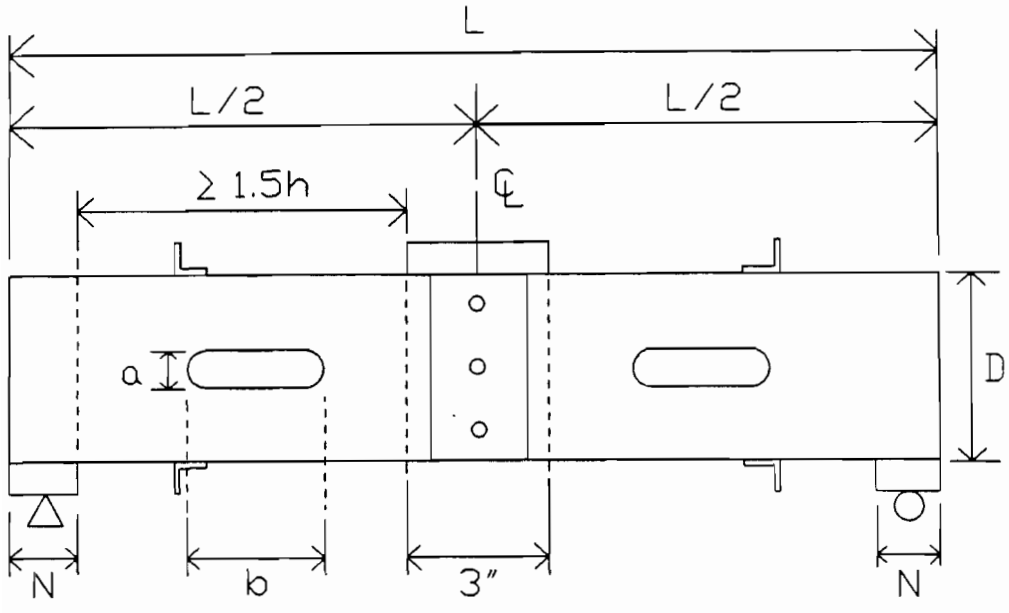

Figure 16. Test Setup for Shear Test Specimens (for 2.5 and 3.625-in. depth sections)

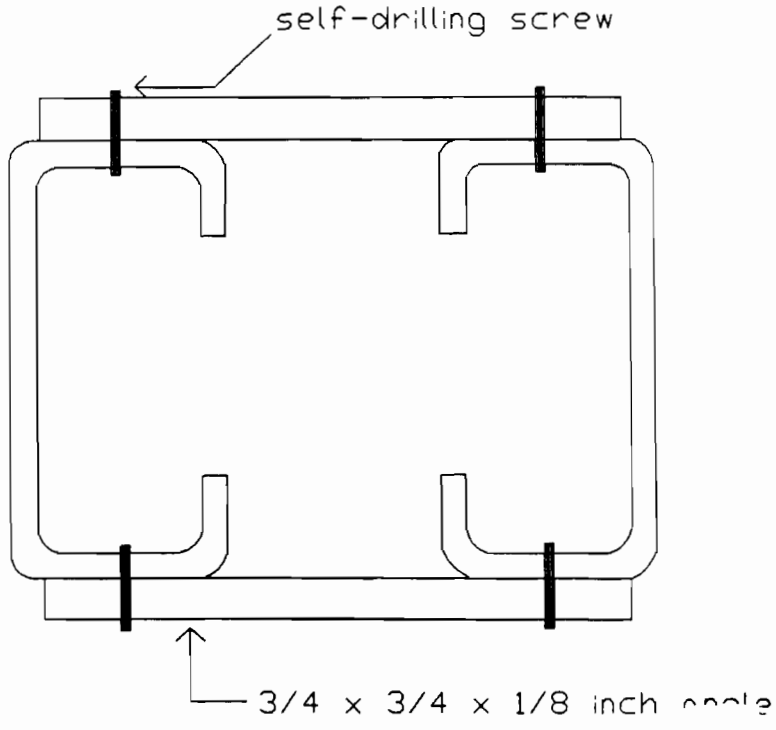

Figure 17. Cross Section of Shear Test Specimens (for 2.5 and 3.625-in. depth sections)

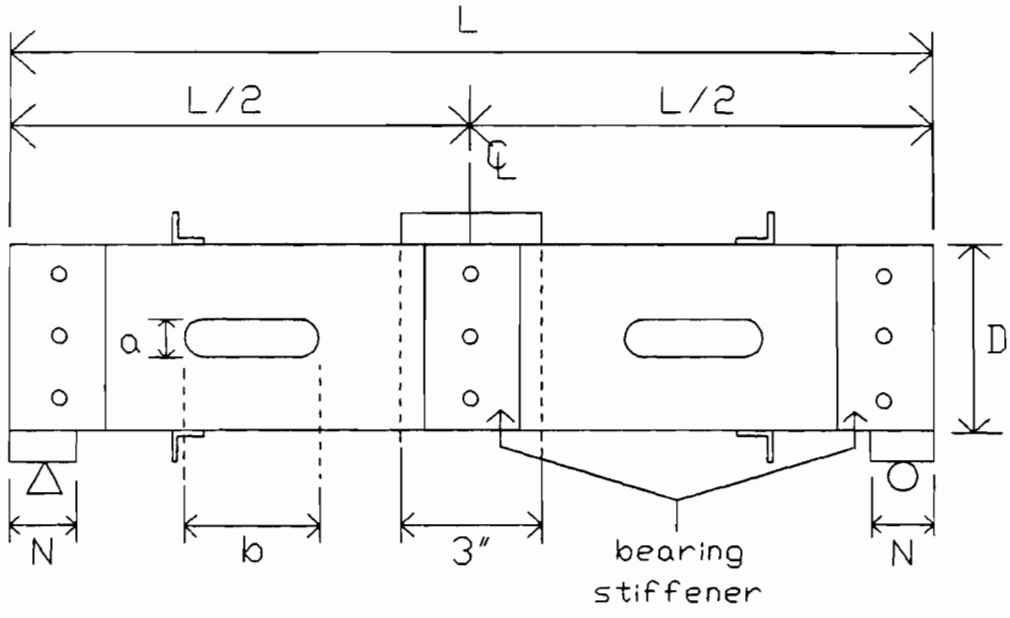

Figure 18. Test Setup for Shear Test Specimens (for 6, 8 and 12-in. depth sections)

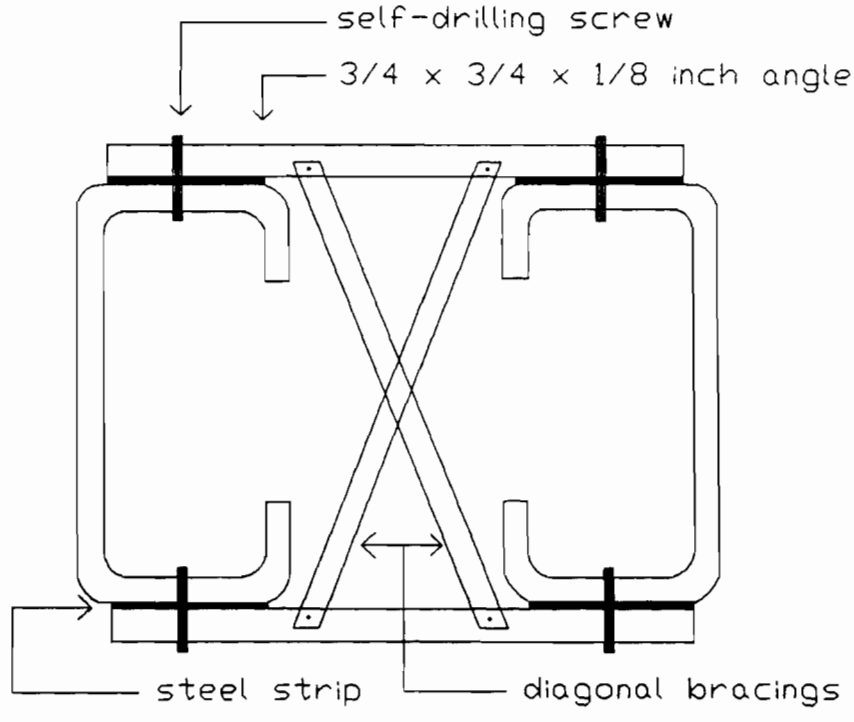

Figure 19. Cross Section of Shear Test Specimens (for 6, 8 and 12-in. depth sections)

F_y = 22.00 to 81.36 ksi.

1. Preparation of Beam Specimens. Five common industry standard C-sections (2.5, 3.625, 6, 8 and 12 inches deep) were tested. Various thicknesses of each C-section were considered. The cross-section dimension, thickness and geometric parameters of each test specimen are recorded in Table XXXIV.

Each beam specimen was fabricated by cutting the C-sections to the required length. In order to prevent lateral-torsional buckling of each individual C-channel section, each beam test specimen consisted of two C-shaped beams connected together using 3/4 x 3/4 x 1/8 inch aluminum angles and self-drilling screws at the compression flange and tension flange. For fabrication details, see Figs. 16, 17, 18 and 19.

When thin steel members with web openings are subjected to concentrated loads, three failure modes may occur: (i) bending, (ii) shear, or (iii) web crippling. The influence of bending was minimized by using members with short span lengths. In this experimental investigation, the span length ranged from 19.10 to 40.56 inches. To preclude web crippling at midspan, two stiffeners were attached vertically to each web at midspan.

For the 6, 8 and 12 inch deep sections (Specimen Nos. SR-12, SR-13, SR-14 and SR-15), vertical stiffeners were also added to each web at the end support. Figure 18 shows the test setup. To provide additional lateral support, two diagonal braces were connected to the angles as shown by Fig.

19. To preclude a bending failure, steel strips were attached to the top and bottom flanges of each 6, 8 and 12 inches C-section. These strips were attached by using self-drilling screws, spaced 1 inch on center.

2. Testing of Specimens

a. Tensile Coupon Tests. The material properties of the steels, for each test specimen, were established by standard tensile coupon specimens cut from the web element of the section. The coupons were prepared in accordance with ASTM A370. The coupons were tested in a 150,000 pound Tinus-Olsen universal testing machine which was linked to the computer software package Labtech Notebook. The average material property values obtained for each material from the coupon tests were used in the analysis of the data. Table XXXV lists the tensile test data for thickness, yield strength (F_y), ultimate tensile strength (F_u) and percent elongation in 2 inches gage length.

b. Testing of Beam Specimens. All test specimens were tested in a Tinius-Olsen universal testing machine as simple supported beams subjected to a concentrate load at midspan. Rollers and bearing plates were used at each end of the beam. One plate was set on the vertical stiffeners at midspan to support the applied load. The appropriate test setups are shown in Figs. 16 and 18. The load was increased gradually until the beam reached failure and could no longer bear additional load.

TABLE XXXV MATERIAL PROPERTIES FOR SHEAR TEST SPECIMENS

Specimen No.	Thickness (in.)	F_y (ksi)	F_u (ksi)	Elongation (%)
SU-4	0.071	81.36	104.28	21.9
SU-5	0.059	53.59	74.74	39.1
SU-6	0.033	67.15	71.50	35.4
SU-8	0.039	33.70	48.02	44.0
SU-9	0.044	46.92	60.32	31.0
SU-10	0.077	63.72	78.42	23.0
SR-12	0.055	49.11	57.50	32.0
SR-13	0.045	72.32	74.49	29.7
SR-14	0.046	47.17	67.06	41.4
SR-15	0.046	22.00	59.06	54.7

Notes: 1. SU: Single Unreinforced (Web)
2. SR: Single Reinforced (Web)

3. Test Results. Twenty-six tests of beams with webs having punchouts were conducted in this experimental investigation. Table XXXVI tabulates the test results. The shear failure load per web, $P_{u(test)}$, is taken as 1/4 of the ultimate midspan load and shown in Table XXXVI. The test data indicates that the shear strength of a beam web was influenced by the depth-to-thickness ratio of the web (h/t), and the ratio of web opening depth to web depth (a/h). From the results of test specimens, SU-6-3 through SU-6-7, it can be

noted that the bearing length, N, was not a principal parameter influencing the reduction in shear capacity.

TABLE XXXVI EXPERIMENTAL DATA FOR SHEAR TEST SPECIMENS

Specimen No.	L (in.)	N (in.)	h/t	a/h	$P_{u(test)}$ (lbs)
SU-4-7	26.54	3.0	44.77	0.472	2760
SU-5-3	19.10	1.0	34.43	0.739	801
SU-5-4	19.10	1.0	34.43	0.739	778
SU-5-5	19.10	1.0	34.43	0.739	775
SU-5-6	19.10	1.0	34.43	0.739	775
SU-5-7	19.10	1.0	34.43	0.739	756
SU-6-3	19.16	1.0	62.00	0.734	338
SU-6-4	19.16	1.0	62.00	0.734	341
SU-6-5	19.16	1.0	62.00	0.734	328
SU-6-6	19.16	1.0	62.00	0.734	325
SU-6-7	19.16	3.0	62.00	0.734	344
SU-8-8	22.11	6.0	54.19	0.355	550
SU-8-9	22.11	6.0	54.19	0.355	438
SU-9-10	27.54	5.0	74.34	0.459	1125
SU-9-11	27.54	6.0	74.34	0.459	929
SU-10-5	34.81	6.0	41.79	0.466	2406
SU-10-6	34.81	6.0	41.79	0.466	2750
SU-10-7	34.81	6.0	41.79	0.466	2556
SR-12-1	40.56	1.0	210.32	0.130	2563
SR-12-2	40.56	1.0	210.32	0.130	3500
SR-13-1	38.00	6.0	167.56	0.199	2263
SR-13-2	38.00	6.0	167.56	0.199	2313
SR-14-1	32.00	6.0	122.64	0.266	2494
SR-14-2	32.00	6.0	122.64	0.266	2594
SR-15-1	38.00	6.0	165.15	0.197	2075
SR-15-2	38.00	6.0	165.15	0.197	2044

Notes: 1. SU: Single Unreinforced (Web)
2. SR: Single Reinforced (Web)

4. Evaluation of Test Data. For solid web elements subjected to shear only, the nominal strength can be estimated by the equations from section C3.2 of 1991 Edition of the AISI LRFD Specification (2). These nominal equations also serve as the basis for the shear strength equations given in the AISI ASD Specification (1). These equations (Eqs. 19, 20 and 21) have been discussed in the Section II.2. Based on these equations for a web element with no opening, the nominal shear strength, V_n, of each test specimen was calculated and listed in Table XXXVII.

TABLE XXXVII EVALUATION OF SHEAR TEST DATA

Specimen No.	h/t	a/h	$P_{u(test)}$ (lbs)	V_n (lbs)	$P_{u(test)}/V_n$
SU-4-7	44.77	0.472	2760	11524	0.240
SU-5-3	34.43	0.739	801	3732	0.215
SU-5-4	34.43	0.739	778	3732	0.208
SU-5-5	34.43	0.739	775	3732	0.208
SU-5-6	34.43	0.739	775	3732	0.208
SU-5-7	34.43	0.739	756	3732	0.203
SU-6-3	62.00	0.734	338	2264	0.149
SU-6-4	62.00	0.734	341	2264	0.151
SU-6-5	62.00	0.734	328	2264	0.145
SU-6-6	62.00	0.734	325	2264	0.144
SU-6-7	62.00	0.734	344	2264	0.152
SU-8-8	54.19	0.355	550	1614	0.341
SU-8-9	54.19	0.355	438	1614	0.271
SU-9-10	74.34	0.459	1125	3371	0.334
SU-9-11	74.34	0.459	929	3371	0.276
SU-10-5	41.79	0.466	2406	9213	0.261
SU-10-6	41.79	0.466	2750	9213	0.298
SU-10-7	41.79	0.466	2556	9213	0.277

TABLE XXXVII (CONTINUED) EVALUATION OF SHEAR TEST DATA

Specimen No.	h/t	a/h	$P_{u(test)}$ (lbs)	V_n (lbs)	$P_{u(test)}/V_n$
SR-12-1	210.32	0.130	2563	2700	0.949
SR-12-2	210.32	0.130	3500	2700	1.296
SR-13-1	167.56	0.199	2263	2010	1.125
SR-13-2	167.56	0.199	2313	2010	1.151
SR-14-1	122.64	0.266	2494	2943	0.847
SR-14-2	122.64	0.266	2594	2943	0.881
SR-15-1	165.15	0.197	2075	2230	0.931
SR-15-2	165.15	0.197	2044	2230	0.917

Notes: 1. SU: Single Unreinforced (Web)
2. SR: Single Reinforced (Web)

5. Development of Reduction Factors. The influence of a web opening on the ultimate shear strength is not accounted for by the current AISI Specification (1,2). Based on the AISI Specification for shear strength of the solid webs, the ratios of $P_{u(test)}/V_n$ (Table XXXVII) show the reduction of the shear strength of a C-section with a web opening.

Based on a plot of the test data, Fig. 20, and using the regression analysis, both a linear and a non-linear shear strength reduction factor q_s ($q_s = P_{u(test)}/V_n$) have been developed. Equations 68 and 69 are the linear relationships.

when $a/h \leq 0.383$:

$$q_s = 1.711 - 3.661(a/h) \leq 1.000 \quad (68)$$

when $0.383 \leq a/h \leq 1.00$:

$$q_s = 0.456 - 0.377(a/h) \quad (69)$$

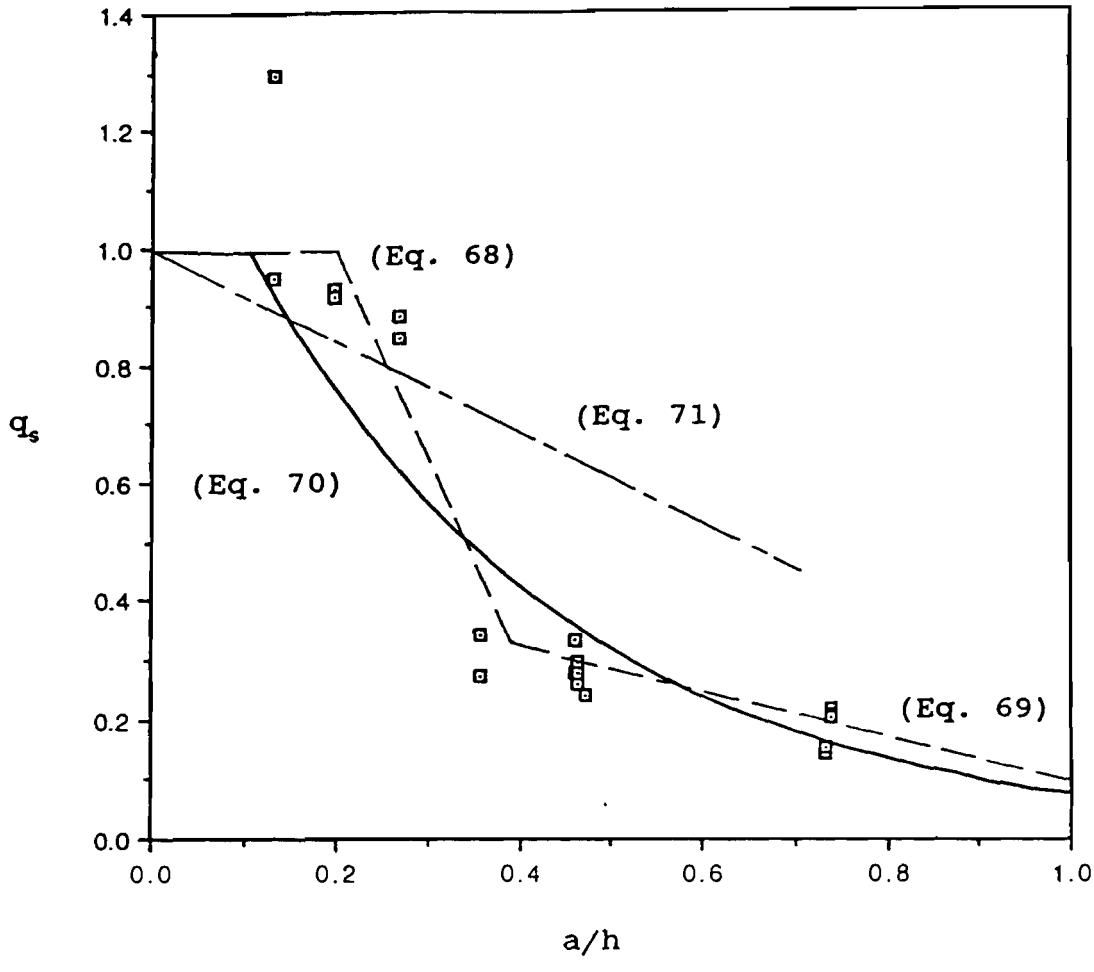

Figure. 20 Load Reduction Factor q_s Verse a/h Ratio

Equation 70 represents the non-linear relationship for the correlation between q_s and a/h as define:

$$q_s = 1.506 * 10^{[-1.33*(a/h)]} \leq 1.000 \qquad (70)$$

Based on the above analysis of test results, Eqs. 68 and 69 or 70 can be used to modify the current AISI design criteria for web design when the web element has an elliptical opening and a limitation of $34.43 \leq h/t \leq 210.32$.

Based on twelve tests of I-beams, Davis and Yu (36) derived Eq. 71 for web design when a circular hole was present at mid-depth in a web element. The experimental results were compared well with the analytical results of Kawai and Ohtsubo, Kroll, and Rockey (36,37).

$$q_s = 1.0 - 1.1(d/h) \qquad (71)$$

where d = The diameter of a circular hole

h = The clear distance between flanges measured along the plane of the web

Equation 71 is limited to $0.0 \leq d/h \leq 0.5$ and $66 < h/t < 100$, and is also shown in Fig. 20. The comparison between Eq. 71 and the test data of this study is indicated in Table XXXVIII and shown in Fig. 20. The unconservative nature of Davis and Yu, is attributed to the web opening geometry; Davis and Yu is based on circular openings, whereas for the tests reported herein, the web openings were elliptical.

6. Comparison of Test Results. Because the maximum shear stress occurs at mid-depth, where web material is removed, and an elliptical web opening creates a stress concentration at the corners of the opening, premature shear failures occurred in the diagonal direction at the location of the web openings. See Fig. 21 for the typical failure pattern. For the configurations used in the tests, the major parameter that appears to influence the shear strength is a/h. This parameter (a/h) was emphasized in the development of the reduction factor, q_s, for evaluating shear strength (Eqs. 68, 69, 70 and 71).

TABLE XXXVIII COMPARISON OF SHEAR CAPACITY WITH DAVIS AND YU'S REDUCTION EQUATION

Specimen No.	a/h	$P_{u(test)}/V_n$	q_s (1)	q_s (2)	q_s (3)
SU-4-7	0.472	0.240	0.278	0.355	0.483
SU-5-3	0.739	0.215	0.177	0.167	---
SU-5-4	0.739	0.208	0.177	0.167	---
SU-5-5	0.739	0.208	0.177	0.167	---
SU-5-6	0.739	0.208	0.177	0.167	---
SU-5-7	0.739	0.203	0.177	0.167	---
SU-6-3	0.734	0.149	0.179	0.159	---
SU-6-4	0.734	0.151	0.179	0.159	---
SU-6-5	0.734	0.145	0.179	0.159	---
SU-6-6	0.734	0.144	0.179	0.159	---
SU-6-7	0.734	0.152	0.179	0.159	---
SU-8-8	0.355	0.341	0.411	0.508	0.615
SU-8-9	0.355	0.271	0.411	0.508	0.615
SU-9-10	0.459	0.334	0.283	0.369	0.494
SU-9-11	0.459	0.276	0.283	0.369	0.494
SU-10-5	0.466	0.261	0.280	0.361	0.494
SU-10-6	0.466	0.298	0.280	0.361	0.494
SU-10-7	0.466	0.277	0.280	0.361	0.494
SR-12-1	0.130	0.949	1.235	1.011	0.857
SR-12-2	0.130	1.296	1.235	1.011	0.857
SR-13-1	0.199	1.125	0.982	0.819	0.780
SR-13-2	0.199	1.151	0.982	0.819	0.780
SR-14-1	0.266	0.847	0.737	0.667	0.703
SR-14-2	0.266	0.881	0.737	0.667	0.703
SR-15-1	0.197	0.931	0.990	0.824	0.780
SR-15-2	0.197	0.917	0.990	0.824	0.780

Notes: (1). Based on two straight lines
(2). Based on an approximate curve
(3). Based on Davis and Yu's Equation

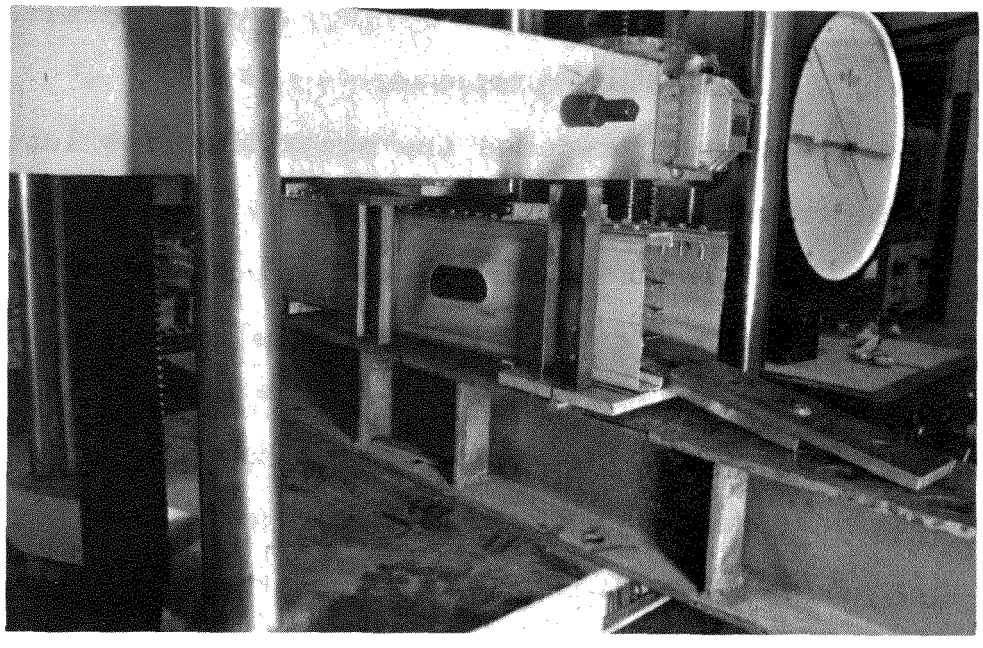

Figure 21. Typical Shear Failure Mode

C. SUMMARY AND DESIGN RECOMMENDATIONS

1. Summary. A primary investigation was conducted to study the behavior of C-shaped members with elliptical web openings subjected to a shear failure load. Based on 26 beam specimen tests, modified equations using either a linear or a non-linear relationship were developed to determine the strength of the web elements having an elliptical opening. The a/h ratio was found to be the primary parameter contributing to the reduction of the capacity for a web element with an opening.

2. Design Recommendations. Based on this investigation, the following design recommendations for the shear capacity of

where

V_n = Nominal shear strength of web

t = Web thickness

h = Depth of the flat portion of the web measured along the plane of the web

k_v = Shear buckling coefficient determined as follows:

1. For unreinforced webs, $k_v = 5.34$
2. For beam webs with transverse stiffeners satisfying the requirements of Section B6

when $a'/h \leq 1.0$

$$k_v = 4.00+5.34/(a'/h)^2 \quad (78)$$

when $a'/h > 1.0$

$$k_v = 5.34+4.00/(a'/h)^2 \quad (79)$$

where a' = The shear panel length for unreinforced web element

= Distance between transverse stiffeners for reinforced web elements

VI. COMBINED BENDING AND SHEAR BEHAVIOR OF WEB ELEMENTS WITH OPENINGS

A. GENERAL

The purpose of this phase of the research has been to investigate the behavior of a single web with openings when subjected to a combined shear force and bending moment. Prior to this phase of the investigation, studies on the ultimate strength of the beam with perforated web subjected to either bending moment or shear force were made.

The interaction between shear forces and bending moments on the ultimate capacity of the web elements with openings was experimentally investigated. The test results are compared with the interaction equations as given in the AISI Specification for a solid web cross section.

The experimental investigation and the evaluation of the test results will be presented and discussed. The following discussion will cover the fabrication of test specimens, test procedure, test results, and analysis of the results. Based on the findings of this study, design recommendations for the interaction relationship have been presented herein.

B. EXPERIMENTAL STUDY

To determine the effects of web openings on the buckling strength, an experimental investigation was conducted to determine the interaction between bending moment and shear force, and the influence of the interaction on the strength of

unreinforced beam webs having openings. From Section V, the significant parameter, the ratio of web opening depth to web depth (a/h), effects the ultimate shear capacity of web element with web openings. Particular consideration on this parameter, a/h, also was given in the analysis of the interaction between bending moment and shear force.

Sixty-eight beam tests were conducted in this study. Beam specimens having three different web opening sizes [(4 x 1.5 inch, 4 x 0.75 inch, and 2 x 0.75 inch)] located at the mid-height of the web were tested. The dimensions of each test specimen and the web openings are listed in Table XXXIX. For the combination of bending and shear behavior, the location of the web opening, the distance x′ as shown in Fig. 22, was also investigated.

The beam test specimens had the following range of material properties:

h/t = 34.43 to 98.23

a/h = 0.352 to 0.740

F_y = 33.70 to 81.36 ksi.

1. Preparation of Beam Specimens. Two common industry standard C-sections (2.5 and 3.625 inches deep) were tested for various thicknesses of each C-section. The cross-section dimension, thickness and geometric parameters of each test specimen are given in Table XXXIX and the test specimen cross-section is shown in Fig. 6.

Each beam specimen was cut to the required length and was fabricated using the same procedure as used for the shear test

specimens. For fabrication details see Section V.B.1 and Figs. 16 and 17.

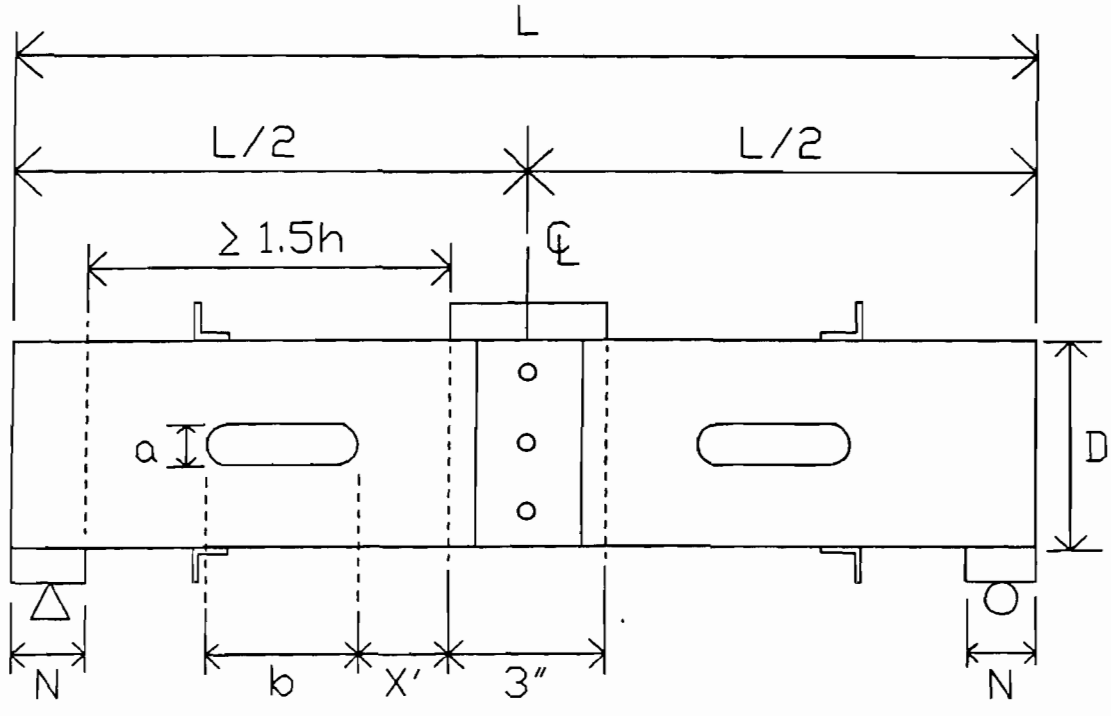

Figure 22. Test Setup for Combined Bending and Shear Test Specimens

2. Testing of Specimens

a. Tensile Coupon Tests. Three tensile coupons were cut from the web element of each section. Standard tensile tests were conducted to determine the mechanical properties of the steel used in this experimental study. All tensile specimens were prepared in accordance with ASTM A370. The coupon were tested in a 150,000 pound Tinus-Olsen universal testing machine which was linked to the computer software package

TABLE XXXIX DIMENSIONS OF TEST SPECIMENS SUBJECTED TO COMBINED BENDING AND SHEAR

Beam Specimen No.	Cross-Section Dimenisions (inches)											Hole Geom. (in.)	
	Thick.	D1	D2	B1	B2	B3	B4	d1	d2	d3	d4	b	a
BS-2-16-1A	0.056	2.55	2.55	1.63	1.63	1.64	1.64	0.50	0.49	0.51	0.49	4	0.75
BS-2-16-2A	0.056	2.55	2.55	1.63	1.63	1.63	1.63	0.50	0.49	0.51	0.50	4	0.75
BS-2-16-1B	0.056	2.54	2.54	1.63	1.63	1.63	1.63	0.51	0.47	0.47	0.51	4	0.75
BS-2-16-2B	0.056	2.54	2.55	1.63	1.63	1.63	1.63	0.51	0.47	0.51	0.50	4	0.75
BS-2-16-1C	0.056	2.54	2.55	1.63	1.63	1.63	1.63	0.47	0.52	0.50	0.48	4	0.75
BS-2-16-2C	0.056	2.55	2.55	1.63	1.63	1.63	1.64	0.47	0.51	0.51	0.47	4	0.75
BSB-2-16-1	0.062	2.51	2.51	1.61	1.61	1.63	1.61	0.40	0.45	0.42	0.43	2	0.75
BSB-2-16-2	0.059	2.46	2.46	1.62	1.63	1.62	1.61	0.47	0.46	0.51	0.51	4	1.50
BSB-2-16-3	0.059	2.47	2.46	1.63	1.62	1.62	1.63	0.47	0.52	0.52	0.46	4	1.50
BSS-2-16-1	0.059	2.47	2.46	1.63	1.63	1.62	1.62	0.47	0.49	0.52	0.49	4	1.50
BSS-2-16-2	0.059	2.47	2.46	1.63	1.63	1.62	1.62	0.47	0.49	0.52	0.49	4	1.50
BSS-2-16-3	0.059	2.47	2.46	1.63	1.63	1.62	1.62	0.47	0.49	0.52	0.49	4	1.50
BSS-2-16-4	0.059	2.47	2.46	1.63	1.63	1.62	1.62	0.47	0.49	0.52	0.49	4	1.50
BSS-2-16-5	0.059	2.47	2.46	1.63	1.63	1.62	1.62	0.47	0.49	0.52	0.49	4	1.50

TABLE XXXIX (CONTINUED) DIMENSIONS OF TEST SPECIMENS SUBJECTED TO COMBINED BENDING AND SHEAR

Beam Specimen No.	Cross-Section Dimenisions (inches)											Hole Geom. (in.)	
	Thick.	D1	D2	B1	B2	B3	B4	d1	d2	d3	d4	b	a
BS-2-20-1A	0.032	2.52	2.51	1.58	1.58	1.57	1.58	0.45	0.48	0.48	0.42	4	0.75
BS-2-20-2A	0.032	2.51	2.51	1.58	1.57	1.57	1.58	0.43	0.48	0.43	0.44	4	0.75
BS-2-20-1B	0.032	2.51	2.51	1.59	1.58	1.58	1.59	0.43	0.47	0.46	0.42	4	0.75
BS-2-20-2B	0.032	2.51	2.51	1.58	1.58	1.57	1.59	0.42	0.47	0.47	0.42	4	0.75
BS-2-20-1C	0.032	2.52	2.51	1.59	1.57	1.57	1.58	0.42	0.48	0.47	0.43	4	0.75
BS-2-20-2C	0.032	2.51	2.52	1.58	1.58	1.58	1.58	0.44	0.48	0.47	0.43	4	0.75
BSB-2-20-1	0.039	2.50	2.48	1.60	1.60	1.60	1.60	0.42	0.41	0.42	0.41	2	0.75
BSB-2-20-2	0.039	2.51	2.52	1.59	1.62	1.58	1.60	0.36	0.42	0.47	0.41	2	0.75
BSB-2-20-3	0.033	2.42	2.42	1.63	1.64	1.63	1.62	0.42	0.42	0.50	0.50	4	1.50
BSB-2-20-4	0.033	2.42	2.43	1.63	1.64	1.63	1.62	0.42	0.41	0.50	0.50	4	1.50
BSS-2-20-1	0.039	2.51	2.50	1.60	1.61	1.59	1.60	0.39	0.42	0.45	0.41	2	0.75
BSS-2-20-2	0.039	2.51	2.50	1.60	1.61	1.59	1.60	0.39	0.42	0.45	0.41	2	0.75
BSS-2-20-3	0.033	2.42	2.43	1.63	1.64	1.63	1.62	0.42	0.42	0.50	0.50	4	1.50
BSS-2-20-4	0.033	2.42	2.43	1.63	1.64	1.63	1.62	0.42	0.42	0.50	0.50	4	1.50
BSS-2-20-5	0.033	2.42	2.43	1.63	1.64	1.63	1.62	0.42	0.42	0.50	0.50	4	1.50
BSS-2-20-6	0.033	2.42	2.43	1.63	1.64	1.63	1.62	0.42	0.42	0.50	0.50	4	1.50
BSS-2-20-7	0.033	2.42	2.43	1.63	1.64	1.63	1.62	0.42	0.42	0.50	0.50	4	1.50

TABLE XXX.X (CONTINUED) DIMENSIONS OF TEST SPECIMENS SUBJECTED TO COMBINED BENDING AND SHEAR

Beam Specimen No.	Cross-Section Dimenisions (inches)											Hole Geom. (in.)	
	Thick.	D1	D2	B1	B2	B3	B4	d1	d2	d3	d4	b	a
BS-3-14-1A	0.067	3.66	3.65	1.63	1.63	1.63	1.63	0.55	0.47	0.49	0.55	4	1.50
BS-3-14-2A	0.067	3.65	3.66	1.63	1.63	1.63	1.64	0.54	0.48	0.49	0.56	4	1.50
BS-3-14-1B	0.067	3.66	3.66	1.63	1.63	1.63	1.63	0.55	0.48	0.48	0.55	4	1.50
BS-3-14-2B	0.067	3.66	3.66	1.63	1.63	1.63	1.63	0.54	0.49	0.50	0.55	4	1.50
BS-3-14-1C	0.067	3.66	3.66	1.62	1.63	1.63	1.62	0.54	0.46	0.48	0.54	4	1.50
BS-3-14-2C	0.067	3.66	3.66	1.63	1.63	1.63	1.63	0.52	0.47	0.50	0.54	4	1.50
BSB-3-14-1	0.077	3.68	3.68	1.65	1.64	1.63	1.63	0.57	0.55	0.56	0.52	4	1.50
BSB-3-14-2	0.077	3.69	3.69	1.63	1.62	1.64	1.63	0.53	0.53	0.62	0.55	4	1.50
BSB-3-14-3	0.071	3.65	3.62	1.62	1.66	1.63	1.63	0.54	0.55	0.49	0.50	4	1.50
BSB-3-14-4	0.071	3.64	3.63	1.63	1.62	1.62	1.63	0.54	0.47	0.49	0.54	4	1.50
BSS-3-14-1	0.077	3.69	3.69	1.64	1.63	1.64	1.63	0.55	0.54	0.59	0.54	4	1.50
BSS-3-14-2	0.077	3.69	3.69	1.64	1.63	1.64	1.63	0.55	0.54	0.59	0.54	4	1.50
BSS-3-14-3	0.071	3.65	3.63	1.63	1.64	1.63	1.63	0.54	0.51	0.49	0.52	4	1.50
BSS-3-14-4	0.071	3.65	3.63	1.63	1.64	1.63	1.63	0.54	0.51	0.49	0.52	4	1.50

TABLE XXXIX (CONTINUED) DIMENSIONS OF TEST SPECIMENS SUBJECTED TO COMBINED BENDING AND SHEAR

Beam Specimen No.	Cross-Section Dimenisions (inches)											Hole Geom. (in.)	
	Thick.	D1	D2	B1	B2	B3	B4	d1	d2	d3	d4	b	a
BS-3-18-1A	0.045	3.63	3.63	1.63	1.63	1.63	1.63	0.48	0.48	0.47	0.49	4	1.50
BS-3-18-2A	0.045	3.66	3.65	1.59	1.59	1.59	1.59	0.46	0.50	0.49	0.45	4	1.50
BS-3-18-1B	0.045	3.65	3.63	1.59	1.63	1.59	1.63	0.44	0.47	0.50	0.44	4	1.50
BS-3-18-2B	0.045	3.65	3.64	1.59	1.63	1.59	1.62	0.50	0.50	0.43	0.47	4	1.50
BS-3-18-1C	0.045	3.64	3.65	1.63	1.59	1.63	1.59	0.49	0.44	0.48	0.51	4	1.50
BS-3-18-2C	0.045	3.65	3.64	1.63	1.63	1.63	1.63	0.47	0.51	0.49	0.47	4	1.50
BSB-3-18-1	0.044	3.75	3.65	1.56	1.56	1.57	1.58	0.58	0.56	0.58	0.54	4	1.50
BSB-3-18-2	0.044	3.65	3.64	1.56	1.58	1.56	1.57	0.56	0.57	0.54	0.54	4	1.50
BSB-3-18-3	0.044	3.61	3.63	1.61	1.61	1.65	1.62	0.51	0.52	0.50	0.50	4	1.50
BSB-3-18-4	0.044	3.62	3.63	1.62	1.66	1.65	1.64	0.50	0.50	0.52	0.52	4	1.50
BSS-3-18-1	0.044	3.70	3.65	1.56	1.57	1.57	1.58	0.57	0.57	0.56	0.50	4	1.50
BSS-3-18-2	0.044	3.70	3.65	1.56	1.57	1.57	1.58	0.57	0.57	0.56	0.50	4	1.50

TABLE XXXIX (CONTINUED) DIMENSIONS OF TEST SPECIMENS SUBJECTED TO COMBINED BENDING AND SHEAR

Beam Specimen No.	Cross-Section Dimenisions (inches)											Hole Geom. (in.)	
	Thick.	D1	D2	B1	B2	B3	B4	d1	d2	d3	d4	b	a
BS-3-20-1A	0.033	3.62	3.62	1.62	1.62	1.61	1.62	0.47	0.42	0.45	0.46	4	1.50
BS-3-20-2A	0.033	3.61	3.61	1.61	1.64	1.62	1.63	0.49	0.48	0.43	0.48	4	1.50
BS-3-20-1B	0.033	3.60	3.60	1.63	1.64	1.64	1.62	0.48	0.47	0.45	0.47	4	1.50
BS-3-20-2B	0.033	3.62	3.60	1.62	1.64	1.64	1.63	0.44	0.45	0.45	0.49	4	1.50
BS-3-20-1C	0.033	3.62	3.61	1.62	1.63	1.62	1.62	0.48	0.46	0.41	0.49	4	1.50
BS-3-20-2C	0.033	3.62	3.62	1.64	1.62	1.62	1.63	0.45	0.44	0.45	0.45	4	1.50
BSB-3-20-1	0.044	3.65	3.71	1.56	1.64	1.55	1.59	0.52	0.56	0.55	0.56	4	1.50
BSB-3-20-2	0.044	3.67	3.69	1.56	1.59	1.55	1.61	0.60	0.56	0.52	0.59	4	1.50
BSB-3-20-3	0.036	3.61	3.60	1.63	1.62	1.63	1.62	0.46	0.47	0.46	0.47	4	1.50
BSB-3-20-4	0.036	3.61	3.61	1.64	1.63	1.64	1.63	0.46	0.47	0.47	0.47	4	1.50
BSB-3-20-5	0.036	3.60	3.60	1.63	1.63	1.62	1.63	0.47	0.46	0.46	0.47	4	1.50

Notes: 1. See Fig. 5 for the symbols used for the hole geometry.
2. See Fig. 6 for the symbols used for dimensions.
3. BS: Combined Bending and Shear
4. BSB: Combined Bending and Shear for Pure Bending behavior
5. BSS: Combined Bending and Shear for Pure Shear behavior
6. Specimen Designation: BS-2-16-1A
2=Nominal Depth, 16=Gage No., 1=Test No.
Type A:x=0.0 in., Type B:x=0.5h in., Type C:x=h in.

Labtech Notebook. The average values obtained from the coupon tests are recorded. Table XXXX lists the tensile test data for thickness, yield strength (F_y), ultimate tensile strength (F_u) and percent elongation in 2 inches gage length.

b. Testing of Beam Specimens. Each specimen was tested as a simply supported beam. The test setup and test procedure are similar to that used for the shear test specimens. A detailed description of the test procedure was presented in Section V.B.2.b.

3. Test Results. A total of 68 tests were completed, 30 tests experienced combined bending and shear, 20 tests failed by pure bending and 18 tests focused on pure shear. The 20 tests that failed by pure bending from Section IV provided information on interaction between the high moment ratios and smaller shear ratios. The 18 tests for pure shear discussed in Section V give an indication of the relationship between smaller moment ratios and high shear ratios.

The test results of V_t and M_t are listed in Table XXXXI. For each test specimens, the failure shear load (V_t) was determined as 1/4 of the maximum midspan load and the bending moment (M_t) was computed on the basis of V_t.

4. Evaluation of Test Data. In order to study the correlation between the bending and shear behavior, two methods were applied to the analysis of the combined shear force and bending moment. The unmodified and modified nominal shear strengths and bending moments were computed as follows:

TABLE XXXX MATERIAL PROPERTIES FOR COMBINED BENDING AND SHEAR TEST SPECIMENS

Specimen No.	Thickness (in.)	F_y (ksi)	F_u (ksi)	Elongation (%)
BS-3-14	0.067	47.88	54.68	41.9
BSB-3-14-1,2	0.077	63.72	78.42	23.0
BSB-3-14-3,4	0.071	81.36	104.28	21.9
BSS-3-14-1,2	0.077	63.72	78.42	23.0
BSS-3-14-3,4	0.071	81.36	104.28	21.9
BS-3-18	0.045	52.75	63.65	41.3
BSB-3-18-1,2	0.044	46.92	60.32	31.0
BSB-3-18-3,4	0.044	53.13	70.16	24.0
BSS-3-18-1,2	0.044	46.92	60.32	31.0
BS-3-20	0.033	58.65	69.18	40.0
BSB-3-20-1,2	0.044	46.82	60.31	31.0
BSB-3-20-3,4,5	0.036	63.71	78.95	29.2
BS-2-16	0.055	55.30	64.75	36.9
BSB-2-16-1	0.062	37.23	48.86	38.0
BSB-2-16-2,3	0.059	53.59	74.74	39.1
BSS-2-16	0.059	53.59	74.74	39.1
BS-2-20	0.032	55.33	68.10	39.2
BSB-2-20-1,2	0.039	33.70	48.02	44.0
BSB-2-20-3,4	0.033	67.15	71.50	35.4
BSS-2-20-1,2	0.039	33.70	48.02	44.0
BSS-2-20-3,4,5,6,7,	0.033	67.15	71.50	35.4

Notes: 1. Specimen designation BS-3-14 is appropriate for test specimens:
BS-3-14-1A
BS-3-14-2A
BS-3-14-1B
BS-3-14-2B
BS-3-14-1C
BS-3-14-2C
2. Specimen designation BSB-3-14-1,2 is appropriate for test specimens:
BSB-3-14-1
BSB-3-14-2
3. See Table XXXIX for other Notes

TABLE XXXXI EXPERIMENTAL DATA FOR COMBINED BENDING AND SHEAR TEST SPECIMENS

Specimen No.	Span Length (in.)	h/t	a/h	V_t (lbs)	M_t (k-in)
BS-3-14-1A	40.0	48.41	0.462	1283	21.78
BS-3-14-2A	40.0	48.41	0.462	1288	21.89
BS-3-14-1B	40.0	48.41	0.462	1320	22.42
BS-3-14-2B	40.0	48.41	0.462	1325	22.53
BS-3-14-1C	40.0	48.41	0.462	1345	22.84
BS-3-14-2C	40.0	48.41	0.462	1350	22.95
BSB-3-14-1	150.0	41.77	0.466	925	75.17
BSB-3-14-2	150.0	41.80	0.466	885	72.01
BSB-3-14-3	150.0	44.78	0.472	1078	86.99
BSB-3-14-4	150.0	44.75	0.472	1065	85.68
BSS-3-14-1	34.8	41.79	0.466	2406	18.21
BSS-3-14-2	34.8	41.79	0.466	2750	21.06
BSS-3-14-3	34.8	41.79	0.466	2556	9.91
BSS-3-14-4	26.5	44.77	0.472	2760	12.03
BS-3-18-1A	40.0	72.61	0.459	650	11.05
BS-3-18-2A	40.0	72.61	0.459	650	11.05
BS-3-18-1B	40.0	72.61	0.459	713	12.11
BS-3-18-2B	40.0	72.61	0.459	638	10.84
BS-3-18-1C	40.0	72.61	0.459	745	12.65
BS-3-18-2C	40.0	72.61	0.459	745	12.65
BSB-3-18-1	150.0	74.99	0.455	338	29.32
BSB-3-18-2	150.0	73.68	0.463	343	29.70
BSB-3-18-3	150.0	73.17	0.466	400	34.15
BSB-3-18-4	150.0	73.25	0.465	378	32.39
BSS-3-18-1	27.5	74.34	0.459	1125	6.90
BSS-3-18-2	29.5	74.34	0.459	929	6.16
BS-3-20-1A	40.0	98.23	0.463	425	7.23
BS-3-20-2A	40.0	98.23	0.463	458	7.76
BS-3-20-1B	40.0	98.23	0.463	475	8.08
BS-3-20-2B	40.0	98.23	0.463	463	7.86
BS-3-20-1C	40.0	98.23	0.463	483	8.18
BS-3-20-2C	40.0	98.23	0.463	508	8.61
BSB-3-20-1	150.0	74.42	0.458	338	29.31
BSB-3-20-2	150.0	74.48	0.458	358	30.78
BSB-3-20-3	150.0	89.50	0.466	300	26.35
BSB-3-20-4	150.0	89.50	0.466	275	24.40
BSB-3-20-5	150.0	89.26	0.467	335	28.88

TABLE XXXXI (CONTINUED) EXPERIMENTAL DATA FOR COMBINED BENDING AND SHEAR TEST SPECIMENS

Specimen No.	Span Length (in.)	h/t	a/h	V_t (lbs)	M_t (k-in)
BS-2-16-1A	40.0	38.68	0.353	645	10.94
BS-2-16-2A	40.0	38.68	0.353	650	11.05
BS-2-16-1B	40.0	38.68	0.353	688	11.69
BS-2-16-2B	40.0	38.68	0.353	658	11.16
BS-2-16-1C	40.0	38.68	0.353	658	11.16
BS-2-16-2C	40.0	38.68	0.353	675	11.48
BSB-2-16-1	150.0	33.43	0.362	260	23.37
BSB-2-16-2	150.0	34.37	0.740	338	29.17
BSB-2-16-3	150.0	34.48	0.737	340	29.47
BSS-2-16-1	19.1	34.43	0.739	800	2.82
BSS-2-16-2	19.1	34.43	0.739	778	3.05
BSS-2-16-3	19.1	34.43	0.739	775	3.51
BSS-2-16-4	19.1	34.43	0.739	775	4.30
BSS-2-16-5	19.1	34.43	0.739	756	2.66
BS-2-20-1A	40.0	66.67	0.352	320	5.42
BS-2-20-2A	40.0	66.67	0.352	320	5.42
BS-2-20-1B	40.0	66.67	0.352	313	5.31
BS-2-20-2B	40.0	66.67	0.352	325	5.53
BS-2-20-1C	40.0	66.67	0.352	320	5.42
BS-2-20-2C	40.0	66.67	0.352	338	5.74
BSB-2-20-1	150.0	53.92	0.362	115	11.85
BSB-2-20-2	150.0	54.46	0.357	115	11.95
BSB-2-20-3	150.0	61.96	0.734	150	14.65
BSB-2-20-4	150.0	62.03	0.733	160	15.33
BSS-2-20-1	19.2	62.00	0.734	338	1.19
BSS-2-20-2	19.2	62.00	0.734	341	1.34
BSS-2-20-3	19.2	62.00	0.734	328	1.49
BSS-2-20-4	19.2	62.00	0.734	325	1.81
BSS-2-20-5	19.2	62.00	0.734	344	1.56
BSS-2-20-6	22.1	54.19	0.355	550	2.78
BSS-2-20-7	22.1	54.19	0.355	438	2.21

Notes: V_t = Tested Shear Strengths
M_n = Tested Moment Capacities

(i). Based on the 1986 AISI Specification equations, the unmodified nominal shear strength, V_n, and moment capacity ,M_n, were calculated and listed in Table XXXXII.

(ii). Based on Eqs. 68 and 69 for the linear shear reduction factor, Eq. 70 for the non-linear shear reduction factor, and the effective net section modulus approach as presented in Section IV, the modified nominal shear strengths and moment capacities, $(V_n)_{m1}$, $(V_n)_{m2}$ and $(M_n)_m$, were evaluated and are given in Table XXXXII.

The shear ratios, V_t/V_n, $V_t/(V_n)_{m1}$ and $V_t/(V_n)_{m2}$, and moment ratios, M_t/M_n and $M_t/(M_n)_m$, were also computed and shown in Table XXXXIII.

5. Comparison of Test Results. For the test specimens that failed by the combined bending and shear behavior, the type of failure mode was indicated in Fig. 23. The failure pattern is defined by a bending failure at midspan and a shear diagonal failure around the corners of the web opening. These two failure patterns almost took place simultaneously when the ultimate load was achieved.

Based on the above analysis of shear ratios and moment ratios, three interaction relationships were examined. The values of V_t/V_n and M_t/M_n (Table XXXXIII) are shown graphically by Fig. 24. Also shown in Fig. 24 is the unit circle which represents the present AISI design approach for combined bending and shear. As indicated by Fig. 24, the AISI Specification does not provide a good relationship between bending and shear for webs with openings.

TABLE XXXXII COMPUTATION OF UNMODIFIED AND MODIFIED NOMINAL SHEAR STRENGTHS AND BENDING MOMENTS FOR COMBINED BENDING AND SHEAR TEST SPECIMENS

Specimen No.	a/h	V_n (lbs)	$(V_n)_{m1}$ (lbs)	$(V_n)_{m2}$ (lbs)	M_n (k-in)	$(M_n)_m$ (k-in)
BS-3-14-1A	0.462	5963	1681	2182	26.39	25.27
BS-3-14-2A	0.462	5963	1681	2182	26.44	27.25
BS-3-14-1B	0.462	5963	1681	2182	26.44	27.64
BS-3-14-2B	0.462	5963	1681	2182	26.54	27.64
BS-3-14-1C	0.462	5963	1681	2182	26.20	25.12
BS-3-14-2C	0.462	5963	1681	2182	26.44	25.36
BSB-3-14-1	0.466	9166	2569	2323	82.30	81.02
BSB-3-14-2	0.466	9166	2569	2323	81.02	72.02
BSB-3-14-3	0.472	11524	3204	2868	89.50	86.42
BSB-3-14-4	0.472	11524	3204	2868	88.68	82.41
BSS-3-14-1	0.466	9213	2583	2335	40.83	40.28
BSS-3-14-2	0.466	9213	2583	2335	40.83	40.28
BSS-3-14-3	0.466	9213	2583	2335	44.55	42.40
BSS-3-14-4	0.472	11524	3204	2868	40.83	40.28
BS-3-18-1A	0.459	3738	1058	968	17.64	16.10
BS-3-18-2A	0.459	3738	1058	968	17.64	16.60
BS-3-18-1B	0.459	3738	1058	968	17.32	15.68
BS-3-18-2B	0.459	3738	1058	968	17.37	16.45
BS-3-18-1C	0.459	3738	1058	968	17.42	16.43
BS-3-18-2C	0.459	3738	1058	968	17.79	16.06
BSB-3-18-1	0.455	3371	959	884	33.93	32.29
BSB-3-18-2	0.463	3371	949	862	33.93	32.26
BSB-3-18-3	0.466	3580	1004	907	34.85	31.88
BSB-3-18-4	0.465	3580	1005	910	35.07	31.33
BSS-3-18-1	0.459	3371	954	873	16.97	16.30
BSS-3-18-2	0.459	3371	954	873	16.97	16.30
BS-3-20-1A	0.463	1586	446	406	13.19	9.58
BS-3-20-2A	0.463	1586	446	406	13.24	9.95
BS-3-20-1B	0.463	1586	446	406	13.48	9.85
BS-3-20-2B	0.463	1586	446	406	13.36	9.72
BS-3-20-1C	0.463	1586	446	406	13.13	9.81
BS-3-20-2C	0.463	1586	446	406	13.36	9.72
BSB-3-20-1	0.458	3371	955	876	33.84	30.79
BSB-3-20-2	0.458	3371	955	876	33.46	32.44
BSB-3-20-3	0.466	2062	578	523	31.86	27.64
BSB-3-20-4	0.466	2062	578	523	31.73	27.68
BSB-3-20-5	0.467	2062	577	521	31.60	27.52
BS-2-16-1A	0.353	3788	1586	1935	15.54	15.17
BS-2-16-2A	0.353	3788	1586	1935	15.54	15.16

TABLE XXXXII (CONTINUED) COMPUTATION OF UNMODIFIED AND MODIFIED NOMINAL SHEAR STRENGTHS AND BENDING MOMENTS FOR COMBINED BENDING AND SHEAR TEST SPECIMENS

Specimen No.	a/h	V_n (lbs)	$(V_n)_{m1}$ (lbs)	$(V_n)_{m2}$ (lbs)	M_n (k-in)	$(M_n)_m$ (k-in)
BS-2-16-1B	0.353	3788	1586	1935	15.37	14.85
BS-2-16-2B	0.353	3788	1586	1935	15.37	14.92
BS-2-16-1C	0.353	3788	1586	1935	15.37	14.85
BS-2-16-2C	0.353	3788	1586	1935	15.43	14.92
BSB-2-16-1	0.362	2745	1059	1364	22.35	22.05
BSB-2-16-2	0.740	3731	660	583	29.90	26.87
BSB-2-16-3	0.737	3731	665	588	30.23	27.30
BSS-2-16-1	0.739	3732	662	585	15.04	13.65
BSS-2-16-2	0.739	3732	662	585	15.04	13.65
BSS-2-16-3	0.739	3732	662	585	15.04	13.65
BSS-2-16-4	0.739	3732	662	585	15.04	13.65
BSS-2-16-5	0.739	3732	662	585	15.04	13.65
BS-2-20-1A	0.352	1934	817	991	7.36	6.25
BS-2-20-2A	0.352	1934	817	991	7.47	6.03
BS-2-20-1B	0.352	1934	817	991	7.41	6.20
BS-2-20-2B	0.352	1934	817	991	7.36	5.98
BS-2-20-1C	0.352	1934	817	991	7.41	6.25
BS-2-20-2C	0.352	1934	817	991	7.41	6.07
BSB-2-20-1	0.362	1614	623	802	12.51	11.97
BSB-2-20-2	0.357	1614	652	815	12.04	11.45
BSB-2-20-3	0.734	2264	406	360	17.19	13.52
BSB-2-20-4	0.733	2264	407	361	17.19	13.50
BSS-2-20-1	0.734	2264	406	360	8.60	6.76
BSS-2-20-2	0.734	2264	406	360	8.60	6.76
BSS-2-20-3	0.734	2264	406	360	8.60	6.76
BSS-2-20-4	0.734	2264	406	360	8.60	6.76
BSS-2-20-5	0.734	2264	406	360	8.60	6.76
BSS-2-20-6	0.355	1614	664	820	2.78	5.93
BSS-2-20-7	0.355	1614	664	820	2.21	5.93

Notes:
- V_n = Nominal Shear Strength Based on the 1986 AISI Specification
- $(V_n)_{m1}$ = Calculation of Shear Strength Based on the Eqs. 68 and 69 for Reduction Factor
- $(V_n)_{m2}$ = Calculation of Shear Strength Based on the Eq. 70 for Reduction Factor
- M_n = Nominal Moment Capacity Based on the 1986 AISI Specification
- $(M_n)_m$ = Calculation of Moment Capacity Based on the Effective Net Section Approach

TABLE XXXXIII EVALUATION OF COMBINED BENDING AND SHEAR TEST DATA

Specimen No.	V_t/V_n	$V_t/(V_n)_{m1}$	$V_t/(V_n)_{m2}$	M_t/M_n	$M_t/(M_n)_m$
BS-3-14-1A	0.215	0.763	0.588	0.825	0.862
BS-3-14-2A	0.216	0.766	0.590	0.828	0.803
BS-3-14-1B	0.221	0.785	0.605	0.848	0.811
BS-3-14-2B	0.222	0.788	0.607	0.849	0.815
BS-3-14-1C	0.226	0.800	0.616	0.872	0.909
BS-3-14-2C	0.226	0.803	0.619	0.868	0.905
BSB-3-14-1	0.101	0.360	0.398	0.913	0.928
BSB-3-14-2	0.097	0.344	0.381	0.889	1.000
BSB-3-14-3	0.094	0.336	0.376	0.972	1.007
BSB-3-14-4	0.092	0.332	0.371	0.966	1.040
BSS-3-14-1	0.298	0.931	1.030	0.446	0.452
BSS-3-14-2	0.277	1.065	1.178	0.516	0.299
BSS-3-14-3	0.240	0.990	1.095	0.222	0.234
BSS-3-14-4	0.261	0.861	0.962	0.295	0.299
BS-3-18-1A	0.174	0.614	0.671	0.627	0.686
BS-3-18-2A	0.174	0.614	0.671	0.627	0.666
BS-3-18-1B	0.191	0.674	0.737	0.699	0.772
BS-3-18-2B	0.171	0.603	0.659	0.624	0.659
BS-3-18-1C	0.199	0.704	0.770	0.726	0.770
BS-3-18-2C	0.199	0.704	0.770	0.711	0.788
BSB-3-18-1	0.100	0.352	0.382	0.864	0.908
BSB-3-18-2	0.102	0.361	0.398	0.875	0.921
BSB-3-18-3	0.112	0.398	0.441	0.980	1.071
BSB-3-18-4	0.106	0.376	0.415	0.924	1.034
BSS-3-18-1	0.334	1.179	1.289	0.407	0.423
BSS-3-18-2	0.276	0.974	1.064	0.363	0.378
BS-3-20-1A	0.268	0.953	1.047	0.548	0.754
BS-3-20-2A	0.289	1.027	1.128	0.586	0.780
BS-3-20-1B	0.299	1.065	1.170	0.599	0.819
BS-3-20-2B	0.292	1.038	1.140	0.588	0.809
BS-3-20-1C	0.305	1.083	1.190	0.623	0.834
BS-3-20-2C	0.320	1.139	1.251	0.644	0.885
BSB-3-20-1	0.100	0.354	0.386	0.866	0.952
BSB-3-20-2	0.106	0.375	0.409	0.920	0.949
BSB-3-20-3	0.145	0.519	0.574	0.827	0.953
BSB-3-20-4	0.133	0.477	0.528	0.769	0.882
BSB-3-20-5	0.162	0.581	0.643	0.914	1.049

TABLE XXXXIII (CONTINUED) EVALUATION OF COMBINED BENDING AND SHEAR TEST DATA

Specimen No.	V_t/V_n	$V_t/(V_n)_{m1}$	$V_t/(V_n)_{m2}$	M_t/M_n	$M_t/(M_n)_m$
BS-2-16-1A	0.170	0.407	0.333	0.704	0.721
BS-2-16-2A	0.172	0.410	0.336	0.711	0.729
BS-2-16-1B	0.182	0.434	0.356	0.760	0.787
BS-2-16-2B	0.174	0.415	0.340	0.726	0.748
BS-2-16-1C	0.174	0.415	0.340	0.726	0.751
BS-2-16-2C	0.178	0.426	0.349	0.744	0.769
BSB-2-16-1	0.095	0.246	0.191	1.046	1.060
BSB-2-16-2	0.091	0.512	0.580	0.976	1.086
BSB-2-16-3	0.091	0.511	0.578	0.975	1.079
BSS-2-16-1	0.214	1.208	1.368	0.188	0.207
BSS-2-16-2	0.208	1.175	1.330	0.203	0.223
BSS-2-16-3	0.208	1.171	1.325	0.233	0.257
BSS-2-16-4	0.208	1.171	1.325	0.286	0.315
BSS-2-16-5	0.203	1.142	1.292	0.177	0.195
BS-2-20-1A	0.165	0.392	0.323	0.737	0.868
BS-2-20-2A	0.165	0.392	0.323	0.726	0.899
BS-2-20-1B	0.162	0.383	0.316	0.717	0.856
BS-2-20-2B	0.168	0.398	0.328	0.751	0.924
BS-2-20-1C	0.165	0.392	0.323	0.726	0.867
BS-2-20-2C	0.175	0.414	0.341	0.774	0.946
BSB-2-20-1	0.071	0.185	0.143	0.947	0.990
BSB-2-20-2	0.071	0.176	0.141	0.993	1.044
BSB-2-20-3	0.066	0.369	0.417	0.852	1.084
BSB-2-20-4	0.071	0.393	0.443	0.892	1.136
BSS-2-20-1	0.149	0.833	0.939	0.138	0.176
BSS-2-20-2	0.151	0.840	0.947	0.156	0.198
BSS-2-20-3	0.145	0.808	0.911	0.173	0.220
BSS-2-20-4	0.144	0.800	0.903	0.210	0.268
BSS-2-20-5	0.152	0.847	0.956	0.181	0.231
BSS-2-20-6	0.341	0.828	0.671	0.453	0.469
BSS-2-20-7	0.271	0.660	0.534	0.360	0.373

See Tables XXXXI and XXXXII for Notes

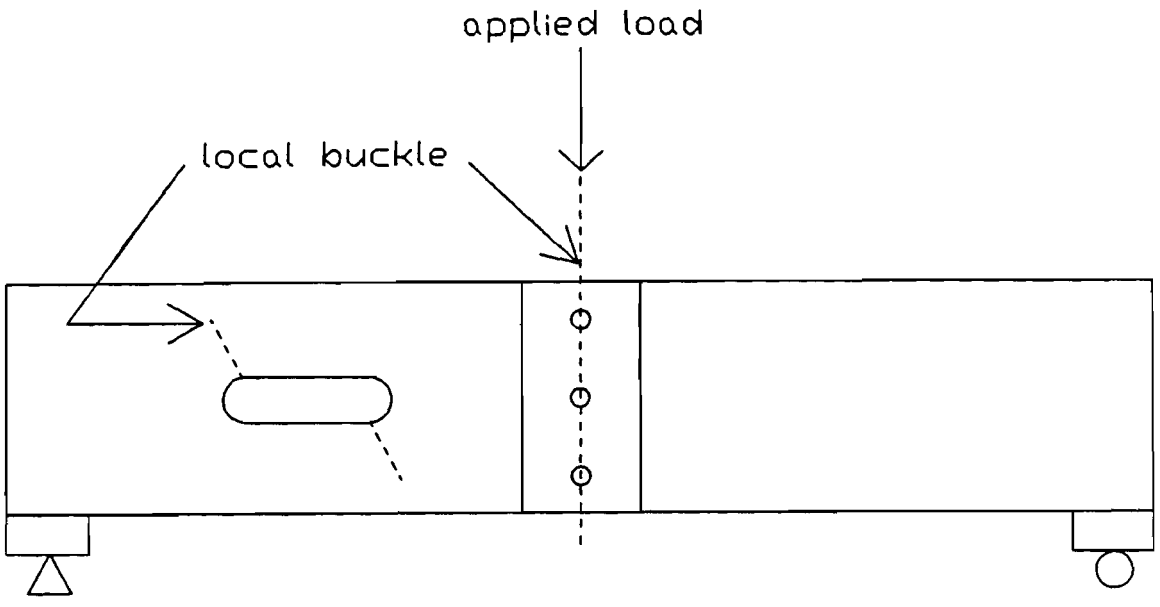

Figure 23. Typical Failure Mode for Combined Bending and Shear

Figure 25 is a plot of the relationship between $V_t/(V_t)_{m1}$ and $M_t/(M_n)_m$ (Table XXXXIII), and Fig. 26 shows the relationship between $V_t/(V_t)_{m2}$ and $M_t/(M_n)_m$ (Table XXXXIII). These two figures present better correlation between bending moment and shear force when compared with the AISI design approach.

Based on a plot of $V_t/(V_n)_{m1}$ and M_t/M_n, and $V_t/(V_n)_{m2}$ and M_t/M_n, Figs. 27 and 28 also demonstrate good interaction between bending moment and shear force for web elements with openings. Figures 27 and 28 consider the shear reduction factor only. Figures 27 and 28 are more appropriate comparisons because at the location of maximum moment, the web did not have an opening.

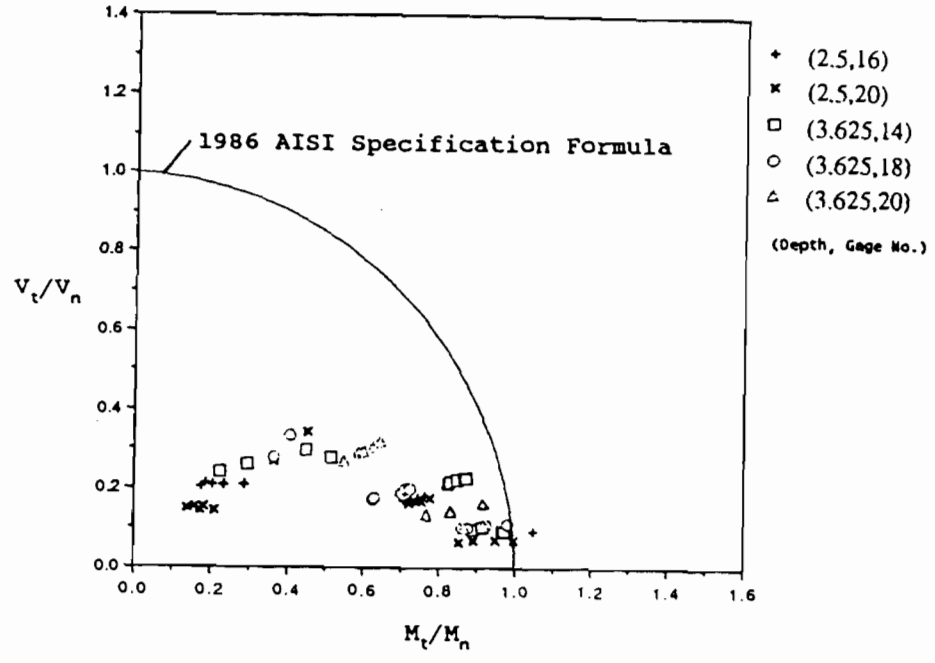

Figure 24. Interaction Diagram for V_t/V_n and M_t/M_n Based on 1986 AISI Specification for Solid Webs

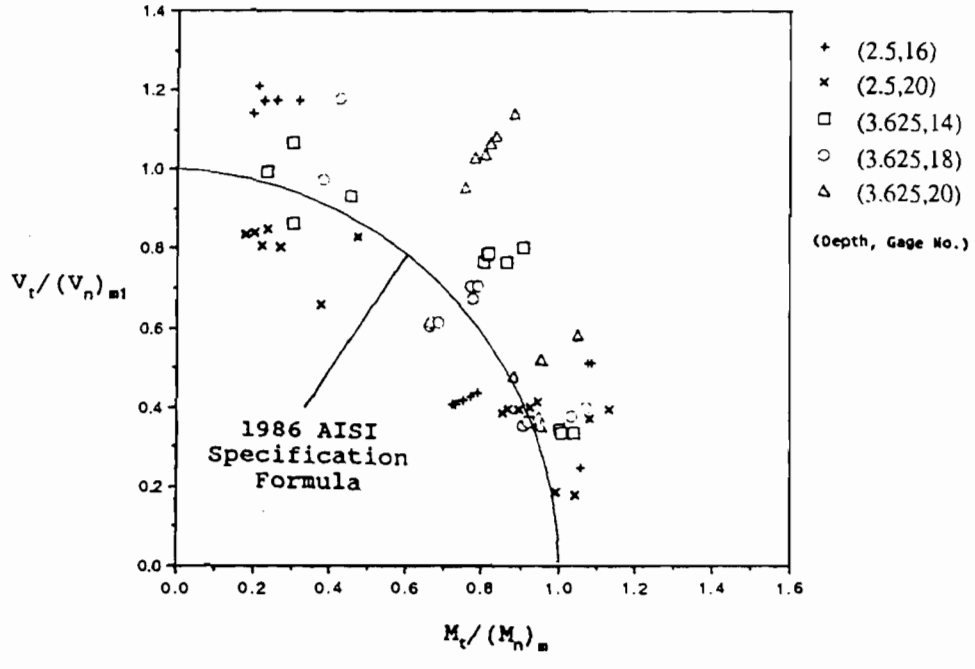

Figure 25. Interaction Diagram for $V_t/(V_n)_{m1}$ and $M_t/(M_n)_m$ Based on the Shear Reduction Factor and Effective Net Section Approach

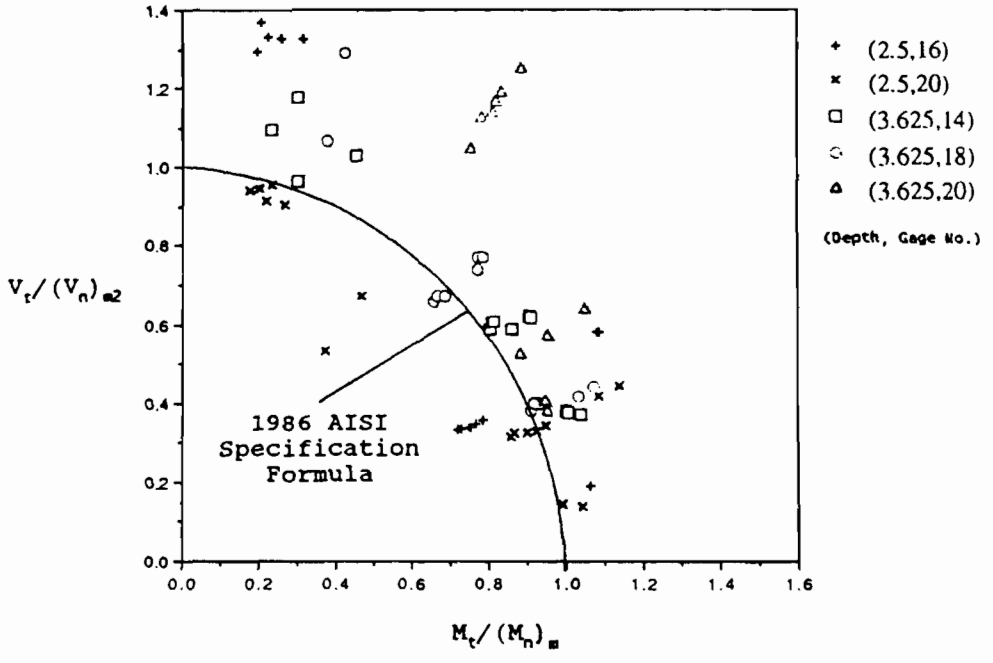

Figure 26. Interaction Diagram for $V_t/(V_n)_{m2}$ and $M_t/(M_n)_m$ Based on the Shear Reduction Factor and Effective Net Section Approach

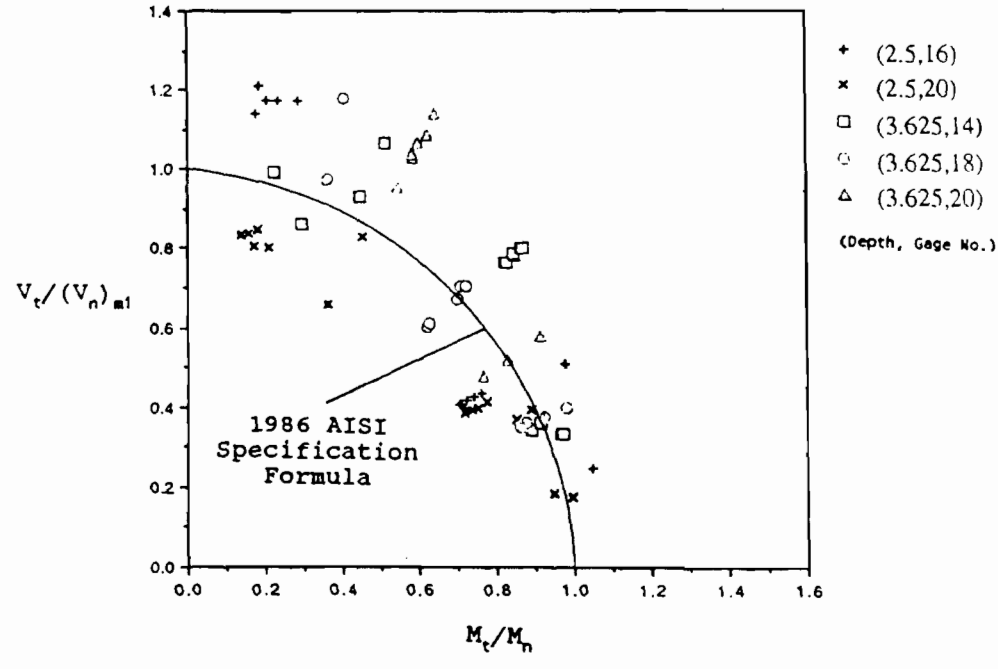

Figure 27. Interaction Diagram for $V_t/(V_n)_{m1}$ and M_t/M_n Based on the Shear Reduction Factor Only

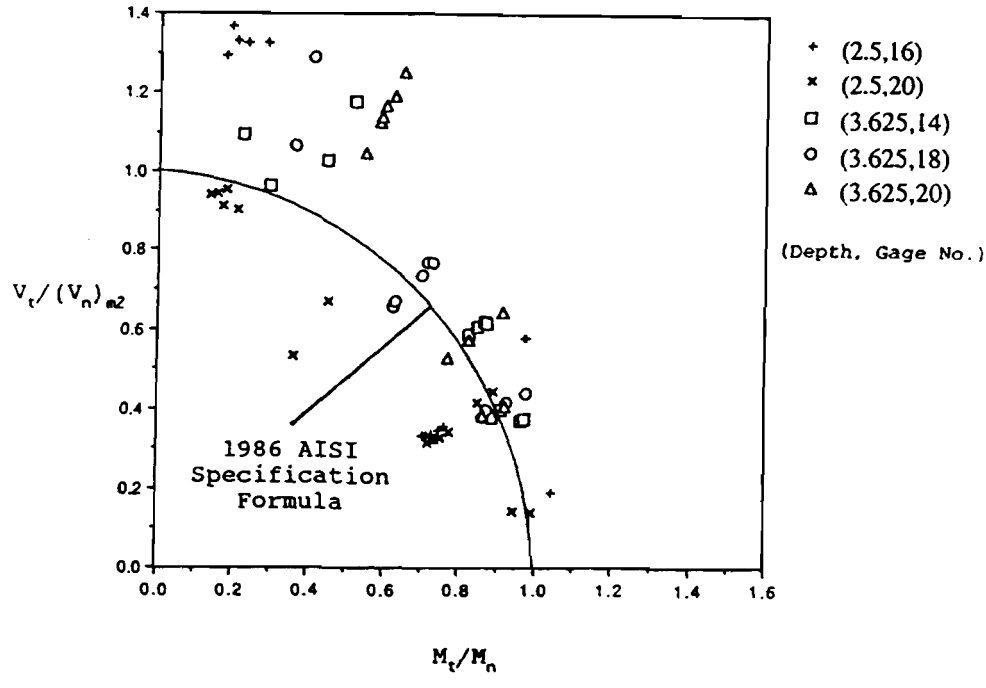

Figure 28. Interaction Diagram for $V_t/(V_n)_{m2}$ and M_t/M_n Based on the Shear Reduction Factor Only

C. SUMMARY AND DESIGN RECOMMENDATIONS

1. Summary. The intent of this investigation was to study the behavior of C-shaped members with elliptical web openings subjected to combined bending moment and shear force. Based on 68 beam specimen tests, the current AISI Specification interaction equation adequately predicts the web capacity if the nominal shear and bending strengths are appropriately modified to account for the web opening.

2. Design Recommendations. Based on the findings of this study, the following design recommendations may be made for a beam with a perforated web subjected to a combined bending moment and shear force.

The AISI Specification interaction equation can be used to predict the strength of a beam web with an opening by using the modified nominal shear strength and bending moment.

$$(M/M_n)^2 + (V/V_{n,m})^2 \leq 1.0 \quad (80)$$

where M = Applied moment

M_n = Nominal moment capacity at the section being investigated

V = Applied shear force

$V_{n,m}$ = Modified shear strength using either the linear or non-linear shear reduction factor

VII. CONCLUSIONS

The objective of this investigation was to study the structural behavior of cold-formed steel members having a perforated web subjected to a pure bending, a pure shear and a combination of bending and shear.

A total of 202 beam specimens were tested, including 108 for pure bending, 26 for pure shear and 68 for combined bending and shear. Based on the findings of this research, the following conclusions were drawn:

1. The presence of web openings reduces the ultimate load-carrying capacity for both pure bending and pure shear.

2. The current AISI Specification can not provide an accurate estimation of moment capacity, shear strength or interaction between bending moment and shear force for C-section members with web openings.

3. The present AISI Specification can predict the moment capacity very well for the members with a solid web governed by local buckling behavior. For the flexural behavior of beam test specimens with web openings having $0.350 \leq a/h \leq 0.740$ and $M_{Rp} < 1.0$ obtained from Eq. 63 which undergo a local buckling mode, design recommendations were presented in Section IV.B.5.a.

4. For beam test specimens with or without web openings having $w/h \leq 0.35$ and $M_{Rp} < 1.0$ determined by using Eqs. 64 or 65 that failed by distortional buckling behavior, possible design approaches were proposed in Section IV.B.5.b.

5. Based on the results of shear test specimens, shear reduction factors were developed and are shown in Section V.B.5. Both linear and non-linear reduction factor equations for use in design of web elements having a elliptical hole and $34.43 \leq h/t \leq 210.32$ are presented.

6. The interaction formula used in the current AISI Specification is applicable for the case of combined bending and shear, if the nominal shear strength and bending strength are modified appropriately.

7. Future studies are needed to obtain a better understanding of the interaction of bending moment and shear force for deeper sections and the edge stiffener's influence on distortional buckling behavior.

APPENDIX -- NOTATION

The following symbols are used in this report:

A = Gross section area of the flange and edge stiffener;

A_h = Length of hole;

A_f = Area of the web;

A_w = Product of D_b and t;

a = Depth of hole;

a' = Shear panel length for unreinforced web element;
= Distance between transverse stiffeners for reinforced web elements;

a'' = Height of hole;

b = Length of hole;

b_e = Effective width of the web element;
= Effective part of the plate width;

$b_{e,f}$ = Effective width of the flange element;

$b_{e,s}$ = Effective width of the lip stiffener;

$b_{e,w}$ = Effective width of the web element;

b_{ue} = Effective width of the portion of the web above the punchout;

b_w = Depth of web;

b_1 = Effective width of the web element;

b_2 = Effective width of the web element;

b' = Half-length of a rectangular hole;

C_w = Warping constant;

D = Plate flexural rigidity per unit width
= $Et^3/[12(1-\nu^2)]$;

D_b = Depth of beam;

d = Diameter of a circular hole;

E = Modulus of elasticity of steel;

$F_{cr,d}$ = Elastic buckling stress;

F_d = Nominal elastic or inelastic distortional buckling stress;

$F_{d,p}$ = Modified elastic or inelastic distortional buckling stress;

F_n = Nominal compressive stress;

F_v = Maximum allowable shear stress;

F_{vH} = Reduced maximum allowable shear stress at section through a hole;

F_y = Yield strength of the material;

F_u = Ultimate tensile strength;

f_1 = Compression stress in web;

f_2 = Tension stress in web;

G = Shear modulus;

H = Depth of hole;

h = Flat width of the web element;

= Clear distance between flanges measured along the plane of the web;

h_x = X coordinate of flange-web junction;

h_y = Y coordinate of flange-web junction;

h_x' = Distance from the web-tension flange junction to the centroid, along an axis parallel to the x-axis;

h_y' = Distance from the web-tension flange junction to the centroid, along an axis parallel to the y-axis;

h' = Clear height of web;

I_x = Moment of inertia about the x-axis (normal to the web);

I_{xy} = Product moment of inertia;

I_y = Moment of inertia about the y-axis (parallel to the web);

I_0 = Polar second moment of area about the shear center;

J = Torsion constant;

k = Web buckling coefficient;

k_v = Shear buckling coefficient;

k_x = Horizontal restraint;

k_y = Elastic extensional spring constant;

k_ϕ = Elastic rotational spring constant;

$k_{\phi,s}$ = Elastic rotational spring constant for a mono-symmetric section with $w_f/t < 400$;

$k_{\phi,as}$ = Elastic rotational spring constant for an unsymmetric section with $w_f/t < 400$;

$k_{\phi,s\text{-}as}$ = Elastic rotational spring constant for unsymmetric and mono-symmetric section with $w_f/t > 400$;

L = Span length;

L_e = Effective unsupported length of the leg;

M = Applied bending moment;

M_{Rp} = Predict moment ratio;

M_T = Plastic moment of tee section;

M_a = Allowable bending moment;

$M_{cr,d}$ = Computed distortional buckling moment in Model B;

M_n = Nominal moment capacity at the section being investigated;

$(M_n)_m$ = Modified moment capacity based on the effective net section approach;

M_t = Tested bending moment;

M_{uc} = Computed ultimate moment based on the AISI Specification;

$M_{uc,d}$ = Computed distortional buckling moment;

$M_{uc,d}$ = Ultimate bending moment;

M_{uen} = Computed ultimate moment based on the effective net section approach;

M_{ufm} = Computed ultimate moment based on the modified effective web area;

M_{ufn} = Computed ultimate moment based on the net section approach;

M_{ut} = Tested ultimate moment;

M_y = Yield moment;

m = Plastic moment of web between adjacent web holes;

n = Number of adjacent web holes;

P = Applied failure load;

P_b = $4(H/D_b)(A_h/H)(1+4A_f/A_w-H/D_b)$;

P_{cr} = Distortional buckling load;

P_f = Lateral compressive force on the rotation of cross section;

P_t = $(1-H/D_b)^2(1+8A_f/A_w-H/D_b)$;

$P_{u(test)}$ = Shear failure load;

p = Center-to-center distance between holes;

Q_y = Intensity of reaction force distributed continuously along the support in the y-direction;

q_s = Shear strength reduction factor;

q'_s = Shear strength reduction factor;

r' = Radius of a circular hole;

S_e = Effective section modulus based on the AISI Specification;

S_{en} = Effective section modulus using AISI effective width equations evaluated at F_n;

$S_{ex,Fk}$ = Effective section modulus evaluated at F_y using modified buckling coefficient;

$S_{ex,d}$ = Effective section modulus based on the nominal elastic or inelastic distortional buckling stress;

$S_{ex,p}$ = Effective section modulus using AISI effective width equations evaluated at $F_{d,p}$;

S_g = Gross section modulus used in Model B;

S_{uen} = Effective section modulus based on the net section at the yield stress, F_y;

S_{ufm} = Effective section modulus evaluated at a yield stress, F_y, with b_2=0.0;

S_{ufn} = Section modulus determined by using the net section approach

s = Minimum width of web post between adjacent web holes;

t = Thickness of element;

u = Horizontal displacement;

V = Applied shear force;

V_a = Allowable shear force;

V_{cr} = Shear buckling force;

V_n = Nominal shear strength of web;

$V_{n,m}$ = Modified shear strength using either the linear or non-linear shear reduction factor;

$(V_n)_{m1}$ = Modified nominal shear strength using a linear shear reduction factor;

$(V_n)_{m2}$ = Modified nominal shear strength using a non-linear shear reduction factor;

V_t = Tested failure shear load;

V_u = Maximum shear force;

V_{uH} = Reduced ultimate shear force;

v = Vertical displacement;

w = Flat width of the web element;

= Flat width of the flange element;

w_u = Flat width of the portion of the web element above the punchout;

w' = Flat width of the flange element;

w_f = Width of the tension flange;

w_w = Depth of the web in the leg under consideration;

x = Distance from the end support to the applied load;

x_o = Location of the shear center relative to the centroid, along an axis parallel to the x-axis;

x' = Distance between hole and plate located at midspan;

y_o = Location of the shear center relative to the centroid, along an axis parallel to the y-axis;

α = $0.75(H/A_h)^2(D_h/H-1)^2$;

β_1 = Geometric parameter;

γ = Ratio of the elastic local buckling stress in the web to the buckling stress required for the web to be fully effective;

η = $(\pi/\lambda)^2$;

λ = $\sqrt{F_y/\sigma_d}$;

ν = Poisson's ratio = 0.3;

σ_d = Elastic distortional or elastic mixed local-distortional mode buckling stress;

σ_{el} = Elastic local buckling stress; and

ϕ = Rotational displacement.

BIBLIOGRAPHY

1. "Specification For the Design of Cold-Formed Steel Structural Members Design," American Iron and Steel Institute, August 19, 1986, with December 11, 1989 Addendum.

2. "Load and Resistance Factor Design Specification for Cold-Formed Steel Structural Members," American Iron and Steel Institute, March 16, 1991.

3. Yu, W.W., "Cold-Formed Steel Design," Second Edition, John Wiley & Sons, Inc., New York, 1991.

4. Redwood, R.G., Discussion of "Elastic Stresses Around Holes in Wide Flange Beams," by Bower, J.E., Journal of the Structural Division, ASCE, Vol. 93, No. ST1., February, 1967.

5. Redwood, R.G., and J.O. McCutcheon, "Experimental Tests of Wide-Flange Beams with Large Unreinforced Web Openings," Department of Civil Engineering and Applied Mechanics, McGill University, Montreal, Quebec, Canada, April, 1967.

6. Redwood, R.G., and J.O. McCutcheon, "Beam Tests with Unreinforced Web Openings," Journal of the Structural Division, ASCE Proceedings, Vol. 94, No. ST1., January, 1968, pp. 1-17.

7. Hoglund, T., "Strength of Thin Plate Girders with Circular or Rectangular Web Holes without Web Stiffeners," Reports of Working Commissions, Vol. 11, International Association for Bridge and Structural Engineering (IABSE) Symposium, London, England, 1971, pp. 353-365.

8. LaBoube, R.A., "Design Guidelines for Web Elements with Openings," Private Correspondence, 1990.

9. Redwood, R.G., H. Baranda, and M.J. Daly, "Test of Thin-Webbed Beams with Unreinforced Holes," Journal of the Structural Division, ASCE Proceedings, Vol. 104, No. ST3., March, 1978, pp. 577-595.

10. Redwood, R.G., and M. Uenoya, "Critical Loads for Webs with Holes," Journal of the Structural Division,ASCE Proceedings, Vol. 105, No. ST10, 1979, pp. 2053-2067.

11. Uenoya, M., and R.G. Redwood, "Buckling of Webs with Openings," Computer and Structures, Vol 9., No. 2, 1978, pp. 191-199.

12. Segner, E.P., Jr., "Reinforcement Requires for Girder Web Openings," Journal of the Structural Division, ASCE, Vol. 90, No. ST3, Proc. Paper 3919, June, 1964, pp. 147-164.

13. Congdon, J,G., and R.G. Redwood, "Plastic Behavior of Beams with Reinforced Holes," Journal of the Structural Division, ASCE Proceedings, Vol. 96, No. ST9., September, 1970, pp. 1933-1955.

14. Redwood, R.G., "Simplified Plastic Analysis for Reinforced Web Holes," Engineering Journal, American Institute of Steel Construction, New York, N.Y., October, 1971.

15. Cooper, P.B., and R.P. Snell, "Test on Beams with Reinforced Web Openings," Journal of the Structural Division, ASCE, Vol. 98, No. ST 3., Proc. Paper 8791, March, 1972, pp. 611-632.

16. Wang, T.M., R.R. Snell, and P.B. Cooper, "Strength of Beams with Eccentric Reinforced Holes," Journal of the Structural Division, ASCE Proceedings, Vol. 101, No. ST9., September, 1975, pp. 1783-1800.

17. Larson, M.A., and K.N. Shah, "Plastic Design of Web Openings in Steel Beams," Journal of the Structural Division, ASCE Proceedings, Vol. 101, No. ST5., May, 1976, pp. 1031-1041.

18. Redwood, R.G., and S.C. Shrivastava, "Design Recommendations for Steel Beams with Web Holes," National Research Council of Canada, Vol. 7, August, 1980, pp. 642-650.

19. Kussman, R.L., and P.B. Cooper, "Design Example for Beams with Web Openings," Engineering Journal, American Institute of Steel Construction, 13(2), 1976, pp. 48-56.

20. Shrivastava, S.C., and R.G. Redwood, "Shear Carried by Flanges at Unreinforced Web Holes," Journal of the Structural Division, ASCE Proceedings, Vol. 105, No. ST8., 1979, pp. 1706-1711.

21. Shanmugam, N.E., and V. Thevendran, "Critical Loads of Thin-Walled Beams Containing Web Openings," Journal of Thin-Walled Structures, Vol. 2, 1992, pp. 291-305.

22. Lau, S.C.W., and G.J. Hancock, "Distortional Buckling Tests of Cold-Formed Channel Sections," Proceedings of the Ninth International Specialty Conference on Cold-Formed Steel Structures, St. Louis, Missouri, November, 1988, pp. 45-73.

23. Kwon, Y.B, and G.J. Hancock, "Tests of Cold-Formed Channels with Local and Distortional Buckling," Journal of the Structural Engineering, ASCE, Vol. 117, No. ST07, July, 1992, pp. 1786-1803.

24. Bernard, E.S., R.Q. Bridge, and G.J. Hancock, "Intermediate Stiffeners in Cold-Formed Profiled Steel Decks. Part 1--'V' Shaped Stiffeners," Research Report No. R653, School of Civil and Mining Engineering, University of Sydney, Australia, 1992.

25. Bernard, E.S., R.Q. Bridge, and Hancock, G.J., "Tests of Profiled Steel Decks with V-Stiffeners," Proceedings of the Eleventh International Specialty Conference on Cold-Formed Steel Structures, St. Louis, Missouri, 1992.

26. Bernard, E.S., R.Q. Bridge, and G.J. Hancock, "Intermediate Stiffeners in Cold-Formed Profiled Steel Decks. Part 1--'Flat Hat' Shaped Stiffeners," Research Report No. R658, School of Civil and Mining Engineering, University of Sydney, Australia, 1992.

27. Charnvarnichborikarn, P., "Distortional Buckling of Cold-Formed Steel Z-Sections," Ph.D. Dissertation, University of Manitoba, April, 1992.

28. Charnvarnichborikarn, P., and D. Polyzois, "Distortional Buckling of Cold-formed Steel Z-section Columns," Proceedings of the Eleventh International Specialty Conference on Cold-Formed Steel Structures, St. Louis, Missouri, October, 1992, pp. 353-378.

29. Narayanan, R., and N.G.V. Der-Avanessian, "Equilibrium Solutions for Predicting the Strength of Webs with Rectangular Holes," Proceedings of the Institute of Civil Engineering, London, England, Part 2, Vol. 75, June, 1983, pp. 265-282.

30. Narayanan, R., N.G.V. Der-Avanessian, and M.M. Ghannam, "Small-Scale Model Tests on Perforated Webs," The Structural Engineering, London, England, Vol. 61B, No. 3, September, 1983, pp. 47-53.

31. Narayanan, R., and N.G.V. Der-Avanessian, "An Equilibrium Method for Assessing the Strength of Plate Girders Having Reinforced Web Openings," Proceedings of the Institute of Civil Engineering, London, England, Part 2, Vol. 77, June, 1984, pp. 107-138.

32. Narayanan, R., and N.G.V. Der-Avanessian, "Elastic Buckling of Perforated Plates under Shear," Thin Walled Structures, Applied Science Publisher, London, England, Vol. 2(1), 1984, pp. 51-73.

33. Narayanan, R., and N.G.V. Der-Avanessian, "Design of Slender Webs Having Rectangular Holes," Journal of Structural Engineering, ASCE, Vol. 111, No. ST4, April, 1985, pp. 777-787.

34. Chow, F.Y., and R. Narayanan, "Buckling of Plates Containing Openings," Proceedings of the Seventh International Specialty Conference on Cold-Formed Steel Structures, University of Missouri-Rolla, Rolla, Missouri, 1984, pp. 39-53.

35. "Suggested Design Guides foe Beams with Web Holes," by the Subcommittee on Beams with Web Holes of the Task Committee on Flexural Members of the Structural Division, John, E., Bower, Chmn., Journal of the Structural Division, ASCE, Vol. 97, No. ST11, Proceeding Paper 8536, November, 1971, pp. 2707-2728.

36. Davis, C.S., and W.W. Yu, "Cold-Formed Steel Members with Perforated Elements," Journal of the Structural Division, ASCE, Vol. 99, No. ST10, Proc. Paper 10059, October 1973, pp. 2061-2077.

37. Davis, C.S., and W.W. Yu, "Buckling Behavior and Post-Buckling Strength of Perforated Stiffened Compression Elements," Proceedings of the First International Specialty Conference on Cold-Formed Steel Structures, (August 1971). University of Missouri-Rolla, Rolla, Missouri, April, 1973, pp. 58-64.

38. Hancock, G.J., "Distortional Buckling of Steel Storage Rack Columns," Journal of Structural Engineering, ASCE, Vol. 111, No. ST12, December, 1985, pp. 2770-2783.

39. Lau, S.C.W., and G.J. Hancock, "Distortional Buckling Formulas for Channel Columns," Journal of Structural Engineering, ASCE, Vol. 113, No. ST05, May, 1987, pp. 1063-1078.

40. Johnston, B.C., Guide to Stability Design Criteria for Metal Structures, Third Edition, John Wiley and Sons, New York, 1976.

41. Kwon, Y.B, and G.J. Hancock, "Design of Channels Against Distortional Buckling," Proceedings of the Eleventh International Specialty Conference on Cold-Formed Steel Structures, St. Louis, Missouri, October, 1992, pp. 323-352.

42. Lundquist, E.E., E.Z. Stowell, and E.H. Schuette, "Principles of Moment Distribution Applied to Stability of Structures Composed of Bars or Plates," NACA Wartime Report L-326, 1943.

43. Lau, S.C.W., and G.J. Hancock, "Distortional Buckling Formulas for Thin-Walled Channel Columns," Research Report No. R521, School of Civil and Mining Engineering, University of Sydney, Sydney, Australia, 1986.

44. Winter, G., "Thin-Walled Structures--Theoretical Solutions and Test Results," Preliminary Publication of the Eighth Congress, IABSE, 1968, pp. 101-112.

45. Serrete, R., and T. Pekoz, "Local and Distortional Buckling of Thin-Walled Beams," Proceedings of the Eleventh International Specialty Conference on Cold-Formed Steel Structures, St. Louis, Missouri, October, 1992, pp. 63-73.

46. Batson, K.D., "Flexural Behavior of Webs with Openings," M.S. Thesis, University of Missouri-Rolla, 1992.

47. Schuster, R.M., "Testing of Perforated C-Stud Sections in Bending," University of Waterloo, Ontario, Canda, March, 1992.